The Hepatic Stellate Cell in Sight:

Targeting Antiproliferative Drugs to the Fibrotic Liver

Rick Greupink

Cover: from top to bottom, a description of the options for the pharmacological treatment of chronic hepatitis/fibrosis in the Netherlands, ± 1850 (in: "zakwoordenboek der therapie voor praktisch genees- en heelkundigen" by Prof. Klencke, 3rd edition, printed by Gieben & Dumont in 1855); collagen III-stained section of a fibrotic rat liver; a desmin-positive hepatic stellate cell in culture; tablets. In the background: liver section stained for collagen III. Together these images nicely reflect the diverse pharmacological, pathological and pharmaceutical aspects of the work described in this thesis.

ISBN printed version: 90-367-2589-5
ISBN electronic version: 90-367-2590-9

Page and cover design: Maaike Baack, Annelies Draaisma and Rick Greupink
Printed by: Febodruk BV te Enschede

RIJKSUNIVERSITEIT GRONINGEN

The Hepatic Stellate Cell in Sight: Targeting Antiproliferative Drugs to the Fibrotic Liver

Proefschrift

ter verkrijging van het doctoraat in de
Wiskunde en Natuurwetenschappen
aan de Rijksuniversiteit Groningen
op gezag van de
Rector Magnificus, dr. F. Zwarts,
in het openbaar te verdedigen op
vrijdag 23 juni 2006
om 14.45 uur

door

Albert Hendrikus Greupink

geboren op 20 september 1976
te Rheden

Promotores:	Prof. dr. K. Poelstra
	Prof. dr. D.K.F. Meijer
Copromotor:	Dr. L. Beljaars
Beoordelingscommissie:	Prof. dr. H. Moshage
	Prof. dr. H.J. Verkade
	Prof. dr. H.J. Haisma

Paranimfen: Hester Bakker
Peer de Graaf

The work presented in this thesis was performed at the department of Pharmacokinetics and Drug Delivery (University of Groningen, The Netherlands), which is part of the research school GUIDE.

This research was funded by grant GFA.5460 from the Dutch Foundation for Technical Sciences (Stichting Technische Wetenschappen).

The printing of this thesis was financially supported by grants of:
Rijksuniversiteit Groningen
Groningen University Institute for Drug Exploration (GUIDE)
Harlan Nederland B.V.
Olympus Nederland B.V.
Roche Nederland B.V.
Nederlandse Vereniging voor Hepatologie

TABLE OF CONTENTS

1

SCOPE OF THE THESIS

Liver fibrosis is characterized by the accumulation of excessive amounts of scar tissue in response to chronic liver injury. Important causes of chronic liver injury are viral hepatitis, metabolic disorders such as Wilson's disease, autoimmune diseases and chronic exposure to certain chemicals, alcohol or drugs. It is also becoming increasingly clear that obesity is a risk factor for steato-hepatitis, finally leading to fibrosis. Although initially the synthesis of scar tissue in the injured liver serves as a repair mechanism to allow proper healing of the damaged tissue, liver fibrosis can be viewed upon as a derailed healing response, in which the deposition of scar tissue is disproportionate to the extent of tissue damage. In its advanced stages the disease is characterized by its self-perpetuating nature, reflected by the fact that fibrosis progresses even after withdrawal of the inciting stimulus. Eventually, fibrosis may develop into an irreversible condition referred to as liver cirrhosis, in which regenerative nodules of still functional liver parenchyma are encapsulated in fibrotic septa, resulting in complete liver failure and, ultimately, death. As outlined in chapter 2, for many patients no effective pharmacological treatment is available and to date a liver transplantation is the only curative option.

Extensive research on the pathophysiology of liver fibrosis has identified the hepatic stellate cell (HSC) as the key fibrogenic cell of the liver. HSC proliferation appears to be a crucial step in fibrogenesis, and attenuating the proliferation of this cell type therefore seems a relevant strategy to inhibit liver fibrosis pharmacologically. However, a serious problem of systemic treatment with antiproliferative drugs would be the unacceptable toxicity in organs other than the liver. Yet, even within the liver systemic treatment with antiproliferative drugs will undesirably affect other cell types. Inhibition of hepatocyte proliferation, for example, may result in an impaired regenerative capacity of the liver, while particularly this process is of great importance for the renewal of the liver parenchyma after massive hepatocyte injury. Because of these serious adverse effects, the use of cytostatics and other potent antiproliferative drugs has not been

examined. One possible approach to reduce the adverse effects is to increase the specificity of antiproliferative agents for activated HSC by cell-selective targeting. With the recent development of the first generation of HSC-selective drug carriers, this has now become an option.

The work described in this thesis focuses on the use of the HSC-selective drug carrier mannose-6-phosphate-modified human serum albumin (M6PHSA). This carrier has been designed to specifically bind to mannose-6-phosphate/insulin-like growth factor-II (M6P/IGF-II) receptors, which are upregulated on the cell surface of activated HSC.

In **chapter 3** the expression of the target receptor is investigated in bile duct-ligated (BDL) rats, since to date no data is available on the M6P/IGF-II receptor expression in this animal model for liver fibrosis. In addition, we evaluated whether the M6P/IGF-II receptor is expressed in fibrogenic cells in a rat model of hypertension-induced fibrotic vascular lesions. We also describe in this chapter how mycophenolic acid (MPA) can be coupled to M6PHSA in such a way that uptake via this receptor is achieved and a cell-selective pharmacologically active construct is obtained. MPA is a known immunosuppressive drug, but we pursued recent observations that suggest a direct antiproliferative effect of this drug on fibrogenic cells as well.

In **chapter 4** the antiproliferative effect of MPA and its mechanism of action are studied for the first time in HSC. Additionally, the pharmacological effects of MPA coupled to the HSC-selective drug carrier, were studied in these cells. *In vivo* experiments with this MPA-containing construct in BDL rats, examining the organ distribution, the intrahepatic distribution over the various liver cell types, as well as the *in vivo* effects on hepatic inflammatory and fibrosis parameters are also reported.

Chapter 5, 6 and 7 focus on the experiments that we have performed with doxorubicin (DOX), a more potent antiproliferative drug than MPA. In **chapter 5**, experiments on the antifibrotic effects of untargeted doxorubicin are described.

These investigations were performed in order to provide evidence for the potential antifibrotic effect of this antiproliferative drug in experimental liver fibrosis in the rat. Additionally, we report in this chapter on the synthesis of a DOX-containing HSC-selective construct, its organ and cellular distribution pattern *in vivo*, as well as its pharmacological effects on HSC *in vitro*. **Chapter 6** focuses in more detail on the pharmacokinetics of the M6PHSA-DOX conjugate in fibrotic rats, whereas in **chapter 7** the effects of this drug targeting preparation on experimental liver fibrosis are investigated.

In summary, the aim of the work presented in this thesis is to investigate the application of two antiproliferative drugs for the treatment of liver fibrosis, with special emphasis on the targeted delivery of these drugs to the hepatic stellate cells. To our knowledge, it is the first study that explores the HSC-selective delivery of antiproliferative drugs as a strategy to treat this chronic disease.

2

GENERAL INTRODUCTION

Liver fibrosis

Liver fibrosis is characterized by the excessive deposition of extracellular matrix (ECM) in response to chronic liver injury of various etiologies of which chronic viral hepatitis, alcohol abuse, and autoimmune diseases are the most common examples (1;2). Moreover, obesity is increasingly recognized as an important risk factor for the development of steato-hepatitis leading to liver fibrosis. Although initially the synthesis of ECM serves as a repair mechanism to allow healing of the injured organ, liver fibrosis can be viewed upon as a derailed healing response, in which the deposition of ECM is excessive, disproportionate to the extent of tissue injury, and deleterious to tissue structure and function. Fibrosis may continue to progress into a severe condition called cirrhosis, which is irreversible and characterized by the formation of regenerative nodules of liver parenchyma that are encapsulated in fibrotic septa (1;3). Eventually, this situation leads to impaired liver function and death. Although the yearly number of deaths from chronic liver disease and cirrhosis is comparatively low in The Netherlands, over the entire European region cirrhosis-related mortality accounts for 20 per 100,000 population, and in the whole of the Western World the disease ranks among the top ten causes of death by disease. Moreover, due to the chronic nature of the disease, costs are also high in terms of hospital admission, loss of productivity and loss of quality of life. The 5-year survival rate among patients with advanced cirrhosis is only approximately 60% and chances of developing a primary hepatocellular carcinoma are increased 60-100 fold, depending on the etiology of the disease (4).

The variety of injurious events that lead to fibrosis, translates into differences in the topographical distribution of fibrosis within the liver. In man, cholestasis mainly leads to liver injury in acinar zone 1 and is characterized by the development of fibrotic septa extending from the portal tracts (portal-portal bridging). In contrast, viral hepatitis-induced liver injury elicits both portal-portal bridging of fibrotic septa as well as the development of scar tissue deposition

between the portal triad and central vein (portal-central bridging). On the other hand, steato-hepatitis induces hepatocellular injury, which is rather evenly distributed throughout the liver lobule and is characterized by perisinusoidal fibrosis in which separate hepatocytes are engulfed by ECM (Fig. 1).

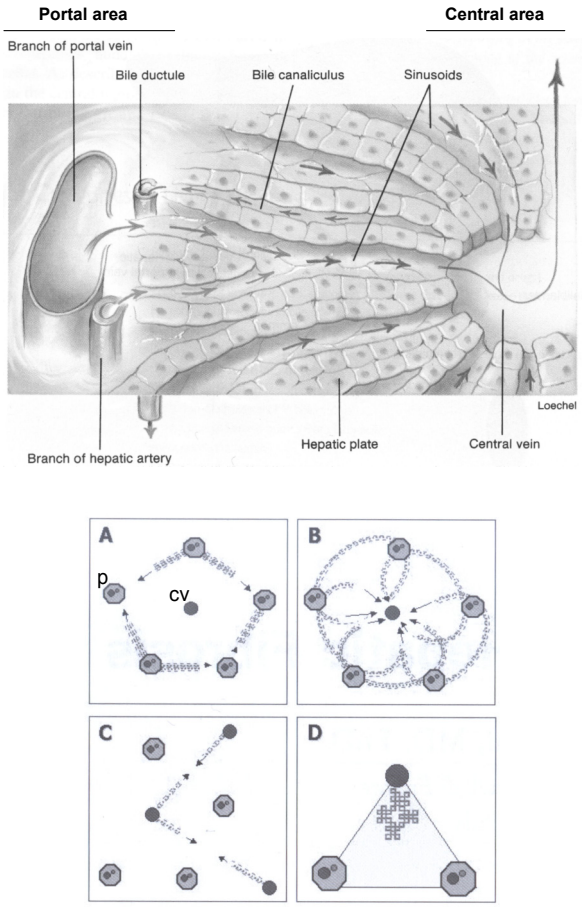

Fig. 1. The upper panel shows a schematic representation of the liver lobule (modified after Stuart, Ira and Fox. The digestive system. In: Human Physiology, 7th ed., McGraw-Hill publishers, p561-599). In the lower panel: a schematic representation of the different topographical distributions of hepatic scarring in the liver. A: portal-portal bridging B: virus-induced, combined portal-portal and portal-central bridging C: central-central bridging D: perisinusoidal fibrosis. p: portal area, cv: central vein. Modified from (1).

In experimental animals these different situations are mimicked as much as possible; bile duct ligation leads to fibrosis in zone 1 of the liver, characterized by portal-portal bridging, whereas administration of the hepatotoxic agent CCl_4 induces mainly hepatocyte injury in zone 3 of the liver, resulting in central-central bridging of fibrotic septa (1).

Current treatment options

To date, therapies that interfere with the underlying cause of the disease represent the best pharmacological treatment options for liver fibrosis. The following paragraphs will therefore give a brief outline of the generally applied pharmacological interventions in patients with this disease. Pharmacological treatment strategies are discussed in relation to the different injurious events leading to liver scarring.

Hepatitis B virus-induced fibrosis

Viral hepatitis is an important cause of chronic liver disease and fibrosis. World wide, approximately 350 million people are chronically infected with hepatitis B virus (HBV), and it is estimated that approximately 25% of these patients will develop liver cirrhosis. The virus infects hepatocytes by binding to certain cell surface receptors, subsequently followed by uncoating of the virus particle and translocation of the HBV genome to the nucleus. Viral DNA resides in hepatocytes very persistently and its clearance appears to be dependent on the clearance of infected hepatocytes by CD8+ T-lymphocytes. This immune response is mainly responsible for the liver injury that follows from HBV infection, although also direct cytopathic effects of HBV have been described in patients with very high viral loads (1;4-6).

Until recently, only (pegylated) interferon-alpha (IFN-α) was available for the treatment of patients with chronic hepatitis B infection. IFN-α is an immune-modulating drug that improves the cytotoxic T-lymphocyte response against

infected hepatocytes. Unfortunately, its use is contra-indicated in patients with clinical cirrhosis. Because IFN-α acts by increasing the clearance of HBV infected hepatocytes, in cirrhotic patients with decompensated liver function, this can result in the loss of a relative large fraction of the remaining functional liver parenchyma and thus in an acute deterioration of liver function. Moreover, an increased incidence of bacterial infections has been associated with the use of IFN-α in cirrhotic patients, which is related to meyelosuppressive effects of the drug (5;6).

However, with the advent of the HBV DNA polymerase inhibitors lamivudine and adefovir, also the treatment of HBV-infected patients with clinical cirrhosis has become an option. In contrast to IFN-α, lamivudine and adefovir have an excellent tolerability and side effect profile. Lamivudine is metabolized intracellularly to its active triphosphate, which acts as a nucleoside analog that inhibits HBV DNA polymerase and causes DNA chain termination. Adefovir is a nucleotide analog to adenosine monophosphate and acts via a similar mechanism (7). Long term mono-therapy with either drug has been shown to exert beneficial effects on fibrosis and inflammation. In HBV-infected patients with cirrhosis and decompensated liver function, treatment with lamivudine extended the time to liver transplantation (8-12).

For all anti-HBV drugs it is necessary to maintain viral suppression for long periods of time, because these drugs only inhibit active viral replication and leave the intracellular reservoir of viral DNA in hepatocytes largely intact. Indeed, relapse occurs in a large percentage of treated patients after cessation of therapy. Furthermore, development of lamivudine-resistant mutants presents a serious problem. Resistance occurs in 28% of treated patients after 1 year of treatment and increases to 68% after 4 years (13;14). Interestingly, no viral resistance has been reported in response to adefovir therapy yet, and therefore adefovir is usually added to lamivudine monotherapy at the first signs of development of drug-resistant mutants (5). New anti-HBV drugs, such as entecavir, clevudine and emtricitabine, are expected to find their way to the clinic soon and it is very well

possible that a combination therapy with mechanistically different acting drugs can improve the response rate to therapy in the near future (7).

Hepatitis C virus-induced fibrosis

World wide, approximately 150 million people are infected with hepatitis C virus (HCV). After HCV infection approximately 85% of patients will develop a chronic hepatitis. Similar to HBV, HCV itself is not directly cytotoxic to hepatocytes, but by continuous stimulation of the immune system, cytotoxic T lymphocyte-mediated clearance of infected hepatocytes forms the main mechanism of hepatic injury. After the initial infection, it may take up to 20 years for these patients to develop advanced fibrosis/cirrhosis and approximately 25-30 years for the development of hepatocellular carcinoma (15). This long asymptomatic period of time often prevents an early onset of therapy.

The number of drugs available for the pharmacological treatment of chronic HCV infection is even smaller than that for HBV-infected patients. Combination therapy of pegylated IFN-α with ribavirin has been proven to be effective in suppressing HCV activity (16). Similar to HBV-infected patients, the treatment aims at reducing viral replication to induce seroconversion and reduce the risk of hepatocellular carcinoma and progression of fibrosis and cirrhosis into end-stage liver disease. Ribavirin is a purine nucleoside analog that inhibits the replication of a wide variety of RNA and DNA viruses (7). Dose-limiting side effects of the drug are anemia and leucopenia, whereas IFN-α therapy is associated with depression, flu-like symptoms, fever and meyelosuppression. Especially in cirrhotic patients a dose reduction is required to avoid drug related morbidity, which generally results in low sustained viral response rates in those patients. Although adjuvant therapy with erythropoietin and granulocyte colony stimulating factor has been proposed in order to reduce anemia and leucopenia in cirrhotic patients, limited clinical evidence for its efficacy is available and treatment of patients with advanced HCV-induced cirrhosis therefore remains very difficult (15;17).

The overall response rate to IFN-α/ribavirin in HCV-infected patients is approximately 50%, and as pointed out in the above paragraphs, for non-responders there is no alternative treatment available. Particularly difficult to treat are the HCV/HIV co-infected and patients with an HCV re-infection of the liver after liver transplantation. These patients often develop fulminant fibrosis, which progresses to end stage liver disease within 5 years (1).

Liver fibrosis due to genetically inheritable factors

Wilson's disease and hemochromatosis are genetically inheritable disorders that can lead to liver fibrosis. Wilson's disease, or copper overload disease, is a result of a mutation in the ATP7B gene which codes for a protein that is essential for copper excretion into the bile. The resulting decrease in copper excretion into the bile leads to its accumulation in the body, which is primarily deposited within the liver, and in a later stage of the disease, also in the brain (18). Hemochromatosis, or iron overload disease, is the result of an increased iron uptake from the small intestine due to a mutation in the HFE gene. It is believed that the increased levels of metal ions in hepatocytes induce necrosis via facilitation of the generation of reactive oxygen intermediates within hepatocytes, which leads to hepatocellular injury and, ultimately, hepatic fibrosis (19;20).

The treatment of cirrhotic patients with Wilson's disease is mainly based on procedures aimed at the reduction of tissue copper levels. A well known anti-copper agent is penicillamine, which acts as a reductive chelator that mobilizes intracellular copper deposits in the liver and brain, and facilitates its urinary excretion. However, the use of penicillamine has become obsolete with the arrival of much safer alternatives. One option is treatment with zinc, which inhibits the copper uptake from the small intestine via the induction of metallothionein in the intestinal wall. Another possibility is treatment with tetrathiomolybdate, which complexes copper in the intestine and in the circulation, thus preventing cellular uptake and favoring its urinary excretion either via faeces or urine. Treatment of

patients with decompensated cirrhosis with these drugs has been shown to improve liver function, often successfully postponing a liver transplantation (18). In analogy to the treatment strategy in Wilson's disease, pharmacological intervention in hemochromatosis also aims at reducing the amount of metal ions in the body. Currently, medical phlebotomy is considered a safe and effective treatment for hemochromatosis (19).

Autoimmune-mediated liver disease

Autoimmune-mediated liver disease can be divided into autoimmune hepatitis (AIH), primary biliary cirrhosis (PBC) and primary sclerosing cholangitis (PSC). Whereas AIH and PBC mostly occur in women, 70% of the patients with PSC are men. Autoimmune diseases in general are the consequence of a breakdown of tolerance to self-antigens. For instance in AIH type II, high circulating levels of anti-CYP2D6 immunoglobulins can be detected, predominantly affecting hepatocytes. In type I and III, other cellular structures are targeted by antibodies, but it is not yet exactly clear which types of immunoglobulins are responsible. In PBC and PSC the small and medium-sized intrahepatic bile ducts are attacked, whereas in PSC especially the large extrahepatic ducts are affected. In all three forms of immune-mediated liver injury liver fibrosis develops, mainly of the periportal type (20).

Although AIH, PSC and PBC are all autoimmune diseases, only AIH responds well to immunosuppressive therapy with corticosteroids and azathioprine. Conversely, for the treatment of PBC, corticosteroid therapy is explicitly not recommended because a worsening of osteoporosis can be expected, of which a higher incidence is associated with the disease already. Especially in PBC patients that are diagnosed in an early stage of hepatic injury, treatment with ursodeoxycholic acid (UDCA) inhibits histopathological progression significantly. However, when hepatic injury has already progressed further, most studies show no beneficial effect of treatment anymore. The mechanism of action of UDCA is

probably related to the reduction of toxic effects of hydrophobic bile acids by a choleretic effect and/or a direct inhibitory effect on bile acid-induced apoptosis of hepatocytes (21).

Even less pharmacotherapeutical options exist for PSC. UDCA appears ineffective and to date no drugs have been identified that show significant therapeutic effects in PSC, except those drugs that provide symptomatic relief of the mainly cholestasis-associated symptoms (22-25).

Drug-induced liver disease, alcoholic and non-alcoholic steatohepatitis

Although the use of certain drugs has been associated with the development of liver fibrosis, most hepatic drug reactions are followed by recovery upon withdrawal of the injurious stimulus, without the occurrence of significant fibrosis. Examples of drugs which have been associated with drug-induced fibrosis are methotrexate, isoniazid, and valproic acid (20;26;27).

Clearly, best known are the detrimental effects of chronic alcohol abuse on the liver. In fact, this drug-induced form of liver fibrosis is the most common cause of cirrhosis in the western world. Chronic exposure to alcohol leads to benign macrovesicular steatosis of the liver in over 90% of alcohol abusers, and generally steatosis will spontaneously resolve upon alcohol abstinence. Nevertheless, in 20-40% of the cases a more severe liver pathology develops as a result of chronic oxidative stress via alcohol metabolites (28). The resulting perivenous infiltration of neutrophils into the fatty liver, typically in combination with ballooning of hepatocytes and the formation of Mallory bodies, is termed alcoholic steatohepatitis (ASH). This is very often accompanied by pericellular fibrosis. Besides alcohol-induced oxidative stress, which results in a cytokine-mediated initiation and perpetuation of the inflammatory and fibrotic process, also antibodies against the ethanol metabolite acetaldehyde, as well as auto-antibodies against alcohol dehydrogenase and CYP2E1 have been implicated in the pathophysiology (20;29). Patients with an acute exacerbation of ASH present with decompensated

liver function, encephalopathy and gastrointestinal bleeding. The one-month survival rate of these patients is only 50% and the survivors of such an exacerbation will generally develop end stage liver cirrhosis within 5 years, despite withdrawal from alcohol use (29).

Non-alcoholic steatohepatitis (NASH) is considered to be the hepatic manifestation of the "metabolic syndrome". The metabolic syndrome is characterized by obesity, insulin resistance and hyperlipidemia and can be considered a typical welfare disease which is the consequence of an unhealthy diet and limited physical activity. The hepatic pathology of NASH is in many ways similar to that of ASH and typical features are ballooning of hepatocytes and lobular inflammation leading to pericellular fibrosis. It is estimated that 10-15% of the patients with NASH will progress to advanced fibrosis and cirrhosis. In the future, NASH may become a more important cause of liver fibrosis because its prevalence is expected to parallel the increase in patients suffering from the metabolic syndrome (20;30).

Currently, weight loss or withdrawal of alcohol or drugs are the main treatments available for patients suffering from NASH, ASH and drug-induced liver fibrosis. If this does not sort any effect and fibrosis still progresses, only symptomatic treatments can be initiated to ensure that the patient survives until a liver transplantation can be performed (28;30).

The hepatic stellate cell in healthy and fibrotic liver

The overview of clinical treatment strategies, given above, shows that the current pharmacological treatment options are not effective in a large percentage of patients, or simply can not be effectively employed because of serious adverse effects. Moreover, most drugs do not affect the perpetuating fibrotic process itself. Additional antifibrotic drugs are therefore urgently needed and, preferably, a pharmacological strategy should become available that can be applied for the attenuation of fibrosis progression of any etiology. Because the hepatic stellate cell

is considered to be the key fibrogenic cell type in the liver, this is an interesting target for the development of drugs that inhibit the fibrotic process itself (1;31;32).

The hepatic stellate cell in the healthy liver

In healthy livers, hepatic stellate cells (HSC) represent approximately 8% of the total number of liver cells present. These cells are localized in the space of Disse and are in close proximity to hepatocytes and hepatic sinusoidal endothelial cells. In Fig. 2 the organization of a hepatic sinusoid is depicted, showing the localization of HSC and other major cell types in the liver.

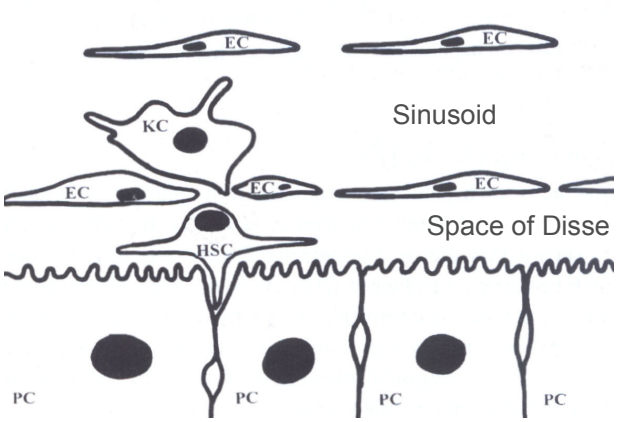

Fig. 2. Schematic representation of the organization of the hepatic sinusoid showing the localization of parenchymal cells (PC), hepatic stellate cell (HSC), Kupffer cell (KC) and sinusoidal endothelial cells (EC) in relation to each other.

The major functions that HSC perform in healthy livers are related to retinol (vitamin A) metabolism and storage, regulation of sinusoidal blood flow by influencing the vascular tone, and regulation of the ECM composition in the space of Disse (33). With respect to retinol metabolism, HSC are responsible for storage of the largest fraction of vitamin A in the body. Of all dietary retinol, 90% is stored in the liver and 75% of this amount is confined within HSC. The high retinol content of HSC results in a positive histochemical goldchloride reaction, and it is with this staining technique by which HSC have initially been identified in tissue

sections of livers (34). Furthermore, the high vitamin A content of HSC compared to other liver cells, allows the isolation of HSC from rat liver by density-gradient-based centrifugation, which enables the possibility of studying this cell type *in vitro* (35;36). The close proximity of HSC to sinusoidal endothelial cells, and the presence of long cytoplasmic processes which surround the endothelial cells, are analogous to that of vascular pericytes. Pericytes are responsible for the regulation of vascular tone in other organs and various studies suggest a similar role for HSC in the liver (37). A third function of HSC in the healthy liver is the maintenance of a correct composition of ECM in the space of Disse. The ECM in the space of Disse in normal livers is of a low-density type, mainly comprising collagen type I, III, IV VI and XVIII, decorin, fibronectin and heparansulphate proteoglycan. The ECM in the space of Disse not only ensures tissue stability, but also has an important role in the regulation of the functions of the various cell types present.

In fibrotic livers the amount of ECM is increased up to 10 fold over that of normal livers. Moreover, the composition of the ECM is different, which in the fibrotic organ consists of larger amounts of the fibrillary collagens I and III. This results in the formation of a high density matrix, which is accompanied by sinusoidal capillarization and loss of hepatocyte microvilli, leading to impaired liver function. The principal cell type in the liver that is responsible for the increased deposition of collagen in the fibrotic liver is the activated hepatic stellate cell (38).

Hepatic stellate cell activation

In response to liver injury, HSC transdifferentiate from a quiescent, vitamin A-storing cell-type into a cell with fibrogenic properties (39). This takes place under the influence of a large number of mediators secreted by multiple liver cell types. Damaged hepatocytes release reactive oxygen intermediates, but also key fibrogenic cytokines or their precursors, such as Transforming Growth Factor-β1 (TGF-β1), Tumor Necrosis Factor-α (TNF-α) , Epidermal Growth Factor (EGF)

and Insulin-like Growth Factor (IGF). These cytokines induce cellular activation in HSC, but also stimulate the secretion of additional inflammatory and fibrogenic cytokines by Kupffer cells (KC) and infiltrated leukocytes. In turn, these cytokines further stimulate HSC activation. Upon activation, HSC themselves begin to produce fibrogenic and inflammatory cytokines. The secretion of TGF-β1, Endothelin-1 (ET-1), Platelet Activating Factor (PAF) and chemotactic factors, such as RANTES and Macrophage Chemotactic Protein-1 (MCP-1), create autocrine and paracrine loops by which the fibrotic process can perpetuate itself (2;31;39).

A typical feature of HSC activation is the increased expression of alpha-smooth muscle actin (α-sma), by which HSC acquire a contractile phenotype. It is believed that HSC contraction in close association with the hepatic sinusoids plays a role in the development of portal hypertension (37). α-sma is considered to be the classical marker for HSC activation, but also other intracellular proteins have been identified to be upregulated upon HSC activation, earlier than α-sma. Examples of these so-called early markers for HSC activation are α-β-crystallin and heat shock protein 47, which are believed to be involved in intracellular collagen transport (40-42).

The synthesis of extracellular matrix proteins by HSC increases upon activation and remodeling of the ECM takes place by the secretion of fibrillary collagens, mainly of type I and III. Also, Tissue Inhibitors of Metalloproteinase (TIMP-1 and TIMP-3) are secreted that additionally inhibit the degradation of newly deposited collagen by Matrix Metalloproteinases (MMPs), thus creating a positive ECM balance. Simultaneously, the secretion of MMPs that degrade the normal low density matrix of the liver is enhanced, resulting in a gradual remodeling of the ECM. During the degradation of normal matrix a number of fibrogenic cytokines are released from it, which further stimulates the remodeling process. In addition, a direct fibrogenic stimulation of HSC has been reported via an interaction of fibrillary collagens with discoidin domain-2 receptors (DDR-2) that are expressed on the cell surface of activated HSC (38;43). In this way another paracrine loop is

created whereby the ECM produced by HSC activates other HSC.

In activated HSC, the receptor expression for certain fibrogenic cytokines on the cell surface is drastically upregulated. Examples of receptors that are upregulated on activated cells, relative to quiescent HSC, are the Platelet Derived Growth Factor-receptor (PDGF-receptor), the Mannose-6-phosphate/Insulin-like growth factor II-receptor (M6P/IGF-II receptor), the ET-1 receptor and many receptors that allow the HSC to interact with the surrounding ECM, an example of which is the collagen VI receptor. The preferential upregulation and presence on the cell surface of activated HSC make them suitable targets for the intracellular delivery of drugs, as will be further discussed below.

Hepatic stellate cell proliferation

HSC proliferation is a prominent feature of fibrogenesis, which occurs mainly under the influence of an isoform of PDGF. This isoform, PDGF-BB, is secreted mainly by Kupffer cells, but in a later stage also by HSC. Many studies show that local proliferation of fibrogenic cells occurs abundantly in experimental liver fibrosis, as well as in human fibrotic livers. Moreover, the profuse expression of PDGF receptors on the interface of fibrotic tissue and functional liver parenchyma suggests that expansion of fibrotic septa occurs mainly by virtue of local HSC proliferation (44-48). In bile duct-ligated rats (BDL), a commonly used animal model for the disease and also the experimental model used in this thesis research, hepatic stellate cell proliferation peaks during the first week after bile duct ligation, in which up to 11% of HSC show proliferative activity. The absolute numbers of activated HSC subsequently reach a plateau 3 weeks after onset of the disease in this animal model, at which point the numbers of α-sma-positive cells have increased more than 10-fold over healthy control animals (49).

Analogy of liver fibrosis with other fibrotic disorders

In fact, the pathophysiological mechanisms described above for liver fibrosis, also take place in other organ systems. Myofibroblast-like cells that fulfill comparable functions to that of the HSC in the fibrotic liver have been identified and extensively characterized in the intestine (intestinal myofibroblast), kidney (mesangial cell, tubulo-interstitial cell), pancreas (pancreatic stellate cell) and blood vessels (vascular smooth muscle cell). Not surprisingly, in the sclerotic and fibrotic processes in these organs, many of the same inflammatory mechanisms, fibrogenic cytokines and cytokine-receptors are involved (50-52).

Experimental drugs inhibiting the fibrotic process itself

Based on the increased understanding of the pathophysiology of liver fibrosis and stellate cell biology, many potential antifibrotic drugs have now been identified (see references (1) and (31) for recent reviews). However, many of them only exert clear effects *in vitro* and fail to act *in vivo*. This can, at least partly, be explained by unfavorable *in vivo* pharmacokinetics of many of these agents, resulting in relatively low and therefore ineffective intracellular drug concentrations within HSC. Another possibility is that the cellular mechanisms through which the drug sorts its effect *in vitro*, turn out to be redundant *in vivo*, and cellular functions are maintained by alternative pathways that are present *in vivo*. There is also a large group of drugs that effectively inhibits liver fibrosis in animal models, but unfortunately displays too many side effects to be applicable in the clinical treatment of liver fibrosis. Examples of such drugs are gliotoxin (non-specific induction of apoptosis in cells), trichostatin A (non-specific histonedeacetylase inhibitor) and the prolyl-4-hydroxylase inhibitors (inhibition of collagen synthesis). Main examples of antifibrotic drugs that have been tested in clinical trials are colchicine (inhibition of collagen synthesis and secretion) and IL-10 (anti-inflammatory action and suppression of collagen synthesis in HSC), but no consistent positive effects could be observed. Moreover, both drugs indeed exert

problematic adverse affects. Currently, ACE inhibitors, angiotensin II blockers and pentoxifylline are being evaluated for their clinical efficacy, but it is clear that drugs with a more specific inhibitory effect on HSC are needed. Table 1 provides an overview of a number of experimental antifibrotic drugs that have been investigated to date. So far, none of the drugs were registered for the treatment of liver fibrosis.

Table 1: Experimental antifibrotic drugs, references are indicated between parentheses.

Drugs with antifibrotic properties *in vitro*	Drugs with antifibrotic effects *in vitro* and in animal models	Drugs tested in a clinical setting
Prostaglandin J2 (53)	Rapamycin (57)	Colchicine (24)
HMG-Co-A reductase inhibitors (54)	Gliotoxin (58)	IL-10 (63)
Trichostatin A (55)	Cariporide (59)	
Pentoxifylline (56)	ACE inhibitors/ AT-II blockers (60)	
	Halofuginone (61)	
	Prolyl-4-hydroxylase inhibitors (62)	

Selective targeting to the HSC

One possible approach to increase intracellular levels of antifibrotic agents in activated HSC *in vivo*, while simultaneously decreasing uptake in non-target tissues, is to selectively deliver these drugs to the HSC. With the recent development of the first generation of HSC-selective drug carriers, this has now become an option (64-66). Generally, these HSC-selective drug carriers consist of a human serum albumin (HSA) core protein to which targeting devices are coupled. These targeting devices are designed to interact with receptors that are preferentially upregulated on the cell surface of activated HSC. To date, drug carriers are available that bind to the M6P/IGF-II receptor, the PDGF-receptor, and the Collagen VI receptor. M6P/IGF-II receptor-specificity is obtained by coupling mannose-6-phosphate groups to the protein backbone, whereas PDGF receptor and

collagen VI receptor-specificity is obtained by coupling receptor-recognizing cyclic peptides to the HSA core. Upon i.v. administration of these proteins to fibrotic rats, 60-70% of the dose accumulated in the liver. Within the liver approximately 70% of the hepatic cells that appeared positive for the constructs after immunohistochemical staining, was also positive for HSC markers. Hepatic uptake and intrahepatic distribution were similar for all carriers, although *in vitro* differences were observed with respect to cellular internalization after binding to the receptor (64-67). The characteristics of these carriers are summarized in table 2.

Table 2: Overview of the characteristics of the available HSC-selective carriers.

HSC-selective carrier	Abbreviation	Target receptor	Internalization after receptor binding
Mannose-6-phosphate modified human serum albumin	M6PHSA	M6P/IGF-IIR	High
Human serum albumin modified with cyclic peptide C*SRNLIDC*	pPB-HSA	PDGF-R	Low
Human serum albumin modified with cyclic peptide C*GRGDSPC*	pCVI-HSA	Collagen VI R	High

Cell-selective delivery of drugs can be achieved by coupling the chosen drug molecules to the protein backbone via covalent conjugation to functional chemical groups in the side chains of amino acids within the protein. After binding of a drug targeting construct to its receptor, the conjugate may remain at the cell surface, or in case of binding to an internalizing receptor, the drug carrier, together with the attached drug, can be taken up by the cell via receptor-mediated endocytosis. By

coupling drugs to the carrier proteins via acid-labile linkers or linkers that can be degraded specifically by lysosomal enzymes, drug release may be obtained intracellularly, whereas the chemical bond between drug and protein remains stable in the circulation. In Fig. 3 this strategy is schematically depicted.

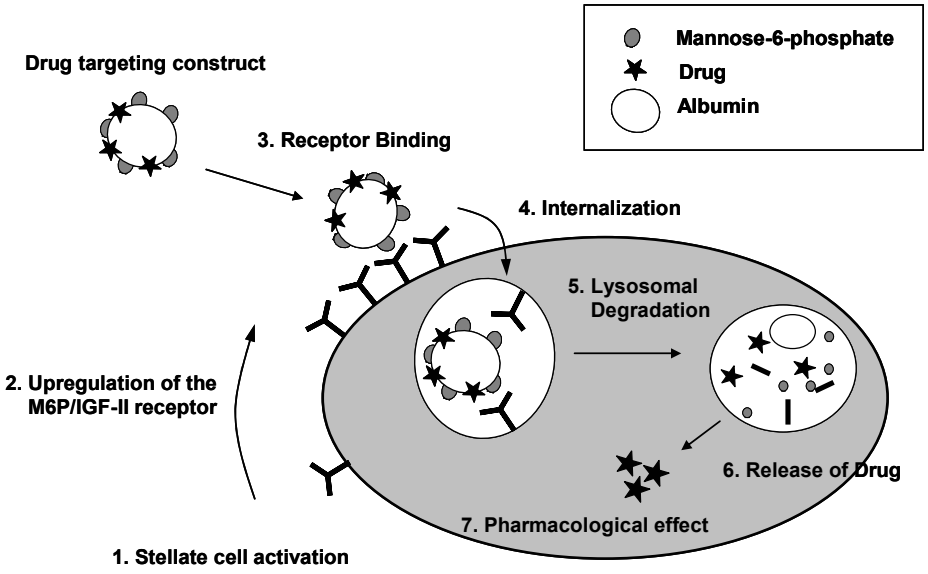

Fig. 3. Schematic representation of the employed targeting strategy.

Especially for M6PHSA, a ligand for the M6P/IGF-II receptor, rapid internalization was found in cultures of HSC. The M6P/IGF-II receptor is a P-type lectin which plays a role in shuttling of proteins to the endosomal compartment within cells. Ten to twenty percent of M6P/IGF-II receptors is expressed on the cell surface in order to facilitate the transport of extracellular lysosomal enzymes to the lysosomes. To date, no signaling functions have been attributed to it, but in fibrogenic cells the M6P/IGF-II receptor is involved in the activation of latent TGF-β into its active form. This physiological role may also explain its preferential upregulation on activated HSC. Furthermore, regulating functions are attributed to the receptor in IGF signaling, by facilitating the lysosomal degradation of this cytokine (68-71).

Alternative targeting strategies

Adrian et al. incorporated M6PHSA into the lipid bi-layer of a liposome, which yielded a liposomal drug targeting preparation that bound to HSC and endothelial cells *in vitro* and, upon administration to fibrotic animals, distributed to the liver, and substantially co-localized with HSC-markers (72). This should make it possible to deliver drugs to HSC by entrapping hydrophilic drugs within the hydrophilic core of the liposome, without having to perform a conjugation reaction between drug and protein. In addition, hydrophobic drugs can be incorporated into the lipid bi-layer of the liposome.

Non-albumin-based drug carriers that target the HSC have been designed as well. Rachmawati et al. studied whether the liver- and HSC-selectivity of IL-10 could be improved by coupling M6P groups directly to the cytokine (73). In addition, Elrick et al. reported a monoclonal human single chain antibody fragment which bound specifically to synaptophysin, a membrane-associated protein in activated HSC. Coupling of a toxin to this carrier resulted in a construct with *in vitro* efficacy, but the *in vivo* organ- and cell-specificity of this construct have yet to be demonstrated (74).

The targeted delivery of genes to the HSC has also been attempted. In an *in vitro* study by Janoschek et al., activated HSC have been successfully transfected with a recombinant, replication-defective adenovirus in which the herpes simplex virus thymidine kinase gene was successfully expressed under control of the TIMP-1 promoter, rendering HSC susceptible for ganciclovir-induced apoptosis (75). *In vivo* studies that describe the efficacy of this gene delivery strategy have, however, not been published yet. One problem of the use of adenoviral vectors for delivering genes to HSC *in vivo* is their preferential uptake by Kupffer cells and hepatocytes. Unpublished results by Schoemaker et al. showed that adenoviral-mediated expression of a transgene by HSC *in vitro* could be enhanced by pre-incubating the virus with a fusion protein recognizing the virus and the PDGF-R. Simultaneously, transfection of hepatocytes could be reduced. Transcriptional

retargeting (i.e. restricting gene expression to target cells by HSC-specific promoters) and transductional retargeting techniques (i.e. HSC-specific targeting of the adenoviral vector) may be combined in the future to increase the HSC-specificity of adenoviral-mediated gene delivery (76).

HSC-selective targeting of antiproliferative drugs: methodology in brief

Because local HSC proliferation is crucial for the formation of fibrotic septa and progression of the fibrotic process, inhibition of HSC proliferation seems a particularly interesting option to inhibit fibrogenesis. To date this intervention has not been extensively tried. The studies described in this thesis explore the use of antiproliferative drugs for the treatment of experimental liver fibrosis in the rat, with special emphasis on the targeted delivery of such drugs to the HSC in order to avoid uptake in non-target tissues and cells.

The a priori selection of suitable drug candidates was based on adherence to the following criteria. First, the drug should have the potential of inhibiting HSC proliferation. Second, the drug should have suitable (physico-)chemical characteristics to allow conjugation to the HSC-selective drug carriers. Third, analytical techniques for the analysis of the drug should be available to allow chemical characterization of the conjugates and bio-analysis in pharmacokinetic studies. In addition, the drug should be available in sufficient amounts to allow chemical characterization of the synthesized constructs, as well as *in vitro* studies and *in vivo* studies in diseased animals. Based on these criteria, the experiments described in this thesis are performed with the antiproliferative drugs mycophenolic acid (MPA) and doxorubicin (DOX). Detailed characteristics of these drugs are discussed in the chapters that describe the experiments performed with them. In view of the molecular targets of MPA (Inosine Monophosphate Dehydrogenase) and DOX (Topoisomerase II, DNA), which are both located intracellularly, a drug carrier was chosen that was internalized after binding to the

receptor. We selected M6PHSA as the most suitable drug carrier for these drugs as previous studies in our lab showed rapid internalization of this carrier.

The *in vitro* evaluation of the developed drug targeting constructs was performed in cultures of 3T3 fibroblasts, an M6P/IGF-II receptor expressing cell-line, as well as cultures of primary isolated rat HSC, the ultimate target cells. These *in vitro* studies served to elucidate whether the synthesized constructs still bound selectively to the fibrogenic cells, and whether pharmacologically active drug was released from the conjugates upon internalization by the target cells. However, the ultimate targeting efficiency and antifibrotic efficacy of HSC-targeted constructs can only be tested in a relevant *in vivo* model of liver fibrogenesis. To this end, we used the rat bile duct ligation model, which is characterized by a quick onset, and subsequent tough and reproducible development of the disease (49).

REFERENCE LIST

1. Pinzani M, Rombouts K, Colagrande S. Fibrosis in chronic liver diseases: diagnosis and management. J Hepatol 2005; 42 Suppl: S22-S36.
2. Friedman SL. Molecular regulation of hepatic fibrosis, an integrated cellular response to tissue injury. J Biol Chem 2000; 275: 2247-50.
3. Cardenas A, Gines P. Management of complications of cirrhosis in patients awaiting liver transplantation. J Hepatol 2005; 42 Suppl: S124-S133.
4. Colombo M, Sangiovanni A. Etiology, natural history and treatment of hepatocellular carcinoma. Antiviral Res 2003; 60: 145-50.
5. Fung SK, Lok AS. Management of patients with hepatitis B virus-induced cirrhosis. J Hepatol 2005; 42 Suppl: S54-S64.
6. Lok AS. Hepatitis B infection: pathogenesis and management. J Hepatol 2000; 32: 89-97.
7. Hardman J, Limbird L, Goodman Gilman A. Goodman and Gilman's the Pharmacological basis of therapeutics, 10th ed, McGraw-Hill publishers, 2001.
8. Hadziyannis SJ, Tassopoulos NC, Heathcote EJ, Chang TT, Kitis G, Rizzetto M, Marcellin P, Lim SG, Goodman Z, Wulfsohn MS, Xiong S, Fry J, Brosgart CL. Adefovir dipivoxil for the treatment of hepatitis B e antigen-negative chronic hepatitis B. N Engl J Med 2003; 348: 800-7.

9. Marcellin P, Chang TT, Lim SG, Tong MJ, Sievert W, Shiffman ML, Jeffers L, Goodman Z, Wulfsohn MS, Xiong S, Fry J, Brosgart CL. Adefovir dipivoxil for the treatment of hepatitis B e antigen-positive chronic hepatitis B. N Engl J Med 2003; 348: 808-16.
10. Dienstag JL, Goldin RD, Heathcote EJ, Hann HW, Woessner M, Stephenson SL, Gardner S, Gray DF, Schiff ER. Histological outcome during long-term lamivudine therapy. Gastroenterology 2003; 124: 105-17.
11. Lau GK, Piratvisuth T, Luo KX, Marcellin P, Thongsawat S, Cooksley G, Gane E, Fried MW, Chow WC, Paik SW, Chang WY, Berg T, Flisiak R, McCloud P, Pluck N. Peginterferon Alfa-2a, lamivudine, and the combination for HBeAg-positive chronic hepatitis B. N Engl J Med 2005; 352: 2682-95.
12. Lai CL, Chien RN, Leung NW, Chang TT, Guan R, Tai DI, Ng KY, Wu PC, Dent JC, Barber J, Stephenson SL, Gray DF. A one-year trial of lamivudine for chronic hepatitis B. Asia Hepatitis Lamivudine Study Group. N Engl J Med 1998; 339: 61-8.
13. Leung NW, Lai CL, Chang TT, Guan R, Lee CM, Ng KY, Lim SG, Wu PC, Dent JC, Edmundson S, Condreay LD, Chien RN. Extended lamivudine treatment in patients with chronic hepatitis B enhances hepatitis B e antigen seroconversion rates: results after 3 years of therapy. Hepatology 2001; 33: 1527-32.
14. Liaw YF, Leung NW, Chang TT, Guan R, Tai DI, Ng KY, Chien RN, Dent J, Roman L, Edmundson S, Lai CL. Effects of extended lamivudine therapy in Asian patients with chronic hepatitis B. Asia Hepatitis Lamivudine Study Group. Gastroenterology 2000; 119: 172-80.
15. Boyer N, Marcellin P. Pathogenesis, diagnosis and management of hepatitis C. J Hepatol 2000; 32: 98-112.
16. Fried MW, Shiffman ML, Reddy KR, Smith C, Marinos G, Goncales FL, Jr., Haussinger D, Diago M, Carosi G, Dhumeaux D, Craxi A, Lin A, Hoffman J, Yu J. Peginterferon alfa-2a plus ribavirin for chronic hepatitis C virus infection. N Engl J Med 2002; 347: 975-82.
17. Everson GT. Management of cirrhosis due to chronic hepatitis C. J Hepatol 2005; 42 Suppl: S65-S74.
18. Brewer GJ, Askari FK. Wilson's disease: clinical management and therapy. J Hepatol 2005; 42 Suppl: S13-S21.
19. Pietrangelo A. Hereditary hemochromatosis--a new look at an old disease. N Engl J Med 2004; 350: 2383-97.
20. Bacon B, Goodman Z, Brunt E. Liver disease in the 21st century: clinico pathologic correlates. Report of the postgraduate course held october 24-25, 2003 by the American Association for the study of Liver Diseases. 2003.

21. Schoemaker MH, Conde dlR, Buist-Homan M, Vrenken TE, Havinga R, Poelstra K, Haisma HJ, Jansen PL, Moshage H. Tauroursodeoxycholic acid protects rat hepatocytes from bile acid-induced apoptosis via activation of survival pathways. Hepatology 2004; 39: 1563-73.
22. Czaja AJ, Bianchi FB, Carpenter HA, Krawitt EL, Lohse AW, Manns MP, McFarlane IG, Mieli-Vergani G, Toda G, Vergani D, Vierling J, Zeniya M. Treatment challenges and investigational opportunities in autoimmune hepatitis. Hepatology 2005; 41: 207-15.
23. Beuers U. Hepatic overlap syndromes. J Hepatol 2005; 42 Suppl: S93-S99.
24. Kaplan MM, Gershwin ME. Primary biliary cirrhosis. N Engl J Med 2005; 353: 1261-73.
25. Cullen SN, Chapman RW. Review article: current management of primary sclerosing cholangitis. Aliment Pharmacol Ther 2005; 21: 933-48.
26. Kaplowitz N. Mechanisms of liver cell injury. J Hepatol 2000; 32: 39-47.
27. Larrey D. Drug-induced liver diseases. J Hepatol 2000; 32: 77-88.
28. Sougioultzis S, Dalakas E, Hayes PC, Plevris JN. Alcoholic hepatitis: from pathogenesis to treatment. Curr Med Res Opin 2005; 21: 1337-46.
29. Tilg H, Diehl AM. Cytokines in alcoholic and nonalcoholic steatohepatitis. N Engl J Med 2000; 343: 1467-76.
30. Wright T, Rockey D. Liver disease: from bench to bedside. Report of the postgraduate course held october 29-30, 2004 by the American Association for the Study of Liver Diseases. 2004.
31. Bataller R, Brenner DA. Liver fibrosis. J Clin Invest 2005; 115: 209-18.
32. Bataller R, Brenner DA. Hepatic stellate cells as a target for the treatment of liver fibrosis. Semin Liver Dis 2001; 21: 437-51.
33. Geerts A. History, heterogeneity, developmental biology, and functions of quiescent hepatic stellate cells. Semin Liver Dis 2001; 21: 311-35.
34. Wake K, Motomatsu K, Senoo H, Masuda A, Adachi E. Improved Kupffer's gold chloride method for demonstrating the stellate cells storing retinol (vitamin A) in the liver and extrahepatic organs of vertebrates. Stain Technol 1986; 61: 193-200.
35. Geerts A, Niki T, Hellemans K, De Craemer D, Van Den Berg K, Lazou JM, Stange G, Van De Winkel M, De Bleser P. Purification of rat hepatic stellate cells by side scatter-activated cell sorting. Hepatology 1998; 27: 590-8.
36. Weiskirchen R, Gressner AM. Isolation and culture of hepatic stellate cells. Methods Mol Med 2005; 117: 99-113.
37. Rockey DC. Hepatic blood flow regulation by stellate cells in normal and injured liver. Semin Liver Dis 2001; 21: 337-49.
38. Schuppan D, Ruehl M, Somasundaram R, Hahn EG. Matrix as a modulator of hepatic fibrogenesis. Semin Liver Dis 2001; 21: 351-72.

39. Eng FJ, Friedman SL. Fibrogenesis I. New insights into hepatic stellate cell activation: the simple becomes complex. Am J Physiol Gastrointest Liver Physiol 2000; 279: G7-G11.
40. Cassiman D, Roskams T, van PJ, Libbrecht L, Aertsen P, Crabbe T, Vankelecom H, Denef C. Alpha B-crystallin expression in human and rat hepatic stellate cells. J Hepatol 2001; 35: 200-7.
41. Lang A, Schrum LW, Schoonhoven R, Tuvia S, Solis-Herruzo JA, Tsukamoto H, Brenner DA, Rippe RA. Expression of small heat shock protein alphaB-crystallin is induced after hepatic stellate cell activation. Am J Physiol Gastrointest Liver Physiol 2000; 279: G1333-G1342.
42. Cassiman D, Libbrecht L, Desmet V, Denef C, Roskams T. Hepatic stellate cell/myofibroblast subpopulations in fibrotic human and rat livers. J Hepatol 2002; 36: 200-9.
43. Olaso E, Ikeda K, Eng FJ, Xu L, Wang LH, Lin HC, Friedman SL. DDR2 receptor promotes MMP-2-mediated proliferation and invasion by hepatic stellate cells. J Clin Invest 2001; 108: 1369-78.
44. Geerts A, Lazou JM, de Bleser P, Wisse E. Tissue distribution, quantitation and proliferation kinetics of fat-storing cells in carbon tetrachloride-injured rat liver. Hepatology 1991; 13: 1193-202.
45. Johnson SJ, Hines JE, Burt AD. Immunolocalization of proliferating perisinusoidal cells in rat liver. Histochem J 1992; 24: 67-72.
46. Ogawa K, Suzuki J, Mukai H, Mori M. Sequential changes of extracellular matrix and proliferation of Ito cells with enhanced expression of desmin and actin in focal hepatic injury. Am J Pathol 1986; 125: 611-9.
47. Burt AD, Robertson JL, Heir J, MacSween RN. Desmin-containing stellate cells in rat liver; distribution in normal animals and response to experimental acute liver injury. J Pathol 1986; 150: 29-35.
48. Jezequel AM, Mancini R, Rinaldesi ML, Ballardini G, Fallani M, Bianchi F, Orlandi F. Dimethylnitrosamine-induced cirrhosis. Evidence for an immunological mechanism. J Hepatol 1989; 8: 42-52.
49. Hines JE, Johnson SJ, Burt AD. In vivo responses of macrophages and perisinusoidal cells to cholestatic liver injury. Am J Pathol 1993; 142: 511-8.
50. Powell DW, Mifflin RC, Valentich JD, Crowe SE, Saada JI, West AB. Myofibroblasts. I. Paracrine cells important in health and disease. Am J Physiol 1999; 277: C1-C9.
51. Schocklmann HO, Lang S, Sterzel RB. Regulation of mesangial cell proliferation. Kidney Int 1999; 56: 1199-207.
52. Zaina S, Nilsson J. Insulin-like growth factor II and its receptors in atherosclerosis and in conditions predisposing to atherosclerosis. Curr Opin Lipidol 2003; 14: 483-9.

53. Li L, Tao J, Davaille J, Feral C, Mallat A, Rieusset J, Vidal H, Lotersztajn S. 15-deoxy-Delta 12,14-prostaglandin J2 induces apoptosis of human hepatic myofibroblasts. A pathway involving oxidative stress independently of peroxisome-proliferator-activated receptors. J Biol Chem 2001; 276: 38152-8.
54. Rombouts K, Kisanga E, Hellemans K, Wielant A, Schuppan D, Geerts A. Effect of HMG-CoA reductase inhibitors on proliferation and protein synthesis by rat hepatic stellate cells. J Hepatol 2003; 38: 564-72.
55. Niki T, Rombouts K, De BP, De SK, Rogiers V, Schuppan D, Yoshida M, Gabbiani G, Geerts A. A histone deacetylase inhibitor, trichostatin A, suppresses myofibroblastic differentiation of rat hepatic stellate cells in primary culture. Hepatology 1999; 29: 858-67.
56. Raetsch C, Jia JD, Boigk G, Bauer M, Hahn EG, Riecken EO, Schuppan D. Pentoxifylline downregulates profibrogenic cytokines and procollagen I expression in rat secondary biliary fibrosis. Gut 2002; 50: 241-7.
57. Zhu J-L, Wu J, Frizell E, Liu S-L, Bashey R, Rubin R, Norton P, Zern MA. Rapamycin inhibits hepatic stellate cell proliferation in vitro and limits fibrogenesis in an in vivo model of liver fibrosis. Gastroenterology 1999; 117: 1198-204.
58. Wright MC, Issa R, Smart DE, Trim N, Murray GI, Primrose JN, Arthur MJ, Iredale JP, Mann DA. Gliotoxin stimulates the apoptosis of human and rat hepatic stellate cells and enhances the resolution of liver fibrosis in rats. Gastroenterology 2001; 121: 685-98.
59. Di Sario A, Bendia E, Taffetani S, Marzioni M, Candelaresi C, Pigini P, Schindler U, Kleemann HW, Trozzi L, Macarri G, Benedetti A. Selective Na+/H+ exchange inhibition by cariporide reduces liver fibrosis in the rat. Hepatology 2003; 37: 256-66.
60. Jonsson JR, Clouston AD, Ando Y, Kelemen LI, Horn MJ, Adamson MD, Purdie DM, Powell EE. Angiotensin-converting enzyme inhibition attenuates the progression of rat hepatic fibrosis. Gastroenterology 2001; 121: 148-55.
61. Pines M, Knopov V, Genina O, Lavelin I, Nagler A. Halofuginone, a specific inhibitor of collagen type I synthesis, prevents dimethylnitrosamine-induced liver cirrhosis. J Hepatol 1997; 27: 391-8.
62. Matsumura Y, Sakaida I, Uchida K, Kimura T, Ishihara T, Okita K. Prolyl 4-hydroxylase inhibitor (HOE 077) inhibits pig serum-induced rat liver fibrosis by preventing stellate cell activation. J Hepatol 1997; 27: 185-92.
63. Nelson DR, Tu Z, Soldevila-Pico C, Abdelmalek M, Zhu H, Xu YL, Cabrera R, Liu C, Davis GL. Long-term interleukin 10 therapy in chronic hepatitis C patients has a proviral and anti-inflammatory effect. Hepatology 2003; 38: 859-68.

64. Beljaars L, Molema G, Weert B, Bonnema H, Olinga P, Groothuis GM, Meijer DK, Poelstra K. Albumin modified with mannose 6-phosphate: A potential carrier for selective delivery of antifibrotic drugs to rat and human hepatic stellate cells. Hepatology 1999; 29: 1486-93.
65. Beljaars L, Molema G, Schuppan D, Geerts A, de Bleser PJ, Weert B, Meijer DK, Poelstra K. Successful targeting to rat hepatic stellate cells using albumin modified with cyclic peptides that recognize the collagen type VI receptor. J Biol Chem 2000; 275: 12743-51.
66. Beljaars L, Weert B, Geerts A, Meijer DK, Poelstra K. The preferential homing of a platelet derived growth factor receptor-recognizing macromolecule to fibroblast-like cells in fibrotic tissue. Biochem Pharmacol 2003; 66: 1307-17.
67. Beljaars L, Olinga P, Molema G, de Bleser P, Geerts A, Groothuis GM, Meijer DK, Poelstra K. Characteristics of the hepatic stellate cell-selective carrier mannose 6-phosphate modified albumin (M6P(28)-HSA). Liver 2001; 21: 320-8.
68. de Bleser PJ, Jannes P, van Buul-Offers SC, Hoogerbrugge CM, van Schravendijk CF, Niki T, Rogiers V, van den Brande JL, Wisse E, Geerts A. Insulinlike growth factor-II/mannose 6-phosphate receptor is expressed on CCl4-exposed rat fat-storing cells and facilitates activation of latent transforming growth factor-beta in cocultures with sinusoidal endothelial cells. Hepatology 1995; 21: 1429-37.
69. de Bleser PJ, Scott CD, Niki T, Xu G, Wisse E, Geerts A. Insulin-like growth factor II/mannose 6-phosphate-receptor expression in liver and serum during acute CCl4 intoxication in the rat. Hepatology 1996; 23: 1530-7.
70. Scharf JG, Knittel T, Dombrowski F, Muller L, Saile B, Braulke T, Hartmann H, Ramadori G. Characterization of the IGF axis components in isolated rat hepatic stellate cells. Hepatology 1998; 27: 1275-84.
71. Dahms NM, Hancock MK. P-type lectins. Biochim Biophys Acta 2002; 1572: 317-40.
72. Adrian J, Poelstra K, Scherphof G, Molema G, Meijer D, Reker-Smit C, Morselt H, Kamps J. Interaction of targeted liposomes with primary cultured hepatic stellate cells: involvement of multiple receptor systems, J Hepatol, 2006, in press
73. Rachmawati H, Beljaars L, Reker-Smit C, Loenen-Weemaes AM, Hagens WI, Meijer DK, Poelstra K. Pharmacokinetic and biodistribution profile of recombinant human interleukin-10 following intravenous administration in rats with extensive liver fibrosis. Pharm Res 2004; 21: 2072-8.
74. Elrick LJ, Leel V, Blaylock MG, Duncan L, Drever MR, Strachan G, Charlton KA, Koruth M, Porter AJ, Wright MC. Generation of a monoclonal human single chain antibody fragment to hepatic stellate cells--a potential mechanism for targeting liver anti-fibrotic therapeutics. J Hepatol 2005; 42: 888-96.

75. Janoschek N, van de LE, Gressner AM, Weiskirchen R. Induction of cell death in activated hepatic stellate cells by targeted gene expression of the thymidine kinase/ganciclovir system. Biochem Biophys Res Commun 2004; 316: 1107-15.
76. Rots MG, Curiel DT, Gerritsen WR, Haisma HJ. Targeted cancer gene therapy: the flexibility of adenoviral gene therapy vectors. J Control Release 2003; 87: 159-65.

3

MANNOSE-6-PHOSPHATE/INSULIN-LIKE GROWTH FACTOR-II RECEPTORS MAY REPRESENT A TARGET FOR THE SELECTIVE DELIVERY OF MYCOPHENOLIC ACID TO FIBROGENIC CELLS

Rick Greupink
Hester I. Bakker
Harry van Goor
Martin de Borst
Leonie Beljaars
Klaas Poelstra

Pharmaceutical Research, in press

ABSTRACT

The insulin-like growth factor axis plays an important role in fibrogenesis. However, little is known about mannose-6-phosphate/Insulin-like growth factor-II receptor (M6P/IGF-IIR) expression during fibrosis. When expressed preferentially on fibrogenic cells, this receptor may be used to selectively deliver drugs to these cells. We investigated M6P/IGF-IIR expression in livers of bile duct-ligated (BDL) rats and in renal vascular walls of renin transgenic TGR(mRen2)27 rats. Both models are characterized by fibrogenic processes. Furthermore, we studied whether drug delivery via M6P/IGF-II-receptor-mediated uptake is possible in fibroblasts. M6P/IGF-IIR mRNA expression was investigated 3, 7 and 10 days after BDL. At all time-points hepatic M6P/IGF-IIR expression was significantly increased compared to healthy controls. Moreover, immunohistochemical staining revealed that α-sma-positive cells were M6P/IGF-IIR-positive. In kidneys of TGR(mRen2)27 rats, the number of M6P/IGF-IIR-positive arteries per microscopic field was increased 5.5 fold over healthy controls. To examine whether M6P/IGF-IIRs could be used as a port of entry for drugs, we coupled mycophenolic acid (MPA) to mannose-6-phosphate-modified human serum albumin (M6PHSA). M6PHSA-MPA inhibited 3T3-fibroblast proliferation dose-dependently, which was reversed by co-incubation with excess M6PHSA, but not by HSA. M6P/IGF-IIRs are expressed by fibrogenic cells and may be used for receptor-mediated intracellular delivery of the antifibrogenic drug MPA.

INTRODUCTION

Fibrotic processes are characterized by an excessive deposition of extracellular matrix proteins and proliferation of fibroblasts in response to chronic tissue injury. Liver fibrosis and fibrotic vascular lesions (atherosclerosis, hypertension-induced vascular thickening) are examples of these disorders and many similarities exist between the processes (1). Both diseases are characterized by the activation of cells from the fibroblast-lineage, which are present in a resting state within healthy tissue. Within the liver, it is the hepatic stellate cell (HSC) that plays a central role in the initiation and perpetuation of fibrosis (2). Quiescent HSC transform into proliferating, α-sma-positive, collagen-producing cells after activation. In analogy to the HSC within the liver, in fibrotic vascular lesions vascular smooth muscle cells differentiate from a quiescent phenotype into a secretory and migrating cell type. This is also accompanied by a proliferation of these cells, associated with a narrowing of the vascular lumen (3-5).

Experimental pharmacological treatments therefore focus on the inhibition of proliferation of fibroblasts or vascular smooth muscle cells. Mycophenolic acid (MPA) is a drug with antiproliferative properties in fibroblast-like cells (6;7). The antiproliferative effect of MPA is the result of a depletion of guanine nucleotides via a non-competitive inhibition of inosine monophosphate dehydrogenase (IMPDH) type II. This enzyme catalyzes the conversion of inosine-5'-monophosphate into xanthine-5'-monophosphate, which is the first and rate-limiting step in de novo guanosine synthesis (8;9). In vascular lesions characterized by vascular smooth muscle cell proliferation, such as atherosclerosis and in-stent restenosis, beneficial effects of MPA have been reported via a direct effect on vascular smooth muscle cells (10;11). More recently, data from our group showed that MPA is capable of inhibiting the proliferation of cultured hepatic stellate cells, as well (12). Hence, patients with fibrosis in various organs may benefit from treatment with MPA. However, because MPA also is a potent immunosuppressive

drug, systemic application of MPA would lead to immunosuppressive effects (8). Although immunosuppression may be very useful, for instance in patients that underwent organ transplantation, it can be considered a side effect in patients with liver fibrosis or fibrotic lesions of the renal vasculature. In these latter cases, no systemic immunosuppression is required. On the contrary, it will increase their risk for developing viral and bacterial infections and in case of a viral hepatitis-induced fibrosis will lead to a flare up of the virus infection (13). Moreover, a suppression of certain T cell subsets may even aggravate fibrosis (14-16). In addition, attenuation of fibroblast proliferation should occur locally, without interfering with this common process in healthy organs. A targeted delivery of MPA to proliferating cells may avoid these matters, while at the same time the antiproliferative effect of MPA is enhanced in fibrogenic cells.

In isolated, culture-activated HSC there is evidence that the mannose-6-phosphate/Insulin-like growth factor-II receptor (M6P/IGF-IIR) is upregulated (17; 18). Also, after acute liver damage due to a single CCl_4 administration to rats, enhanced M6P/IGF-II receptor expression has been documented (19). Therefore, this receptor may be used as a target receptor for drug targeting strategies and indeed we have shown that coupling mannose-6-phosphate (M6P) groups to human serum albumin (HSA) leads to selective accumulation of this modified albumin in HSC (20). However, when designing an effective pharmacological therapy based on receptor-mediated drug targeting principles, it is pivotal to know at which time points the M6P/IGF-II receptor is expressed during ongoing experimental liver fibrosis *in vivo*. Additionally, if the M6P/IGF-II receptor is also over-expressed in blood vessels that are at risk for fibrotic vascular lesions, this strategy may also be applied to treat this disease. Yet, to our knowledge M6P/IGF-II receptor expression has not been investigated with respect to this.

In the present study, we therefore explored the time-course of M6P/IGF-II receptor expression during experimental liver fibrosis, induced by ligation of the common bile duct. In addition, we investigated whether this receptor is expressed

in the renal vasculature of homozygous TGR(mRen2) rats, that display enhanced DNA synthesis in vascular smooth muscle cells and exhibit mild thickening of renal capillary walls (21;22). Furthermore, we studied whether delivery of MPA to M6P/IGF-II receptor-expressing fibroblasts is possible via receptor-mediated uptake *in vitro*, and whether this leads to pharmacological effects within these cells.

MATERIALS AND METHODS

Experimental animals

Liver fibrosis was induced in male Wistar rats (220-240g, Harlan, Horst, The Netherlands) by ligation of the common bile duct according to standard procedures (20). The resulting fibrotic process in the liver is characterized by increased proliferation of bile duct epithelial cells, which are surrounded by collagens, mainly of type I and III and increased numbers of α-sma-positive cells (23). Livers were harvested 3, 7 and 10 days after surgery and were frozen in isopentane at –80 °C. The livers from healthy animals served as controls.

Kidneys from 11-week old, male homozygous Ren2 transgenic rats (Max Delbrueck Centre for Molecular Medicine, Berlin, Germany) were used to study receptor expression in the renal vasculature. These transgenic animals are characterized by an increased activity of the renin angiotensin system and vascular hypertrophy (21;22). Kidneys from age-matched male Sprague-Dawley rats (Max Delbrueck Centre for Molecular Medicine) were used as controls.

The animals had free access to tap water and standard lab chow. All experiments were approved by the local committee for care and use of laboratory animals and were performed according to strict governmental and international guidelines for the use of experimental animals.

Immunohistochemical staining procedures

Cryostat liver and kidney sections of 4 µm thickness were prepared, and after acetone fixation the sections were stained according to standard indirect immunohistochemical techniques. The presence of M6P/IGF-II receptor was demonstrated with a goat polyclonal antibody purchased from Santa Cruz Biotechnology, Santa Cruz, CA and immunohistochemical staining for α-smooth muscle actin (α-sma) was performed with a mouse monoclonal antibody obtained from Sigma, Gillingham, UK.

RT-PCR and gel electrophoresis

RNA isolation from whole liver and kidney samples and the synthesis of cDNA were performed according to standard procedures. To assess the expression levels of M6P/IGF-II receptor mRNA relative to GAPDH, reverse transcriptase PCR was performed using the following primers in a concentration of 50 µM. FW 5'-GTGTCCTCTGGGTGTGGACT, RV 5'-CTCCTCCTTGCTGACCTTTG (M6P/IGF-IIR); FW 5'-GCTGGTGCTGAGTATGTCG, RV 5'-CTGTGGTCATGAGCCCTTCC (GAPDH). After the PCR reaction, products were run on a 2% agarose gel, at 90V charge over a period of 45 minutes, and the bands were subsequently quantified by image analysis.

Synthesis and characterization of the M6P-constructs

The synthesis of M6PHSA was performed as described earlier (20). The characterization of this neo-glycoprotein was done by analysis of mannose-, phosphate- and protein content of the construct according to standard procedures (20). MPA (Sigma) was coupled to M6PHSA via an ester bond by activation with 2-iodoethanol. To 20 mg of MPA dissolved in 800 µl of dichloromethane (Merck, Darmstadt, Germany), 20 µl of $SOCl_2$ (Sigma) and 0.4 µl of dimethylformamide (Merck) were added and stirring was maintained at room temperature for 5 hours.

The reaction mixture was evaporated to dryness, redissolved in 800 µl of dichloromethane and reacted with 200 µl of 2-iodoethanol (Sigma) for 90 minutes on ice, protected from light. The 2-iodoethanol ester of MPA was separated from the excess of 2-iodoethanol by elution of the reaction mixture with dichloromethane:acetone:acetonitrile = 8:1:1 on a Silica G column (Merck). The identity of the reaction product was confirmed by mass spectrometry. MPA-2-iodoethanol ester was coupled to the sulfhydryl groups of M6PHSA which were incorporated via S-acetylthioglycolic acid N-hydroxysuccinimide ester derivatization (SATA, Sigma) according to Duncan et al. (24). The reaction mixture was purified by filtration and dialysis against water, subsequently freeze dried and stored at -20 ºC. The drug:protein ratio was assessed by HPLC using a Zorbax SB-AQ 3.5 µm; 4.6x150 mm column (Agilent technologies, USA), after hydrolysis of the ester bond between MPA and the carrier at pH=12. Samples were eluted with acetonitrile:PBS = 25:75, flow 1.0 ml/min and detected with a Waters UV detector (model 441) at 254 nm. Protein content was assessed by the Biorad protein assay. Drug loading was then calculated by determination of the molar ratio of MPA to protein. The monomeric protein content was assessed by size exclusion chromatography on an FPLC HR 10/30 Superdex 200 column.

Culture of 3T3-fibroblasts

NIH/3T3-fibroblasts were cultured at 37 °C in Dulbecco's modified Eagles Medium (Biowithaker, Verviers, Belgium) containing 5% FCS, supplemented with 100 U/ml penicillin, 100 µg/ml streptomycin and 2 mM L-glutamine (Gibco, Paisley, UK). One day prior to proliferation experiments, cells were seeded in 96-well plates at a density of 5000 cells/well.

Effects on cell proliferation

The effect of test compounds on cell proliferation was assessed in 3T3-fibroblasts, and was measured by bromodeoxyuridine (BrdU)-incorporation assays,

using standard ELISA techniques. During proliferation experiments, 3T3-fibroblasts were cultured in the described medium, supplemented with 10 μM BrdU and treated with MPA, HSA, M6PHSA, M6PHSA-MPA or vehicle for 4 hours. In competition experiments, 120 μg/ml of the conjugate was co-incubated for 4 hours with M6PHSA or HSA (1 mg/ml) to establish whether the effect of the (targeted) drug could be inhibited by an excess of receptor ligand.

Effects on cell viability

Cell viability of 3T3-fibroblasts was assessed by the Alamar Blue assay for mitochondrial activity according to the instructions of the manufacturer (Serotec, Kidlington, UK). Cells were seeded in 96-well plates as described above, and were incubated with MPA and Alamar Blue simultaneously for 4 hours. Alamar Blue conversion was measured fluorimetrically at an excitation wavelength of 560 nm and an emission wavelength of 590 nm.

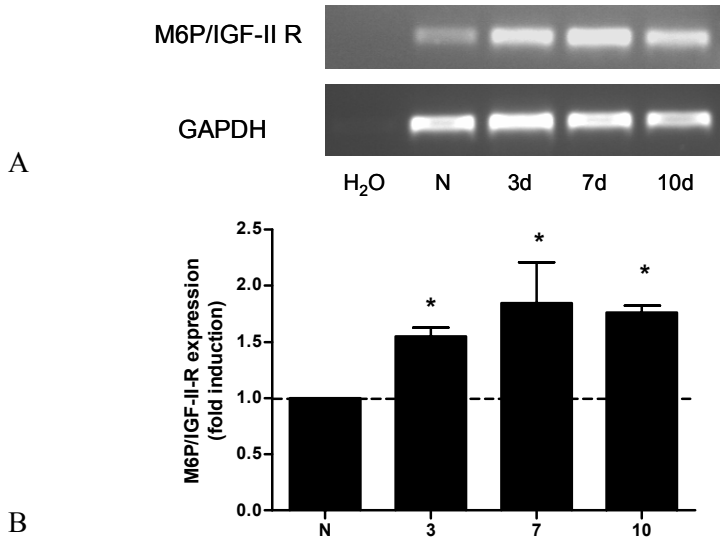

Fig. 1. A: Expression of M6P/IGF-IIR mRNA in livers of normal livers (N) and livers of BDL rats at 3, 7 and 10 days after BDL. B: Quantification of the mRNA expression, using image analysis. Data represent the average of 3 animals ± SD. * indicates $P < 0.05$.

Statistical analysis

Data were expressed as the average ± SD and subjected to a two-tailed Student's t-test. When multiple means were compared, one-way analysis of variance was performed, followed by the LSD post-hoc test. Differences were considered statistically significant at $P<0.05$.

RESULTS

M6P/IGF-IIR expression in the liver after BDL

RT-PCR analysis of liver specimens revealed that M6P/IGF-IIR mRNA expression in the livers was already increased during the early stages after bile duct ligation. At 3, 7 and 10 days after BDL, mRNA expression in the livers increased to 1.5 ± 0.2, 1.8 ± 0.4 and 1.8 ± 0.1 fold over control, respectively (Fig. 1; $P< 0.05$).

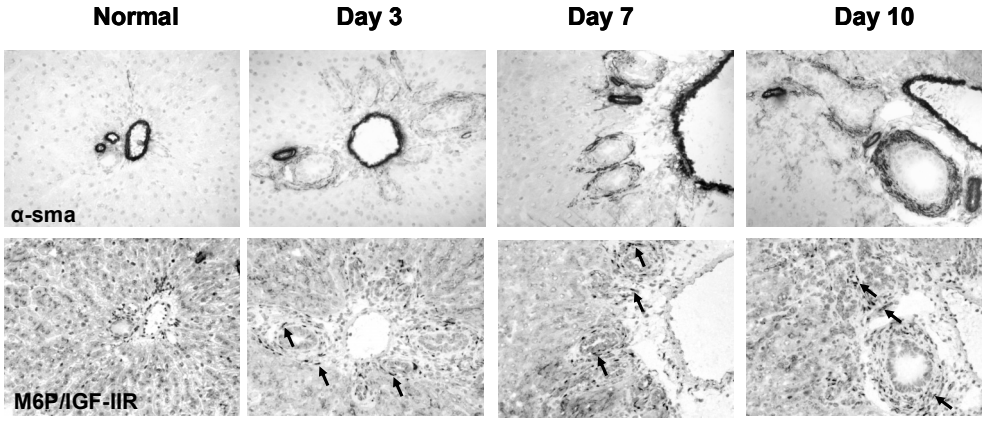

Fig 2. Representative microphotographs of sequential sections of rat livers, stained for the myofibroblast marker α-sma and for the presence of M6P/IGF-II receptor in normal liver and at day 3, 7 and 10 after BDL (original magnification 200x). Arrows indicate the M6P/IGF-II receptor-positive non-parenchymal cells (a full color version of this figure can be found in the appendix).

Immunohistochemical staining of liver sections revealed that cells with spindle-shaped nuclei, which were mainly found around the proliferating bile duct epithelial cells, clearly stained positive for the M6P/IGF-II receptor. In order to verify the specificity of the observed staining, we co-incubated the antibody with a blocking peptide prior to application to the sections. This procedure completely abolished staining, confirming the M6P/IGF-IIR specificity of the procedure. Immunohistochemical analysis of consecutive sections for α-sma revealed that the M6P/IGF-II receptor-expressing cells were also positive for this myofibroblast marker. Besides expression in the non-parenchymal α-sma-positive cells, the M6P/IGF-II receptor could also be detected in hepatocytes of both healthy livers and livers from bile duct-ligated rats (Fig. 2).

M6P/IGF-IIR expression in vessels of TGR(mRen2)27 rats

Immunohistochemical staining of cryostat sections of kidney for the M6P/IGF-IIR revealed that in Ren2 transgenic rats, the receptor expression in the arterial vessel walls was increased compared to SD controls (Fig. 3A). To quantify this, the number of M6P/IGF-II receptor-positive vessels was counted per microscopic field and related to the total number of arteries that were identified by staining for α-sma. Results showed an increase from 0.8 ± 0.4 M6P/IGF-II-positive arteries in controls to 4.4 ± 1.3 in transgenic animals, a 5 fold induction (Fig. 3B). The presence of the receptor was demonstrated in glomeruli and tubular epithelial cells. Although in glomeruli no differences between control and Ren2 rats could be observed with respect to receptor expression, within tubular epithelial cells, M6P/IGF-IIR staining appeared to be reduced in Ren2 animals. Evaluation of M6P/IGF-IIR mRNA expression levels in whole kidney samples revealed no significant differences between normal and Ren2 rats (Fig. 3C).

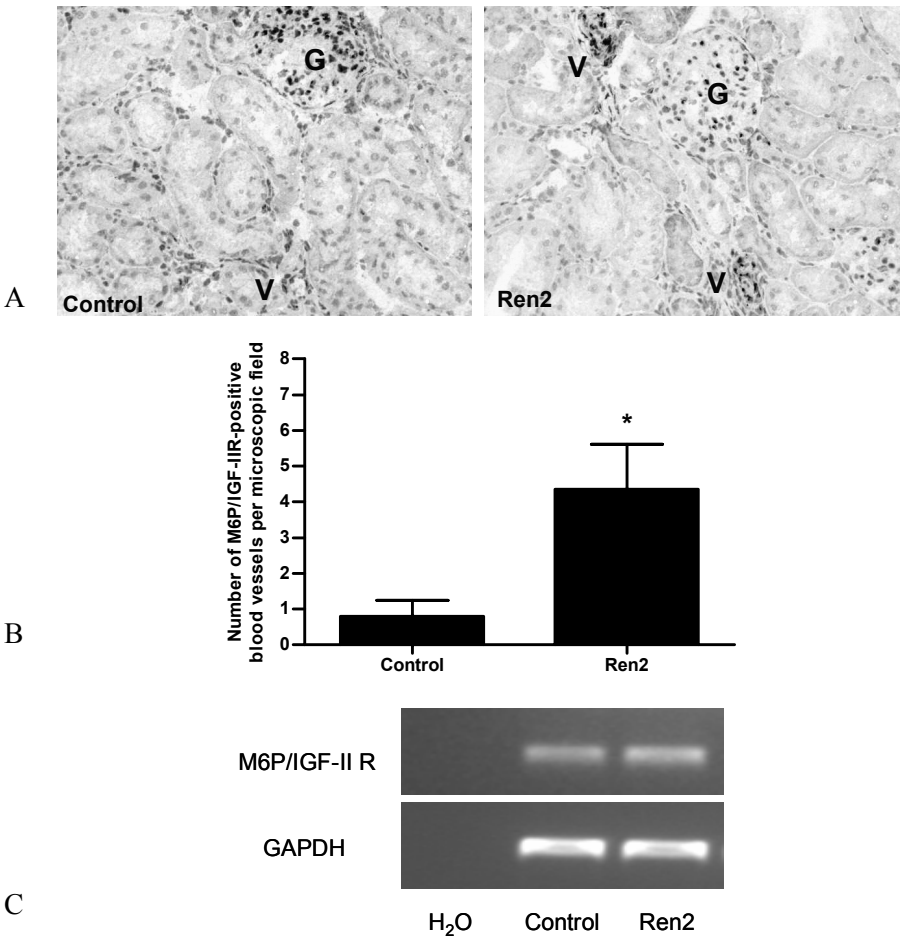

Fig. 3A: Representative microphotographs of kidney sections stained for M6P/IGF-IIR. G = glomerulus, V = blood vessel (Original magnification 200x, a full color version of this figure can be found in the appendix). B: Quantification of the number of M6P/IGF-IIR-positive blood vessels per microscopic field, counted at a magnification of 100x. Data represent the average ± SD of 5 animals per group. * indicates $P<0.05$. C: No significant differences could be observed in M6P/IGF-IIR mRNA expression between Ren2 rats and SD controls (at least 4 animals per group).

Synthesis and characterization of M6P constructs

Mannose-6-phosphate was successfully coupled to HSA. Assays for the amounts of sugar, phosphate and protein showed that a total of 29 mannose-6-phosphate groups were coupled per HSA core protein. After conjugation of MPA

and subsequent purification, HPLC-analysis revealed that coupling of MPA to M6PHSA resulted in a drug to protein ratio of 0.4:1. This low coupling ratio was the result of a relatively inefficient reaction between the 2-iodoethanolester of MPA and the –SH groups on the protein backbone, which could not be enhanced. Still, drug loading was sufficient for pharmacological evaluation of the targeting concept. FPLC analysis showed that more than 70% of the total amount of the protein was present in the monomeric form.

A

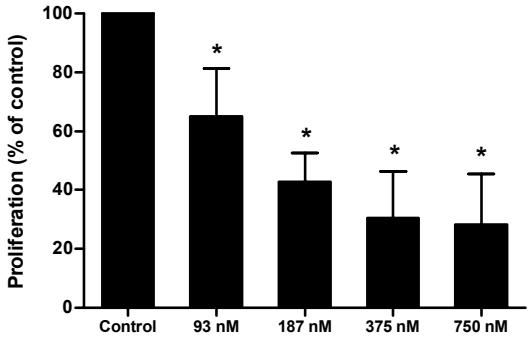

B

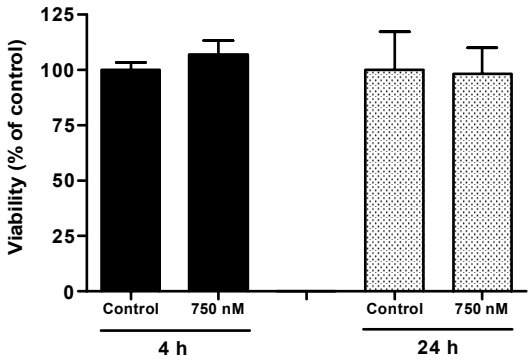

Fig 4. Effect of 4 hour incubations with increasing concentrations of MPA on the BrdU-incorporation in cultures of 3T3-fibroblasts (A). MPA decreases the proliferation of these cells dose-dependently, whereas cell viability is not affected after 4 or 24 hr incubation with MPA (B). The data represent the average ± SD of 3 independent experiments. * indicates $P<0.05$ compared to control.

Pharmacological effect of MPA on fibroblasts

Immunohistochemical staining of 3T3-fibroblasts revealed that this cell type expressed the M6P/IGF-II receptor (data not shown). In fig. 4A, the effect of MPA in cultures of 3T3-fibroblasts is shown. The drug affected fibroblast proliferation in a dose-dependent manner, inhibiting BrdU-incorporation by 72 ± 17% at a concentration of 750 nM after 4 hours of incubation. Cell viability, as assessed by measurement of mitochondrial activity with the Alamar Blue assay, was not affected (Fig. 4B) and also cell morphology, as assessed with a phase contrast microscope, was similar to vehicle-treated control cultures.

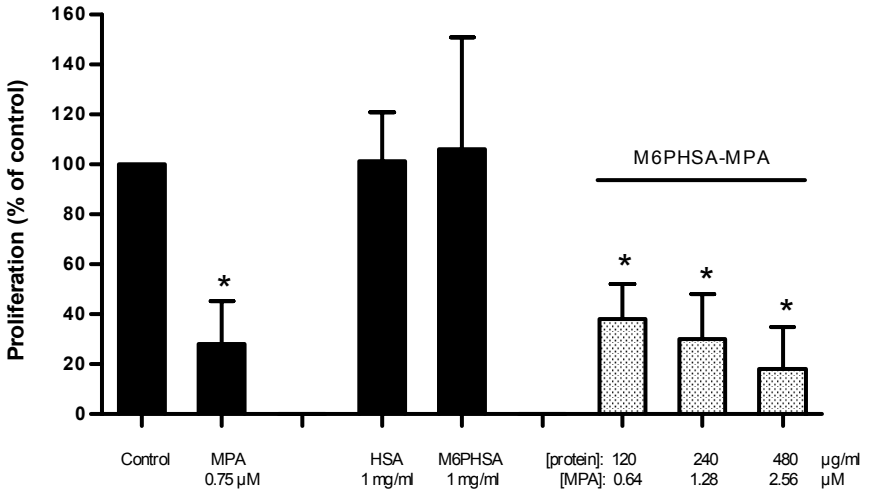

Fig 5. The effect of M6PHSA-MPA on the proliferation of 3T3-fibroblasts. Note that M6PHSA-MPA induces a dose-dependent decrease in BrdU-incorporation, whereas HSA and M6PHSA do not inhibit cell proliferation. The effect of free MPA is shown as a reference. Data represent the average ± SD of at least 3 independent experiments. * indicates $P<0.05$ compared to control.

Pharmacological effect of M6PHSA-MPA on fibroblasts

In fig. 5 it can be seen that increasing concentrations of the conjugate inhibited BrdU-incorporation in cultures of 3T3-fibroblasts in a dose dependent manner. BrdU-incorporation was inhibited by 82 ± 17 % at the highest concentration of 480

µg/ml M6PHSA-MPA, which corresponds to 2.56 µM MPA ($P<0.05$). HSA and M6PHSA alone did not affect cell division at all.

Competition experiments

To assess whether the M6PHSA-MPA construct is specifically internalized by receptors, the effect of M6PHSA, as a competitive receptor ligand, on the antiproliferative action of M6PHSA-MPA was tested. In fig. 6 it is shown that an excess of M6PHSA strongly reduced the effect of the conjugate ($P<0.05$) whereas HSA alone had no significant effect. This excess of M6PHSA did not influence the effect of free MPA (data not shown). These experiments indicate that the effect of M6PHSA-MPA is the result of drug release after receptor-mediated uptake of the conjugate.

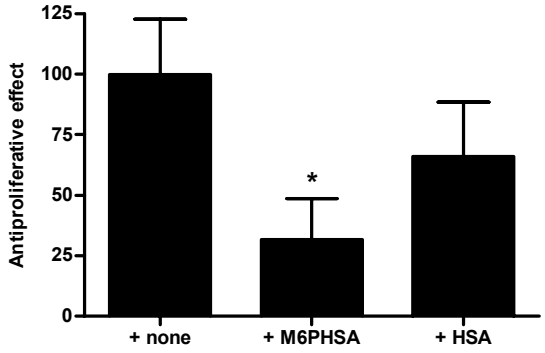

Fig 6. The effect of co-incubation of M6PHSA-MPA (120 µg/ml) with 1 mg/ml M6PHSA or 1 mg/ml HSA. It can be seen that M6PHSA reduces the effect of the conjugate significantly whereas HSA has no significant effect (all groups n=3). * indicates $P<0.05$ compared to control.

DISCUSSION

In this paper we show that the M6P/IGF-II receptor is upregulated already in the early stages after bile duct ligation and increased expression is also found in renal blood vessels of homozygous Ren2 transgenic rats. This is in line with reports that show that the insulin-like growth factor axis plays an important role in

development of liver fibrosis and the development of fibrotic vascular lesions (25-29). Although the role of the IGF-axis in fibrogenesis is generally accepted, to our knowledge no reports exist that describe M6P/IGF-II receptor expression and upregulation in an early stage in the animal models that we investigated. In both animal models the receptor is present on cells with spindle-shaped nuclei, which both are α-sma-positive, two typical features of fibroblast-like cells and vascular smooth muscle cells.

The M6P/IGF-II receptor plays a role in the shuttling of proteins to the early and late endosomes (30). In line with this, the receptor is also found in hepatocytes and in tubular epithelial cells. Importantly, previous studies from our group showed no binding of M6PHSA at all to these cells after iv administration of the protein, whereas a co-localization with markers for hepatic stellate cells was clearly notable (20). This indicates that M6P/IGF-II receptors on the cell surface of fibroblasts are accessible, but M6P/IGF-II receptors within hepatocytes are not accessible for iv administered M6P-containing proteins.

The physiological function of M6P/IGF-II receptor upregulation during fibrosis is still unclear. In contrast to the IGF-I receptor, the M6P/IGF-II receptor has no well described signaling function upon binding of insulin-like growth factor. However, it can regulate local levels of insulin-like growth factor by binding and subsequent lysosomal degradation (30). In addition, M6P/IGF-II receptor-mediated cleavage of latent TGF-beta into the active profibrogenic cytokine has been reported in cultures of activated HSC. This would allow activation of this potent fibrogenic cytokine in the direct surroundings of cells of the fibroblast lineage (31). Moreover, with respect to the vascular pathology that develops in renin transgenic rats, and the recent understanding that angiotensin II plays an important role in liver fibrosis as well (32), it is of note that pro-renin can also bind to M6P/IGF-II receptors (33; 34). The early upregulation of M6P/IGF-II receptor expression on HSC and vascular smooth muscle cells in Ren2 and BDL rats may therefore also point to a role of this receptor in the regulation of renin levels in the direct vicinity

of these cells during fibrogenesis, thus indirectly influencing local angiotensin II levels.

Although a clearly enhanced staining for M6P/IGF-II receptors was found by using immunohistochemical methods in fibrotic livers as well as in renal arteries, mRNA levels for this receptor were only increased in liver samples and not in kidney samples. This is probably related to the fact that M6P-IGF-IIR expression in the kidney is only very locally enhanced so that these local changes can not be clearly measured against the background of the expression levels of the surrounding tubular epithelial cells.

As an *in vitro* model for the testing of drug targeting preparations directed to cells that express the M6P/IGF-II receptor, we used 3T3-fibroblasts (35). The sensitivity of this cell-line to treatment with MPA described here, confirms a previous report. This report demonstrated that high concentrations of MPA in cultures of 3T3 cells resulted in cytotoxicity, mainly in proliferating cells (36). We now show that MPA affects cell proliferation at low concentrations without significant loss of cell viability. Using this model system, we demonstrated that our M6PHSA-MPA conjugate inhibits fibroblast proliferation dose-dependently (Fig. 5). Furthermore, data from competition experiments indicated that the effect of M6PHSA-MPA is mediated by receptor-mediated endocytosis, a process which can be saturated by competitive ligands. M6PHSA attenuated the anti-proliferative effect of MPA-constructs significantly, in contrast to HSA itself (Fig. 6), indicating that the effect of this MPA-construct is mediated by receptors that recognize M6P-ligands, most likely M6P/IGF-II receptors. This *in vitro* finding provides a basis for the effective targeting *in vivo*, since it shows that passive diffusion, which is the major mechanism by which MPA accumulates in leukocytes and other non-target cells, is now largely disqualified. In addition, the rapid metabolism of MPA in hepatocytes after systemic injection (37) would also be prevented by the delivery of pharmacologically active MPA to fibrogenic cells. The current observations support and extend previous data from our lab on the binding and uptake of ^{125}I-

labeled M6PHSA-MPA in cultures of rat HSC (12).

We did not measure the release of native MPA from the carrier within target cells. However, the fact that a pharmacological effect was found suggests that this is the case. In a previous study we showed that MPA, which was conjugated via an acid-stable amide bond to the drug carrier, did not exert any antiproliferative effect (12). This strengthens the notion that MPA must be released from the carrier in its native form in order to exert its growth-inhibiting properties.

The feasibility of using M6P/IGF-IIR-mediated uptake for the selective intracellular delivery of therapeutic modalities is further exemplified by a paper written by the group of Sly (38). They demonstrated that it is possible to enhance the lysosomal delivery of human β-glucuronidase into fibroblasts in a murine model for mucopolysaccharidosis by fusing the enzyme at its C-terminus with an M6P/IGF-IIR-recognizing peptide. In addition to M6P/IGF-IIR targeting, data from our group indicate that targeting of the Platelet Derived Growth Factor receptor or collagen VI receptor also holds promise for the selective delivery of drugs to fibrogenic cells (39; 40).

In conclusion: the M6P/IGF-II receptor is upregulated on fibroblast-like cells in fibrotic livers in an early stage after bile duct ligation and in renal vascular walls of homozygous Ren2 transgenic rats. It may also provide a relevant port of entry for antifibrogenic drugs, thus enabling selective drug delivery to pathogenic cells at an early stage of fibrotic diseases.

ACKNOWLEDGEMENTS

This study was financially supported by the Dutch Foundation for Technical Sciences (STW), grant no GFA.5460. Prof. D.K.F. Meijer is gratefully acknowledged for valuable scientific discussion and review of the manuscript.

REFERENCES

1. D. W. Powell, R. C. Mifflin, J. D. Valentich, S. E. Crowe, J. I. Saada, and A. B. West. Myofibroblasts. I. Paracrine cells important in health and disease, Am. J. Physiol, 277:C1-C9 (1999).
2. S. L. Friedman. Molecular regulation of hepatic fibrosis, an integrated cellular response to tissue injury, J. Biol. Chem., 275:2247-2250 (2000).
3. M. N. Babapulle and M. J. Eisenberg. Coated stents for the prevention of restenosis: Part I, Circulation, 106:2734-2740 (2002).
4. M. N. Babapulle and M. J. Eisenberg. Coated stents for the prevention of restenosis: Part II, Circulation, 106:2859-2866 (2002).
5. D. P. Faxon, V. Fuster, P. Libby, J. A. Beckman, W. R. Hiatt, R. W. Thompson, J. N. Topper, B. H. Annex, J. H. Rundback, R. P. Fabunmi, R. M. Robertson, and J. Loscalzo. Atherosclerotic Vascular Disease Conference: Writing Group III: pathophysiology, Circulation, 109:2617-2625 (2004).
6. I. A. Hauser, L. Renders, H. H. Radeke, R. B. Sterzel, and M. Goppelt-Struebe. Mycophenolate mofetil inhibits rat and human mesangial cell proliferation by guanosine depletion, Nephrol. Dial. Transplant., 14:58-63 (1999).
7. C. Heinz, T. Hudde, K. Heise, and K. P. Steuhl. Antiproliferative effect of mycophenolate mofetil on cultured human Tenon fibroblasts, Graefes Arch. Clin. Exp. Ophthalmol., 240:408-414 (2002).
8. A. C. Allison and T. Eunson. Mycophenolate mofetil and its mechanisms of action, Immunopharmacology, 47:85-118 (2000).
9. Y. Ji, J. Gu, A. M. Makhov, J. D. Griffith, and B. S. Mitchell. Regulation of the interaction of inosine monophosphate dehydrogenase with mycophenolic Acid by GTP, J. Biol. Chem., 281:206-212 (2006).
10. H. Shimizu, M. Takahashi, S. Takeda, S. Inoue, J. Fujishiro, Y. Hakamata, T. Kaneko, T. Murakami, K. Takeuchi, I. Takeyoshi, Y. Morishita, and E. Kobayashi. Mycophenolate mofetil prevents transplant arteriosclerosis by direct inhibition of vascular smooth muscle cell proliferation, Transplantation, 77:1661-1667 (2004).
11. F. Romero, B. Rodriguez-Iturbe, H. Pons, G. Parra, Y. Quiroz, J. Rincon, and L. Gonzalez. Mycophenolate mofetil treatment reduces cholesterol-induced atherosclerosis in the rabbit, Atherosclerosis, 152:127-133 (2000).
12. R. Greupink, H. I. Bakker, C. Reker-Smit, A. M. Loenen-Weemaes, R. J. Kok, D. K. Meijer, L. Beljaars, and K. Poelstra. Studies on the targeted delivery of the antifibrogenic compound mycophenolic acid to the hepatic stellate cell, J. Hepatol., 43:884-892 (2005).

13. D. R. Nelson, Z. Tu, C. Soldevila-Pico, M. Abdelmalek, H. Zhu, Y. L. Xu, R. Cabrera, C. Liu, and G. L. Davis. Long-term interleukin 10 therapy in chronic hepatitis C patients has a proviral and anti-inflammatory effect, Hepatology, 38:859-868 (2003).
14. J. J. Maher. Interactions between hepatic stellate cells and the immune system, Semin. Liver Dis., 21:417-426 (2001).
15. T. Poynard, P. Mathurin, C. L. Lai, D. Guyader, R. Poupon, M. H. Tainturier, R. P. Myers, M. Muntenau, V. Ratziu, M. Manns, A. Vogel, F. Capron, A. Chedid, and P. Bedossa. A comparison of fibrosis progression in chronic liver diseases, J. Hepatol., 38:257-265 (2003).
16. Z. Shi, A. E. Wakil, and D. C. Rockey. Strain-specific differences in mouse hepatic wound healing are mediated by divergent T helper cytokine responses, Proc. Natl. Acad. Sci. U. S. A, 94:10663-10668 (1997).
17. P. J. de Bleser, P. Jannes, S. C. van Buul-Offers, C. M. Hoogerbrugge, C. F. van Schravendijk, T. Niki, V. Rogiers, J. L. van den Brande, E. Wisse, and A. Geerts. Insulinlike growth factor-II/mannose 6-phosphate receptor is expressed on CCl4-exposed rat fat-storing cells and facilitates activation of latent transforming growth factor-beta in cocultures with sinusoidal endothelial cells, Hepatology, 21:1429-1437 (1995).
18. J. A. Weiner, A. Chen, and B. H. Davis. E-box-binding repressor is down-regulated in hepatic stellate cells during up-regulation of mannose 6-phosphate/insulin-like growth factor-II receptor expression in early hepatic fibrogenesis, J. Biol. Chem., 273:15913-15919 (1998).
19. P. J. de Bleser, C. D. Scott, T. Niki, G. Xu, E. Wisse, and A. Geerts. Insulin-like growth factor II/mannose 6-phosphate-receptor expression in liver and serum during acute CCl4 intoxication in the rat, Hepatology, 23:1530-1537 (1996).
20. L. Beljaars, G. Molema, B. Weert, H. Bonnema, P. Olinga, G. M. Groothuis, D. K. Meijer, and K. Poelstra. Albumin modified with mannose 6-phosphate: A potential carrier for selective delivery of antifibrotic drugs to rat and human hepatic stellate cells, Hepatology, 29:1486-1493 (1999).
21. M. H. de Borst, G. Navis, R. A. de Boer, S. Huitema, L. M. Vis, W. H. van Gilst, and H. van Goor. Specific MAP-kinase blockade protects against renal damage in homozygous TGR(mRen2)27 rats, Lab Invest, 83:1761-1770 (2003).
22. M. J. Brosnan, A. M. Devlin, J. S. Clark, J. J. Mullins, and A. F. Dominiczak. Different effects of antihypertensive agents on cardiac and vascular hypertrophy in the transgenic rat line TGR(mRen2)27, Am. J. Hypertens., 12:724-731 (1999).
23. L. Beljaars, K. Poelstra, G. Molema, and D. K. Meijer. Targeting of sugar- and charge-modified albumins to fibrotic rat livers: the accessibility of hepatic cells after chronic bile duct ligation, J. Hepatol., 29:579-588 (1998).

24. R. J. Duncan, P. D. Weston, and R. Wrigglesworth. A new reagent which may be used to introduce sulfhydryl groups into proteins, and its use in the preparation of conjugates for immunoassay, Anal. Biochem., 132:68-73 (1983).
25. S. Zaina and J. Nilsson. Insulin-like growth factor II and its receptors in atherosclerosis and in conditions predisposing to atherosclerosis, Curr. Opin. Lipidol., 14:483-489 (2003).
26. S. Zaina, L. Pettersson, B. Ahren, L. Branen, A. B. Hassan, M. Lindholm, R. Mattsson, J. Thyberg, and J. Nilsson. Insulin-like growth factor II plays a central role in atherosclerosis in a mouse model, J. Biol. Chem., 277:4505-4511 (2002).
27. R. Novosyadlyy, K. Tron, J. Dudas, G. Ramadori, and J. G. Scharf. Expression and regulation of the insulin-like growth factor axis components in rat liver myofibroblasts, J. Cell Physiol, 199:388-398 (2004).
28. J. G. Scharf, T. Knittel, F. Dombrowski, L. Muller, B. Saile, T. Braulke, H. Hartmann, and G. Ramadori. Characterization of the IGF axis components in isolated rat hepatic stellate cells, Hepatology, 27:1275-1284 (1998).
29. G. Pugliese, F. Pricci, N. Locuratolo, G. Romeo, G. Romano, S. Giannini, B. Cresci, G. Galli, C. M. Rotella, and U. Di Mario. Increased activity of the insulin-like growth factor system in mesangial cells cultured in high glucose conditions. Relation to glucose-enhanced extracellular matrix production, Diabetologia, 39:775-784 (1996).
30. N. M. Dahms and M. K. Hancock. P-type lectins, Biochim. Biophys. Acta, 1572:317-340 (2002).
31. P. A. Dennis and D. B. Rifkin. Cellular activation of latent transforming growth factor beta requires binding to the cation-independent mannose 6-phosphate/insulin-like growth factor type II receptor, Proc. Natl. Acad. Sci. U. S. A, 88:580-584 (1991).
32. R. Bataller, E. Gabele, C. J. Parsons, T. Morris, L. Yang, R. Schoonhoven, D. A. Brenner, and R. A. Rippe. Systemic infusion of angiotensin II exacerbates liver fibrosis in bile duct-ligated rats, Hepatology, 41:1046-1055 (2005).
33. P. J. Admiraal, C. A. van Kesteren, A. H. Danser, F. H. Derkx, W. Sluiter, and M. A. Schalekamp. Uptake and proteolytic activation of prorenin by cultured human endothelial cells, J. Hypertens., 17:621-629 (1999).
34. M. M. van den Eijnden, J. J. Saris, R. J. de Bruin, E. de Wit, W. Sluiter, T. L. Reudelhuber, M. A. Schalekamp, F. H. Derkx, and A. H. Danser. Prorenin accumulation and activation in human endothelial cells: importance of mannose 6-phosphate receptors, Arterioscler. Thromb. Vasc. Biol., 21:911-916 (2001).

35. T. Braulke and G. Mieskes. Role of protein phosphatases in insulin-like growth factor II (IGF II)-stimulated mannose 6-phosphate/IGF II receptor redistribution, J. Biol. Chem., 267:17347-17353 (1992).
36. D. F. Smee, M. Bray, and J. W. Huggins. Antiviral activity and mode of action studies of ribavirin and mycophenolic acid against orthopoxviruses in vitro, Antivir. Chem. Chemother., 12:327-335 (2001).
37. H. Tedesco-Silva, M. C. Bastien, L. Choi, C. Felipe, J. Campestrini, F. Picard, and R. Schmouder. Mycophenolic acid metabolite profile in renal transplant patients receiving enteric-coated mycophenolate sodium or mycophenolate mofetil, Transplant. Proc., 37:852-855 (2005).
38. J. H. LeBowitz, J. H. Grubb, J. A. Maga, D. H. Schmiel, C. Vogler, and W. S. Sly. Glycosylation-independent targeting enhances enzyme delivery to lysosomes and decreases storage in mucopolysaccharidosis type VII mice, Proc. Natl. Acad. Sci. U. S. A, 101:3083-3088 (2004).
39. L. Beljaars, G. Molema, D. Schuppan, A. Geerts, P. J. de Bleser, B. Weert, D. K. Meijer, and K. Poelstra. Successful targeting to rat hepatic stellate cells using albumin modified with cyclic peptides that recognize the collagen type VI receptor, J. Biol. Chem., 275:12743-12751 (2000).
40. L. Beljaars, B. Weert, A. Geerts, D. K. Meijer, and K. Poelstra. The preferential homing of a platelet derived growth factor receptor-recognizing macromolecule to fibroblast-like cells in fibrotic tissue, Biochem. Pharmacol., 66:1307-1317 (2003).

4

STUDIES ON THE TARGETED DELIVERY OF THE ANTIFIBROGENIC COMPOUND MYCOPHENOLIC ACID TO THE HEPATIC STELLATE CELL

Rick Greupink
Hester I. Bakker
Catharina Reker-Smit
Anne-miek van Loenen-Weemaes
Robbert-Jan Kok
Dirk K.F. Meijer
Leonie Beljaars
Klaas Poelstra

Journal of Hepatology 2005; 43: 884-892

ABSTRACT

Hepatic stellate cell (HSC) activation and proliferation are key events in the pathology of liver fibrosis. Inhibiting these parameters therefore is a relevant option to treat liver fibrosis pharmacologically. The immunosuppressive drug mycophenolic acid (MPA) has been shown to inhibit proliferation and activation of various types of fibroblasts. In an effort to circumvent the immunosuppression and at the same time enhance this antifibrotic effect, we coupled MPA to the HSC-selective drug carrier mannose-6-phosphate modified human serum albumin and evaluated this conjugate for its specificity and antifibrotic activity. We found that MPA inhibited proliferation of HSC *in vitro*. The drug coupled to the drug carrier bound specifically to HSC and reduced HSC proliferation *in vitro*. *In vivo* studies in bile duct-ligated rats demonstrated that our conjugate accumulated selectively in the liver with significant uptake in HSC apart from Kupffer and endothelial cells, whereas primary and secondary lymphoid tissues were avoided. Treatment of bile duct-ligated rats with this conjugate reduced hepatic inflammation and hepatic α-β-crystallin mRNA expression, a marker for HSC activation. In conclusion, this study shows that targeted delivery of MPA to HSC results in a decrease in HSC activation, making it the first drug that is successfully delivered to this cell type.

INTRODUCTION

During liver fibrosis, hepatic stellate cells (HSC) change from a quiescent cell type into activated cells with a myofibroblastic phenotype that extensively proliferate and produce an excess of extracellular matrix proteins. This gradually causes an impairment of liver function (1, 2). Inhibiting HSC functioning therefore is an interesting strategy to develop an effective pharmacological treatment for this disease (3-7).

The immunosuppressive drug mycophenolic acid (MPA) is a potential inhibitor of HSC proliferation and activation. In the treatment of the fibrotic process in the kidney, MPA has been successfully used to ameliorate fibrosis in two animal models (8-10). *In vitro* studies showed that MPA has a direct antiproliferative effect and inhibits cell activation in cultures of mesangial cells, the fibrogenic cells within glomeruli (11, 12). Other studies report that MPA is able to inhibit the proliferation of tenon fibroblasts and vascular smooth muscle cells, which are main players in fibrotic processes in the eye and during atherosclerosis, respectively (13, 14). This may imply that MPA can also act on HSC.

The ideal antifibrotic drug for liver fibrosis should be organ-specific and, if possible, even HSC-specific. Inhibition of fibroblast proliferation other than HSC, in principle, can result in impaired wound healing elsewhere in the body, which is not desired. In addition to that, systemically administered MPA would lead to suppression of T and B lymphocyte functioning, which may seriously affect the host-defence system of patients.

In order to avoid immunosuppression and at the same time to deliver MPA specifically to the HSC, we coupled the drug to the HSC-selective drug carrier mannose-6-phosphate-modified human serum albumin (M6PHSA). M6PHSA has been shown to accumulate selectively in activated HSC *in vivo*, through binding to Mannose-6-Phosphate/Insuline-like Growth Factor-II receptors (M6P/IGF-II receptors) (15). These receptors are abundantly present on activated HSC (16, 17).

In this study we explore the potential of MPA conjugated to M6PHSA to achieve specific delivery to the HSC in order to treat HSC activation and proliferation, making this the first drug to be targeted to the HSC.

MATERIALS AND METHODS

Preparation of drug targeting construct

Synthesis of M6PHSA-MPA via ester bond

M6PHSA was synthesized as described (15). MPA (Sigma, Gillingham, UK) was coupled to M6PHSA via an ester bond by activation with 2-iodoethanol. Briefly, MPA (20 mg) was reacted with 20 µl of $SOCl_2$ (Sigma) and 0.4 µl of dimethylformamide (Merck, Darmstadt, Germany) in dichloromethane (Merck) for 5 hours. The reaction mixture was evaporated to dryness. The remaining product was reacted with 200 µl of 2-iodoethanol (Sigma) in dichloromethane for 90 minutes on ice, protected from light. The resulting MPA-2-iodoethanol ester was coupled to the sulfhydryl groups of M6PHSA which were incorporated via S-acetylthioglycolic acid N-hydroxysuccinimide ester (Sigma) derivatization (18). The final product was purified by filtration followed by dialysis against water and was then lyophilized. The protein content was assessed by the Biorad protein assay. Drug content was assessed by HPLC after hydrolysis of the ester bond between MPA and M6PHSA at pH=12. Drug loading was calculated from the molar ratio between MPA and protein. The percentage of monomeric protein in the preparation was assessed by size exclusion chromatography as described previously (15).

Synthesis of M6PHSA-MPA via amide bond

To enhance drug loading to the carrier, MPA was also coupled to M6PHSA via an amide bond. Briefly, MPA (8 mg) was reacted in PBS with M6PHSA (10 mg) and 5 mg 1-ethyl-3-(3-dimethylaminopropyl)-carbodiimide (Sigma). Purification was performed as described above. The amount of conjugated MPA was

determined as described above, after degradation of the conjugate overnight at 120 °C in 6 N HCl.

Experimental Animals

For HSC isolation, male Wistar rats of 400-500g (Harlan, Horst, The Netherlands) were housed under a 12-hour dark/light cycle, at constant humidity and temperature. Animals had free access to tap water and standard lab chow (Harlan). For *in vivo* experiments male Wistar rats of 220-240g were used. All experiments were approved by the local committee for care and use of laboratory animals and were performed according to strict governmental and international guidelines for the use of experimental animals.

In vitro experiments

HSC isolation

HSC were isolated and cultured according to the method of Geerts et al. (19). After 9 days of culture, when cells had an activated phenotype, the cells were plated in 24-well plates at a density of 30,000 cells/well and were allowed to attach to the plates overnight before performing experiments.

Effects on cell proliferation

To assess the effect of test substances on cell proliferation, HSC were cultured with MPA, M6PHSA (1 mg/ml), M6PHSA-MPA (1 mg/ml) or vehicle for 48 hours. Immunohistochemical staining was performed to assess BrdU-incorporation. The number of BrdU-positive cells was counted and expressed relative to the total number of cells counted. HSC were cultured in the presence of 10 μM BrdU with 50 ng/ml human recombinant PDGF-BB (Peprotech, Rocky Hill, NJ, USA) and 10% FCS to stimulate proliferation.

To verify whether MPA acts by decreasing intracellular guanosine synthesis, MPA-treated HSC (1.5 μM) were co-incubated with 1 mM guanosine (Sigma) for 48 hours and cell proliferation was measured by assessment of BrdU incorporation.

Binding of M6PHSA-MPA to HSC in vitro

To authenticate specific binding of the conjugate to HSC, binding assays were performed with ^{125}I-labeled M6PHSA-MPA. Cells (10 days after isolation) were pre-incubated with 1% BSA in DMEM to block non-specific binding. HSC were then incubated at 37 °C with 100,000 cpm of ^{125}I-labeled M6PHSA-MPA in the absence of a competitor for receptor binding, in the presence of 1 mg/ml HSA or with 1 mg/ml M6PHSA. After 2 hours, cells were washed and the cell-associated radioactivity was measured on a γ-counter (Riastar, Packard instruments, Palo Alto, USA).

Inosine monophosphate dehydrogenase (IMPDH) mRNA expression in HSC

RNA was isolated from primary isolated rat HSC with the Absolutely RNA microprep kit (Stratagene, La Jolla, CA, USA) after culture-activation of the cells on plastic for 3, 7 or 10 days. cDNA was synthesized according to standard techniques and real time PCR was performed on an ABI PRISM 7900HT Sequence Detection System to assess the expression of IMPDH type 2 mRNA relative to GAPDH. SYBR Green (Applied Biosystems, Warmington, UK) was used for fluorescent detection of the amplified product. Appropriate primers were used in a concentration of 50 μM.

In vivo experiments

Organ distribution

Organ distribution experiments were performed in bile duct-ligated rats (BDL) as described previously (15). Three weeks after BDL, animals were injected i.v. with a tracer dose of ^{125}I-labeled M6PHSA-MPA under O_2/N_2O/Isoflurane anaesthesia. Ten minutes after injection, the animals were sacrificed by heart puncture. The organs were removed and washed with saline, before measuring radioactivity with a γ-counter.

Intra-hepatic distribution

Three BDL rats received i.v. injections with PBS from day 3 until day 10 after BDL and a final injection of M6PHSA-MPA (4 mg/kg) 10 minutes before sacrifice. Another three BDL rats were injected daily from day 3 until day 10 after BDL with conjugate before their final injection, 10 minutes prior to sacrifice. This allowed us to study the difference in distribution after single and multiple dosing. Immunohistochemical double-stainings were performed for the conjugate and markers for HSC (desmin/GFAP), Kupffer cells (ED2) and endothelial cells (RECA-1) on 4 μm acetone-fixed cryostat sections of liver, as described earlier (15). The number of double-positive cells per microscopic field was counted at a magnification of 200x. In each microscopic field this number of double-positive cells was related to the total number of HSA-positive cells. This yielded a relative accumulation of M6PHSA-MPA by each cell type. At least 5 microscopic fields per section were analyzed.

In vivo effect study

BDL rats were i.v. injected daily with PBS, M6PHSA-MPA (4 mg/kg/day), M6PHSA (4 mg/kg/day) or M6PHSA (4 mg/kg/day) in combination with 8 μg/kg/day of uncoupled MPA which is equivalent to the amount of MPA present in the conjugate. Animals were treated from day 3 after BDL until sacrifice at day 10 after BDL. Staining for oxygen-free radical-producing cells, using diaminobenzidine (DAB) was performed on 4 μm cryostat sections of liver as described (20). The staining was quantified by counting the number of DAB-positive cells in 6 microscopic fields per section (magnification 10 x 10). The extent of fibrosis and the number of desmin/GFAP-positive cells were assessed by picrosirius red staining and immunohistochemical staining for desmin/GFAP, respectively, followed by morphometric analysis with Image J software (NIH, Bethesda, USA).

Real-time RT-PCR for hepatic α-β-crystallin mRNA, a marker for HSC activation was performed as described above (21-23).

Statistical analysis

Results were expressed as the mean +/- SD. Data were subjected to a one-way ANOVA followed by the LSD post-hoc test. The differences were considered statistically significant at $P < 0.05$.

Table 1: Characteristics of the synthesized M6PHSA-MPA constructs

	Coupling	Chemical structure	maximal Drug:protein Ratio	Pharmacological activity
Conjugation of MPA To M6P-HSA	Via ester	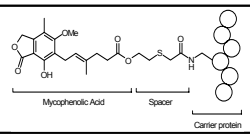	1.2	Yes
	Via amide	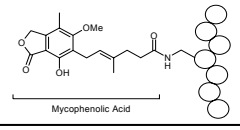	22	No

RESULTS

Characterization of M6PHSA-MPA conjugates

Synthesis of M6PHSA-MPA via an ester bond

HPLC-analysis revealed that the maximum drug to protein ratio that could be achieved was 1.2:1 (Table 1). Bulk synthesis yielded lower coupling ratios and the construct used in the *in vitro* studies, therefore, had a drug to protein ratio of 0.4:1. The conjugate that was used for *in vivo* studies had a near equal drug to protein ratio of 0.5:1. Size exclusion chromatography showed that more than 70% of the conjugate consisted of monomeric protein.

Synthesis of M6PHSA-MPA via an amide bond

Analysis of the construct for the coupling ratio of MPA to M6PHSA showed that a total of 22 drug molecules were coupled per carrier molecule (Table 1).

In vitro experiments with MPA

When HSC were incubated with increasing concentrations of MPA, BrdU-incorporation decreased strongly in a dose-dependent manner (Fig. 1), whereas cell viability was not affected (data not shown).

Since it is possible that MPA acts by decreasing intracellular guanosine synthesis through inhibition of IMPDH, we investigated whether HSC express mRNA for IMPDH. In Fig. 2A it can be seen that IMPDH type 2 mRNA is expressed after 3, 7 and 10 days of culture activation. In addition, Fig. 2B shows that the effect of MPA is completely blocked when exogenous guanosine is added to the culture medium.

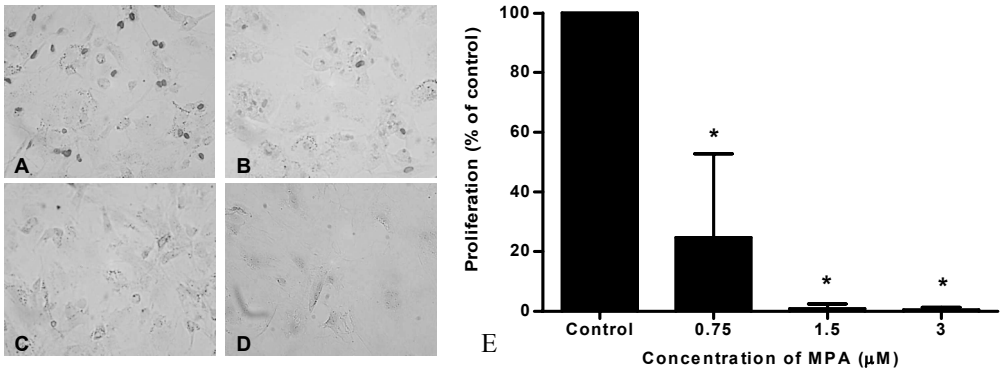

Fig. 1. Representative microphotographs of the immunohistochemical detection of BrdU-incorporation (red staining) in nuclei of primary isolated rat HSC, 11 days in culture. Figures show cultures treated for 48 hours with vehicle (A), or treated with 0.75 (B), 1.5 (C) and 3 µM (D) MPA. Magnification 200x. E: Percentage of BrdU-positive cells expressed as a percentage of control. Data represent the average of 3 independent experiments. * indicates $p < 0.05$.

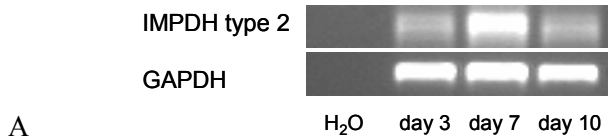

A

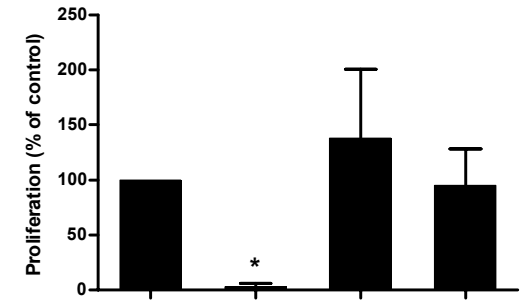

B

Fig. 2. A: Expression of IMPDH type 2 mRNA in primary isolated rat HSC after culture activation for 3, 7 and 10 days. B*:* The effect of co-incubation of HSC with guanosine (1 mM) and MPA (1.5 μM) on cell proliferation. Note that the response of HSC to MPA is attenuated when exogenous guanosine is supplemented to the culture medium. * indicates $P < 0.05$ compared to control. Data represent the average +/- SD of 3 experiments, from 3 different HSC isolations.

In vitro activity of M6PHSA-MPA conjugates

In experiments with 3T3-fibroblasts, the conjugate in which MPA was linked to M6PHSA via an ester bond significantly inhibited BrdU-incorporation, whereas MPA that was conjugated via an amide bond to the drug carrier, displayed no pharmacological activity at all, in spite of the much higher amount of MPA that was coupled to the protein (Table 1). In subsequent experiments we therefore only tested the pharmacologically active M6PHSA-MPA conjugate in cultures of HSC, the ultimate target cells. Incubation of HSC with this conjugate, strongly reduced BrdU-incorporation, whereas M6PHSA alone was completely inactive (Fig. 3).

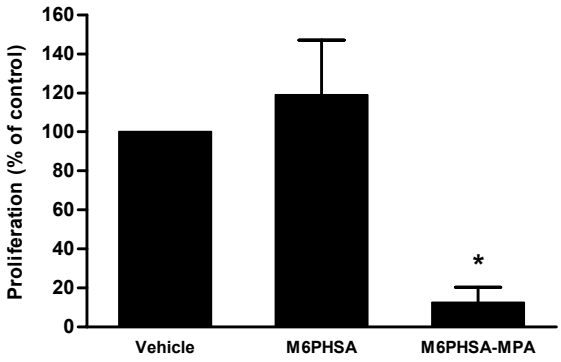

Fig. 3. The effect of M6PHSA (1 mg/ml) and M6PHSA-MPA (conjugation via ester bond, 1 mg/ml) on BrdU incorporation in cultures of primary isolated HSC (10 days in culture). Data represent the average of 3 independent experiments, from 3 different HSC isolations. * indicates $P < 0.05$ compared to control.

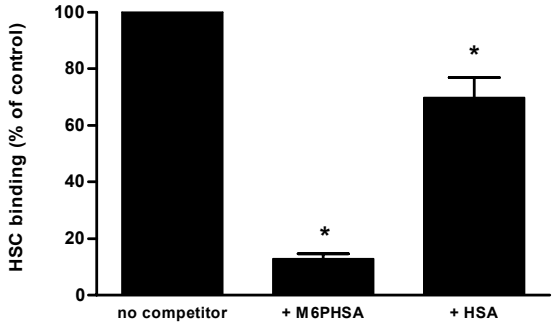

Fig. 4. The influence of competitors on the binding and uptake of ^{125}I-labeled M6PHSA-MPA by primary isolated HSC (10 days in culture). Note that M6PHSA, a ligand for the M6P/IGF-II receptor reduces binding of the conjugate by 87 +/- 2%, whereas the control protein HSA, only reduces binding by 30 +/- 7%. * indicates $P < 0.05$. Data are the average of 3 independent experiments from 3 different HSC isolations.

Binding of M6PHSA-MPA to HSC in vitro

To verify that M6PHSA-MPA binds specifically to receptors on HSC, we performed binding studies on culture activated HSC with ^{125}I-labeled M6PHSA-MPA. Binding to HSC was strongly inhibited by M6PHSA, an M6P/IGF-II receptor ligand, whereas the control protein HSA only had a minor effect (Fig 4).

In vivo distribution of M6PHSA-MPA

All *in vivo* experiments were performed with the conjugate in which MPA was coupled to M6PHSA via an ester bond.

Organ distribution

Ten minutes after i.v. administration of a tracer dose of ^{125}I-labeled M6PHSA-MPA to animals with liver fibrosis, the conjugate distributed only to the liver. Thymus and spleen, which are organs with resident T and B lymphocytes, did only take up minor amounts of conjugate. Accumulation in other major organs like heart, kidney and lung was also very low (Fig. 5). In bone marrow no significant radioactivity was found (data not shown).

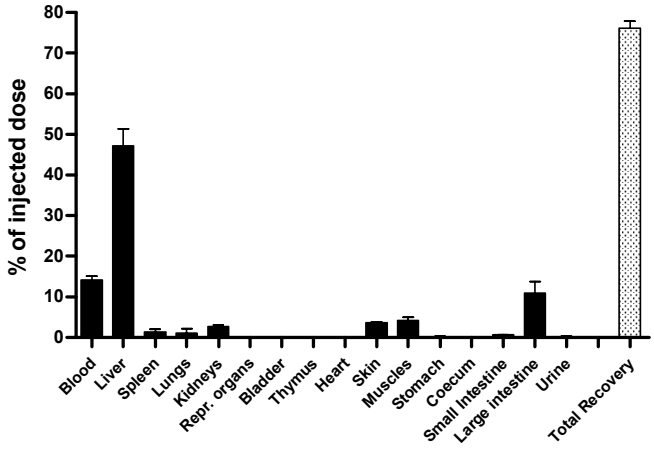

Fig. 5. Organ distribution of ^{125}I-labeled M6PHSA-MPA, 10 minutes after i.v. injection (penal vein) in rats, 3 weeks after BDL (n=2).

Intra-hepatic distribution

Immunohistochemical staining for HSA within the liver showed a distribution to the non-parenchymal cells, 10 minutes after injection. Double-staining indicated co-localization of HSA with the HSC markers desmin/GFAP (Fig. 6A). However, double-staining for endothelial cells (EC) and HSA, and double staining for Kupffer cells (KC) and HSA also showed double-positive cells (Fig. 6B and 6C). Quantification of the particular staining patterns revealed an equal distribution to HSC, EC and KC (Fig. 6D). The intra-hepatic distribution in the multiple-dose and single-dose groups was similar.

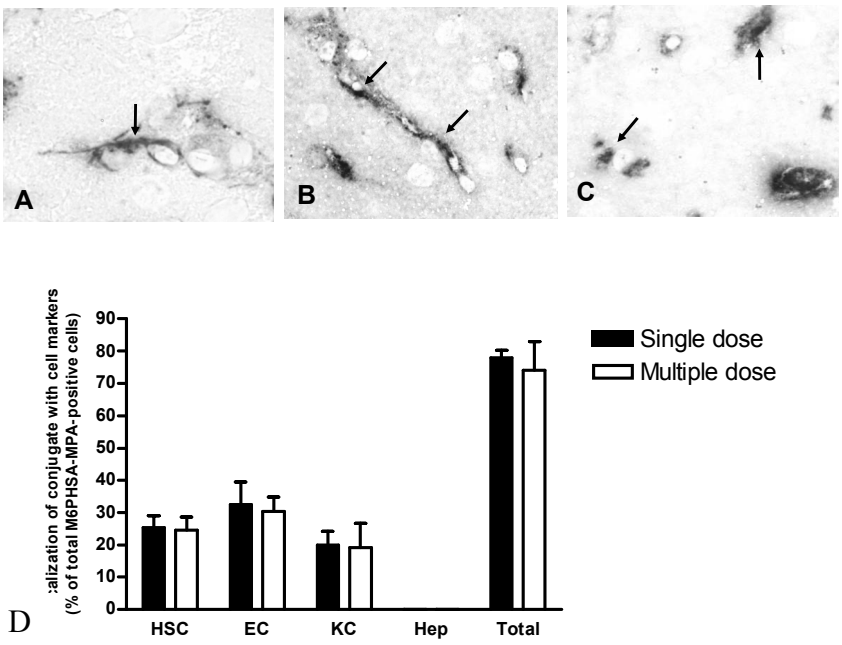

Fig. 6. Co-localisation of M6PHSA-MPA with HSC (A), EC (B) and KC (C) in rat livers, demonstrated by immunohistochemical double-staining for the conjugate (α-HSA, red staining) and non-parenchymal cell types (KC, EC and HSC were identified with the antibodies ED2, RECA-1 and anti-desmin/GFAP respectively; blue staining) in 4 µm cryostat sections. Magnification 1000x. D: Quantification of the intra-hepatic cellular distribution of M6PHSA-MPA in the livers of fibrotic rats after a single dose and after multiple injections (n=3). HSC: hepatic stellate cell, EC: endothelial cell, KC: Kupffer cell and Hep: hepatocyte.

In vivo effects

To assess the effects of test compounds on the liver, we treated BDL animals for 7 days. We started dosing at day 3 after BDL because M6P/IGF-II receptor expression is being up regulated from this time point on (data not shown) and we stopped at day 10 when signs of fibrosis are evident but not excessive yet.

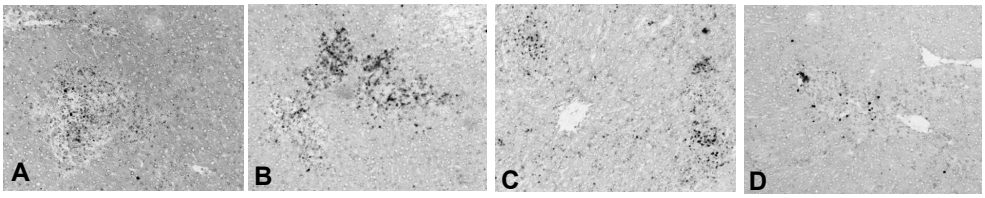

E

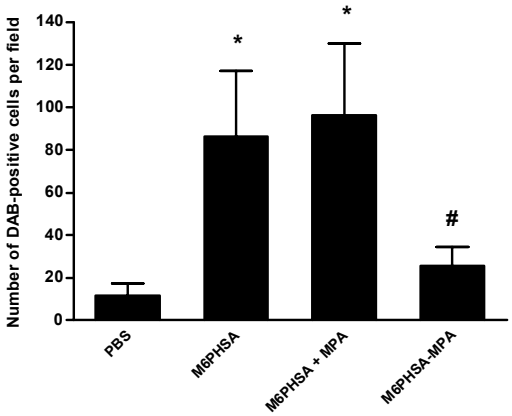

Fig. 7. Representative microphotographs of a DAB-staining for the amount of oxygen-free radical-producing cells in livers of bile duct ligated rats (n=5 per group) after daily i.v. injections with PBS (A), M6PHSA 4 mg/kg (B), M6PHSA 4 mg/kg combined with an equimolar amount of uncoupled MPA as present in bound form in the conjugate (C), and conjugate 4 mg/kg (D). Animals were injected from BDL day 3 until BDL day 10. Magnification 200x. E: Quantification of DAB staining by counting the number of DAB-positive cells per microscopic field (magnification 10 x 10). Per rat 6 fields were counted, each group consisted of 5 animals (average +/- SD). * indicates $P < 0.05$ compared to the PBS-treated group, # indicates $p < 0.05$ compared to both the M6PHSA-treated animals and the M6PHSA + uncoupled MPA-treated animals.

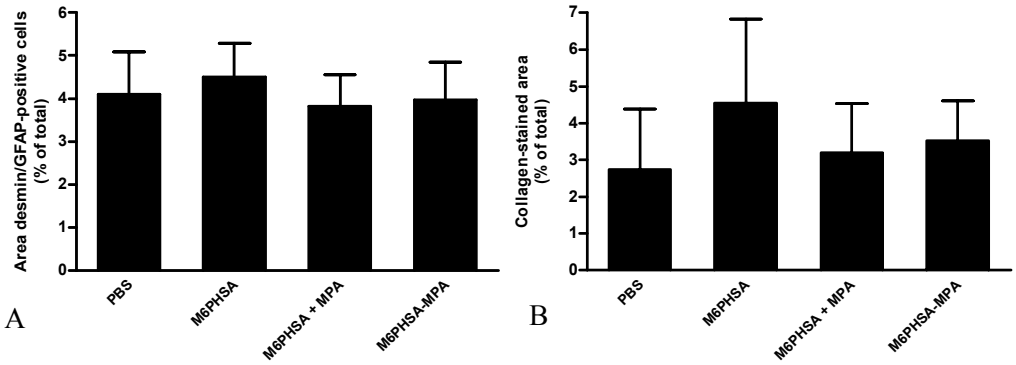

Fig. 8. A*:* Results of a morphometric analysis of liver sections stained for desmin/GFAP. The area of desmin/GFAP positive cells is expressed as a percentage of the total area. B: Results of the morphometric analysis of liver sections stained for collagen with picrosirius red. Data present the average of 5 animals per group +/- SD. For both stainings no significant differences were observed between the groups.

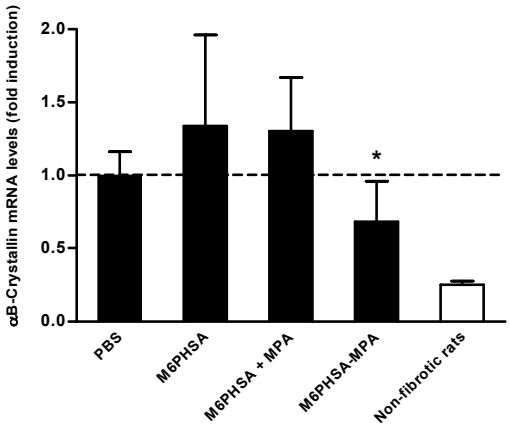

Fig. 9. Effect of drugs and control substances on the hepatic mRNA levels of α-β-Crystallin expression after daily i.v. injections (penal vein) with PBS, conjugate (4 mg/kg), M6PHSA (4 mg/kg) and M6PHSA (4 mg/kg) that was combined with an equimolar amount of uncoupled MPA compared to the amount present in the conjugate. Animals were treated from day 3 to day 10 after bile duct ligation (n=5 per group). As a reference α-β-Crystallin mRNA expression in healthy, non-fibrotic rats is showed. * indicates $P < 0.05$ compared to both the M6PHSA-treated animals and the M6PHSA + MPA-treated group.

Oxygen-free radical-producing cells

Treatment with carrier alone or with M6PHSA + unconjugated MPA elevated the number of DAB-positive cells in the liver, reflecting an increase in the number of oxygen-free radical-producing neutrophils and monocytes (Fig. 7). In contrast, the M6PHSA-MPA conjugate significantly lowered the amount of DAB-positive cells compared to these two groups. The dose of unconjugated MPA was equimolar to the amount of coupled MPA in conjugate-treated animals.

Extent of hepatic collagen deposition and amount of desmin/GFAP-positive cells

The extent of collagen deposition and the amount of desmin/GFAP-positive cells did not differ between the groups (Fig. 8). Because these late markers for the extent of liver fibrosis were not affected by either targeted or untargeted MPA, we assessed the influence of the various test substances on an early marker for hepatic stellate cell activation, i.e. α-β-Crystallin (21-23).

α-β-Crystallin mRNA levels

Fig. 9 shows the effect of treatment on α-β-Crystallin mRNA expression. When the conjugate-treated group was compared to the animals treated with M6PHSA + unconjugated MPA or the M6PHSA-treated animals, a significant decrease in expression of α-β-Crystallin mRNA levels could be seen. This indicates that this early marker for HSC activation is lowered by the targeted form of MPA only.

DISCUSSION

In the present study we investigated the antifibrogenic potential of mycophenolic acid and of a conjugate of mycophenolic acid coupled to the HSC-selective drug carrier M6PHSA. We report here, for the first time, that MPA also has antiproliferative effects in culture-activated rat HSC.

Since long-term administration of immunosuppressive drugs will cause problems in patients with liver fibrosis, we addressed the issue of avoiding adverse

effects by exploring the antifibrotic effects of MPA after coupling it to an HSC-selective drug carrier. We showed that, for effective targeting of MPA, a construct in which the drug is coupled via an ester bond to the carrier backbone has to be used, since a conjugate in which MPA was linked via a non-peptide-like amide bond exerted no effect *in vitro*. Most likely this is due to the inability to degrade non-peptide like amide bonds within lysosomes of cells (24, 25).

Distribution studies *in vivo* showed uptake of the conjugate selectively in the liver, whereas lymphocyte-containing organs were avoided. Within the liver, the conjugate accumulated in HSC, although uptake of the construct by EC and KC was also evident. Quantitative estimations of drug concentrations within target cells can not be easily done based on these immunohistochemical data, but it is highly likely that the drug concentration in HSC after administration of uncoupled drug, which distributes throughout the body, is only a fraction compared to the targeted situation, in which the drug accumulates within the liver, in only a limited part of the cells.

A possible reason for the uptake of conjugate in KC and EC may be the presence of protein polymers in the construct which can be taken up by KC. Another possibility is that the negatively charged protein backbone of the construct is recognized by scavenger receptors on KC and EC (26, 27). Yet, the delivery of MPA to these cell types is not expected to produce profibrotic or pro-inflammatory effects. In fact, MPA may exert anti-inflammatory and antifibrotic effects in these cell types. In human umbilical chord vein endothelial cells (HUVEC), MPA attenuated the expression of adhesion molecules, and incubation of monocytes and macrophages with MPA caused a reduced cell adhesion and a reduced cytokine and nitric oxide production by these cells (28, 29). Based on these findings, MPA delivery to EC and KC in the liver may even attenuate hepatic inflammation.

In vivo, the targeted delivery of MPA clearly reduced inflammation compared to the group that was treated with untargeted MPA mixed with carrier. This effect may be explained by the actions of MPA in EC and KC as outlined above. Yet, an

active role of HSC in hepatic inflammation has also been suggested and the delivery of MPA to this cell type may also contribute to the observed effects (30, 31). Although inflammation in rats treated with M6PHSA-MPA was reduced compared to the group injected with carrier alone or the group that received carrier + untargeted MPA, the number of activated neutrophils was still higher compared to PBS-treated controls. This may be due to a pro-inflammatory effect of the carrier counteracting the anti-inflammatory effect of targeted MPA. Possibly this is effected by KC that take up a portion of the injected carrier protein (15). Both lowering the amount of protein aggregates in the preparation and limiting the overall negative charge of the conjugate may circumvent this KC uptake.

When studying the antifibrotic effects of targeted MPA we could not find a significant effect on the amount of desmin/GFAP positive cells in the liver, which was anticipated because of the antiproliferative properties of MPA.

Because recently it was reported that MPA reduced the activation of cultured mesangial cells (12) we also evaluated our liver samples for the expression of an early, sensitive and specific marker for HSC activation, α-β-Crystallin (21-23). Data show that in contrast to untargeted MPA, an equimolar concentration of targeted MPA reduced the expression of α-β-Crystallin in fibrotic animals, reflecting reduced HSC activation.

In conclusion: MPA appears to be a potent inhibitor of HSC proliferation *in vitro* and therefore may be a promising antifibrotic agent in liver fibrosis. We showed that the targeted delivery of MPA to the HSC in the liver is possible, and results in an anti-inflammatory effect and in signs of reduced HSC activation *in vivo*. Simultaneously, the uptake in extrahepatic tissues in which side effects of MPA may occur is avoided. The mild pharmacological effect of targeted MPA within the liver however stresses the need for additional structure-activity and dose-dependency studies on this targeting construct. This includes investigations on the targeting of even more potent drugs. Yet, the construct presented in this

report may be the first of a generation of antifibrotic drug targeting preparations that accumulates in HSC.

ACKNOWLEDGEMENTS

This study was financially supported by the Dutch Foundation for Technical Sciences.

REFERENCE LIST

1. Eng FJ, Friedman SL. Fibrogenesis I. New insights into hepatic stellate cell activation: the simple becomes complex. Am J Physiol Gastrointest Liver Physiol 2000 Jul;279(1):G7-G11.
2. Friedman SL. Molecular regulation of hepatic fibrosis, an integrated cellular response to tissue injury. J Biol Chem 2000 Jan 28;275(4):2247-2250.
3. Kurikawa N, Suga M, Kuroda S, Yamada K, Ishikawa H. An angiotensin II type 1 receptor antagonist, olmesartan medoxomil, improves experimental liver fibrosis by suppression of proliferation and collagen synthesis in activated hepatic stellate cells. Br J Pharmacol 2003 Jul;139(6):1085-1094.
4. Rombouts K, Kisanga E, Hellemans K, Wielant A, Schuppan D, Geerts A. Effect of HMG-CoA reductase inhibitors on proliferation and protein synthesis by rat hepatic stellate cells. J Hepatol 2003 May;38(5):564-572.
5. Caligiuri A, De Franco RM, Romanelli RG, Gentilini A, Meucci M, Failli P, et al. Antifibrogenic effects of canrenone, an antialdosteronic drug, on human hepatic stellate cells. Gastroenterology 2003 Feb;124(2):504-520.
6. Di Sario A, Bendia E, Svegliati BG, Ridolfi F, Casini A, Ceni E, et al. Effect of pirfenidone on rat hepatic stellate cell proliferation and collagen production. J Hepatol 2002 Nov;37(5):584-591.
7. Niki T, Rombouts K, De Bleser P, De Smet K, Rogiers V, Schuppan D, et al. A histone deacetylase inhibitor, trichostatin A, suppresses myofibroblastic differentiation of rat hepatic stellate cells in primary culture. Hepatology 1999 Mar;29(3):858-867.
8. Badid C, Vincent M, McGregor B, Melin M, Hadj-Aissa A, Veysseyre C, et al. Mycophenolate mofetil reduces myofibroblast infiltration and collagen III deposition in rat remnant kidney. Kidney Int 2000;58:51-61.

9. Romero F, Rodriguez-Iturbe B, Parra G, Gonzalez L, Herrera-Acosta J, Tapia E. Mycophenolate mofetil prevents the progressive renal failure induced by 5/6 renal ablation in rats. Kidney Int 1999 Mar;55(3):945-955.
10. Van den Branden C, Ceyssens B, Pauwels M, Van Wichelen G, Heirman I, Jie N, et al. Effect of mycophenolate mofetil on glomerulosclerosis and renal oxidative stress in rats. Nephron Exp Nephrol 2003;95(3):e93-e99.
11. Hauser IA, Renders L, Radeke HH, Sterzel RB, Goppelt-Struebe M. Mycophenolate mofetil inhibits rat and human mesangial cell proliferation by guanosine depletion. Nephrol Dial Transplant 1999 Jan;14(1):58-63.
12. Dubus I, Vendrely B, Christophe I, Labouyrie JP, Delmas Y, Bonnet J, et al. Mycophenolic acid antagonizes the activation of cultured human mesangial cells. Kidney Int 2002 Sep;62(3):857-867.
13. Heinz C, Hudde T, Heise K, Steuhl KP. Antiproliferative effect of mycophenolate mofetil on cultured human Tenon fibroblasts. Graefes Arch Clin Exp Ophthalmol 2002 May;240(5):408-414.
14. Moon JI, Kim IS, Kim MS, Kim EH, Kim HJ, Park K. Effect of cyclosporin, mycophenolic acid, and rapamycin on the proliferationof rat aortic vascular smooth muscle cells: in vitro study. Transplant Proc 2000;32:2026-2027.
15. Beljaars L, Molema G, Weert B, Bonnema H, Olinga P, Groothuis GM, et al. Albumin modified with mannose 6-phosphate: A potential carrier for selective delivery of antifibrotic drugs to rat and human hepatic stellate cells. Hepatology 1999 May;29(5):1486-1493.
16. de Bleser PJ, Jannes P, van Buul-Offers SC, Hoogerbrugge CM, van Schravendijk CF, Niki T, et al. Insulinlike growth factor-II/mannose 6-phosphate receptor is expressed on CCl4-exposed rat fat-storing cells and facilitates activation of latent transforming growth factor-beta in cocultures with sinusoidal endothelial cells. Hepatology 1995 May;21(5):1429-1437.
17. Weiner JA, Chen A, Davis BH. E-box-binding repressor is down-regulated in hepatic stellate cells during up-regulation of mannose 6-phosphate/insulin-like growth factor-II receptor expression in early hepatic fibrogenesis. J Biol Chem 1998 Jun 26;273(26):15913-15919.
18. Duncan RJ, Weston PD, Wrigglesworth R. A new reagent which may be used to introduce sulfhydryl groups into proteins, and its use in the preparation of conjugates for immunoassay. Anal Biochem 1983 Jul 1;132(1):68-73.
19. Geerts A, Niki T, Hellemans K, De Craemer D, Van Den Berg K, Lazou JM, et al. Purification of rat hepatic stellate cells by side scatter-activated cell sorting. Hepatology 1998 Feb;27(2):590-598.

20. Poelstra K, Hardonk MJ, Koudstaal J, Bakker WW. Intraglomerular platelet aggregation and experimental glomerulonephritis. Kidney Int 1990 Jun;37(6):1500-1508.
21. Cassiman D, Roskams T, van PJ, Libbrecht L, Aertsen P, Crabbe T, et al. Alpha B-crystallin expression in human and rat hepatic stellate cells. J Hepatol 2001 Aug;35(2):200-207.
22. Cassiman D, Libbrecht L, Desmet V, Denef C, Roskams T. Hepatic stellate cell/myofibroblast subpopulations in fibrotic human and rat livers. J Hepatol 2002 Feb;36(2):200-209.
23. Lang A, Schrum LW, Schoonhoven R, Tuvia S, Solis-Herruzo JA, Tsukamoto H, et al. Expression of small heat shock protein alphaB-crystallin is induced after hepatic stellate cell activation. Am J Physiol Gastrointest Liver Physiol 2000 Dec;279(6):G1333-G1342.
24. Franssen EJ, Koiter J, Kuipers CA, Bruins AP, Moolenaar F, de Zeeuw D, et al. Low molecular weight proteins as carriers for renal drug targeting. Preparation of drug-protein conjugates and drug-spacer derivatives and their catabolism in renal cortex homogenates and lysosomal lysates. J Med Chem 1992 Apr 3;35(7):1246-1259.
25. Nelson PH, Eugui E, Wang CC, Allison AC. Synthesis and immunosuppressive activity of some side-chain variants of mycophenolic acid. J Med Chem 1990 Feb;33(2):833-838.
26. Jansen RW, Molema G, Harms G, Kruijt JK, van Berkel TJ, Hardonk MJ, et al. Formaldehyde treated albumin contains monomeric and polymeric forms that are differently cleared by endothelial and Kupffer cells of the liver: evidence for scavenger receptor heterogeneity. Biochem Biophys Res Commun 1991 Oct 15;180(1):23-32.
27. Terpstra V, van Amersfoort ES, van Velzen AG, Kuiper J, van Berkel TJ. Hepatic and extrahepatic scavenger receptors: function in relation to disease. Arterioscler Thromb Vasc Biol 2000 Aug;20(8):1860-1872.
28. Jonsson CA, Carlsten H. Mycophenolic acid inhibits inosine 5'-monophosphate dehydrogenase and suppresses production of pro-inflammatory cytokines, nitric oxide, and LDH in macrophages. Cell Immunol 2002 Mar;216(1-2):93-101.
29. Glomsda BA, Blaheta RA, Hailer NP. Inhibition of monocyte/endothelial cell interactions and monocyte adhesion molecule expression by the immunosuppressant mycophenolate mofetil. Spinal Cord 2003 Nov;41(11):610-619.
30. Maher JJ, Lozier JS, Scott MK. Rat hepatic stellate cells produce cytokine-induced neutrophil chemoattractant in culture and in vivo. Am J Physiol 1998 Oct;275(4 Pt 1):G847-G853.
31. Maher JJ. Interactions between hepatic stellate cells and the immune system. Semin Liver Dis 2001 Aug;21(3):417-426.

5

THE ANTIPROLIFERATIVE DRUG DOXORUBICIN INHIBITS LIVER FIBROSIS IN BILE DUCT-LIGATED RATS AND CAN BE SELECTIVELY DELIVERED TO HEPATIC STELLATE CELLS IN VIVO

Rick Greupink
Hester I. Bakker
Wilma Bouma
Catharina Reker-Smit
Dirk K.F. Meijer
Leonie Beljaars
Klaas Poelstra

Journal of Pharmacology and Experimental Therapeutics 2006; 317(2):514-521

ABSTRACT

Hepatic stellate cell (HSC) proliferation is a key event in liver fibrosis and, therefore, pharmacological intervention with antiproliferative drugs may result in antifibrotic effects. In this paper, the antiproliferative effect of three cytostatic drugs is tested in cultured rat HSC. Subsequently, the antifibrotic potential of the most potent drug was evaluated *in vivo*. As a strategy to overcome drug-related toxicity, we additionally studied how to deliver this drug specifically to HSC by conjugating it to the HSC-selective drug carrier mannose-6-phosphate-modified human serum albumin (M6PHSA). We investigated the effect of cisplatin, chlorambucil and doxorubicin on BrdU-incorporation in cultured HSC, and found DOX to be the most potent drug. Treatment of bile duct-ligated (BDL) rats with daily i.v. injections of 0.35 mg/kg DOX from day 3 to day 10 after BDL, reduced α-smooth muscle actin-stained area in liver sections from 8.5±0.8 to 5.1±0.9% ($P< 0.01$) and collagen-stained area from 13.1±1.3 to 8.9±1.5% ($P<0.05$). DOX was coupled to M6PHSA and the organ distribution of this construct (M6PHSA-DOX) was investigated. Twenty minutes after i.v. administration, 50±6% of the dose was present in the livers and co-localization of M6PHSA-DOX with HSC-markers was observed. Additionally, *in vitro* studies showed selective binding of M6PHSA-DOX to activated HSC. Moreover, M6PHSA-DOX strongly attenuated HSC proliferation *in vitro*, indicating that active drug is released after uptake of the conjugate. In conclusion, DOX inhibits liver fibrosis in BDL rats and HSC-selective targeting of this drug is possible. This may offer perspectives for the application of antiproliferative drugs for antifibrotic purposes.

INTRODUCTION

Liver fibrosis is the common response to chronic liver injury. The activated hepatic stellate cell (HSC) is generally considered as the key cell that is responsible for the excessive collagen deposition during this disease. New antifibrotic strategies therefore mainly focus on the discovery of drugs that inhibit stellate cell functioning (1-7).

Since HSC proliferation is the hallmark of liver fibrosis, the question emerges what would happen if HSC proliferation is inhibited during the fibrotic process. Cytostatic drugs are among the most potent inhibitors of cell proliferation and effects of these drugs on wound healing are well known (8). However, to our knowledge no attempts to test cytostatic drugs in fibrotic animals have been made. Obviously, an important concern when using such drugs is the occurrence of serious side effects in non-hepatic tissues. Even within the liver, treatment with antiproliferative drugs may result in unwanted effects. For instance, inhibition of hepatocyte proliferation may be detrimental to the renewal of functional liver parenchyma, a crucial process in the fibrotic liver (9).

In recent years, HSC-selective drug carriers have become available, which allow drugs to be delivered to HSC with increased specificity (10-12). Conjugating very potent inhibitors of cell proliferation to the HSC-selective drug carrier mannose-6-phosphate-modified human serum albumin (M6PHSA) has therefore now become an option. M6PHSA has been shown to accumulate in HSC *in vivo* via binding to mannose-6-phosphate/insulin-like growth factor-II receptors, which are upregulated on the cell surface of activated HSC (10;13;14). Ligands bound to the receptor are subject to receptor-mediated endocytosis and are routed to the acidic lysosomal compartment, where degradation of the construct and subsequent release of the coupled drug may take place (15;16). If cytostatic drugs can be targeted to the HSC by employing this strategy, this could result in a reduction of

systemic side effects and may improve the applicability of potent antiproliferative agents for antifibrotic purposes, in the future.

The present study first evaluates the antiproliferative effect of three cytostatic drugs in culture-activated rat HSC. Subsequently, the most promising drug from these experiments, doxorubicin (DOX), was tested in a rat experimental model for liver fibrosis, in order to provide better rationale for its use as an antifibrotic drug. Finally, we use *in vitro* and *in vivo* techniques to investigate whether DOX can be selectively delivered to the HSC in a pharmacologically active form by coupling it to M6PHSA.

MATERIALS AND METHODS

HSC isolation

HSC were isolated from the livers of male Wistar rats (> 400 g, Harlan, Horst, The Netherlands) according to the method of Geerts et al. (17). After isolation, HSC were cultured at 37 ºC in a 95% air, 5% CO_2 atmosphere in Dulbecco's Modified Eagles Medium with glutamax-1 (Gibco, Breda, The Netherlands), supplemented with 10% FCS (Biowithaker), 100 U/ml penicillin (Sigma, Gillingham, UK) and 100 µg/ml streptomycin (Sigma). The purity of the HSC culture was assessed after 9 days of culture in the described medium, during which HSC activation spontaneously occurs. In these cultures, always more than 95% of the cells were positive for the activated HSC marker α-smooth muscle actin (α-sma), as assessed by immunohistochemical staining and cell counting.

Effect of drugs on HSC proliferation in vitro

After 9 days in culture, when HSC displayed an activated phenotype, cells were seeded in 24-wells plates at a density of 30,000 cells per well. Cells were incubated with various concentrations of chlorambucil (Sigma), doxorubicin (Pfizer, Capelle

aan den IJssel, The Netherlands) or cisplatin (Sigma) in the presence of 10% FCS, 50 ng/ml Platelet Derived Growth Factor-BB (PDGF-BB) and 10 μM 5-bromo-2'-deoxyuridine for 24h (BrdU, Sigma) to allow detection of proliferating cells by immunohistochemistry. BrdU-incorporation was subsequently quantified by cell counting as described previously (18).

Antifibrotic potential of doxorubicin in BDL rats

Experimental animals

Male Wistar rats of 220-240g were used. Animals had free access to tap water and standard lab chow (Harlan, Horst, The Netherlands). All experiments were approved by the local committee for care and use of laboratory animals and were performed according to strict governmental and international guidelines for the use of experimental animals. Liver fibrosis was induced by ligation of the common bile duct as described previously (10).

Experimental setup

Ten animals were subjected to bile duct ligation under isoflurane/N_2O/O_2 anaesthesia at day 0 of the protocol. On day 3, the animals were randomly divided into two groups and were treated with either PBS (n=5) or DOX (n=5) at a dose of 0.35 mg/kg/day. A total of 7 i.v. injections was given, starting on day 3 of the protocol and the animals were sacrificed 24 hours after the last injection on day 10. Three additional rats were not submitted to bile duct ligation and served as control group.

Number of activated HSC and the extent of liver fibrosis

The number of activated HSC in the liver was assessed by staining for α-sma (Sigma, Gillingham, UK) on 4 μm cryostat sections, according to standard indirect immunohistochemical techniques. To study the extent of fibrosis, cryostat sections of livers were stained for collagen type III (Southern Biotechnology, Birmingham, UK). Also, formalin-fixed paraffin-embedded tissue samples were stained with

picrosirius-red dye to stain all collagens (Sigma). Microphotographs of both stainings were taken at an original magnification of 4x10. The fibrotic area per liver section was quantified by morphometric analysis of the sections using the Image J software package (NIH, Bethesda, ML, USA). Secondary to the antifibrotic effects, also adverse effects were assessed. General toxicity was monitored by analysis of body weight (BW), whereas intrahepatic toxicity of DOX towards liver cells was examined by analysis of serum AST, ALT, AP and γ-GT levels. Inflammatory cell influx in the livers was assessed by diaminobenzidine (DAB) staining as described previously, as well as by evaluation of haematoxylin/eosin-stained liver sections (18;19). To evaluate the effect of DOX on the bile duct epithelial cell proliferation, staining with a monoclonal antibody raised against cytokeratin 7 (Santa Cruz Biotechnology, Santa Cruz, CA, USA) was performed, according to standard indirect immunohistochemical techniques.

Synthesis and characterization of M6PHSA-DOX

M6PHSA was synthesized as described by Beljaars et al. (10). DOX was coupled to this drug carrier via cisaconitic acid according to the method of Shen and Ryser, covalently linking the drug and the carrier via an acid-sensitive spacer, which allows drug release within the acidic lysosomal compartment of cells (20). M6PHSA-DOX was subsequently purified by dialysis against PBS and size-exclusion chromatography on a HiLoad 16/60 Superdex 200 column (Amersham Biosciences, Uppsala, Sweden). After further dialysis against water, the product was lyophilized and stored at –20 °C until use.

Chemical characterization M6PHSA-DOX

The total amount of coupled DOX was assessed by spectrophotometric analysis (21;22). In brief, the conjugate was dissolved in PBS in a concentration of 1 mg/ml. The absorption at 480 nm was measured and the total amount of DOX in the preparation was calculated from a calibration curve. The amount of free drug

was subsequently assessed on an HPLC system fitted with a pump (model 510, Waters, Milford, MA), a Thermoquest 250 x 4.6 mm 5 µm Hypersil BDS C8 column (Thermo Electron Corporation, Waltham, MA) and a UV detector (model 441, Waters) at 254 nm. A solution of 6.7 g trisodiumcitrate in 760 ml water and 240 ml acetonitril (pH adjusted to 4 with formic acid) was used for elution at a flow of 1 ml/min. Monomeric protein content was analyzed by standard SDS-PAGE techniques, using a 10% polyacrylamide gel. The net negative charge of M6PHSA-DOX and control proteins was assessed by anion exchange chromatography on a mono Q column as described previously (10).

In vivo distribution of DOX and M6PHSA-DOX

In vivo organ distribution of ^{125}I-labeled M6PHSA-DOX

One week after bile duct ligation (BDL), animals were injected i.v. with a tracer dose of ^{125}I-labeled M6PHSA-DOX under O_2/N_2O/Isoflurane anaesthesia. Twenty minutes after injection, blood samples were taken by heart puncture (5-10 ml), and the animals were subsequently sacrificed by bleeding after severing the aorta. Organs were harvested and processed as described before. All urine present in the bladder was collected in order to measure the amount of radioactivity that was excreted into the urine. The organ-associated radioactivity was expressed per whole organ, and was corrected for blood-derived radioactivity. The latter was calculated from the radioactivity present in each organ of BDL rats that were injected with ^{125}I-labeled HSA, which is known to remain in the blood. The percentage of the dose of M6PHSA-DOX in blood was calculated from the amount of radioactivity in the 5-10 ml blood sample, by extrapolation to the corresponding value for the total blood volume in rats (60 ml/kg) (10).

Localization of the untargeted and targeted drug

To investigate the distribution of DOX, 20 minutes after i.v. injection of the uncoupled form (2mg/kg), after injection of M6PHSA-DOX (30 mg/kg, which

contains an amount of 2 mg/kg DOX), or after injection of PBS, the animals were sacrificed and 4 μm cryostat sections of liver, kidney and heart were made. These sections were examined by fluorescence microscopy, without embedding the sections in a mounting medium first, since this may corrupt the original localization of DOX. Microphotographs were taken with an Olympus C5050 zoom digital camera and were converted to blue-scale images, so the localization of DOX could be better discerned.

Cellular localization of M6PHSA-DOX

One week after BDL, animals were injected i.v. with 30 mg/kg M6PHSA-DOX. After 20 minutes the animals were sacrificed and tissues were excised and frozen in isopentane at -80 °C. Cryostat sections (4 μm) of liver, heart and kidney were acetone-fixed and stained for the presence of the conjugate with an antibody directed against human serum albumin (HSA, Cappel, Zoetermeer, The Netherlands). In addition, we investigated whether there was co-localization of the injected construct with HSC markers. To this end, double-stainings were performed for HSA and HSC-markers. As a marker for HSC, two monoclonal antibodies were combined: a mouse monoclonal IgG directed against desmin (Sigma) and mouse monoclonal IgG anti-GFAP (Neomarkers, Fremont, CA, USA) (23).

In vitro studies with M6PHSA-DOX

To investigate whether the *in vivo* binding to HSC was mediated by specific binding of M6PHSA-DOX to receptors on HSC, the protein backbone of the conjugate was labeled with ^{125}I according to the chloramine-T method. Culture-activated HSC were exposed to 100,000 cpm of ^{125}I-labeled M6PHSA-DOX at 37 °C, in the absence of a competitor for receptor binding, or in the presence of either 1 mg/ml HSA or 1 mg/ml M6PHSA. After 2 hours, the cell-associated radioactivity was measured on a γ-counter (Riastar, Packard instruments, Palo Alto, USA). The effect of M6PHSA-DOX was investigated as described above for the uncoupled

drugs. The cells were incubated with 10 μg/ml M6PHSA-DOX, an equivalent amount of control protein, or PBS.

Statistical analysis

Results were expressed as the mean ± SEM. One-way ANOVA was used to compare means, and differences were considered statistically significant at $P < 0.05$. For statistical analysis the SPSS software package was used (SPSS Inc, Chicago, IL, USA).

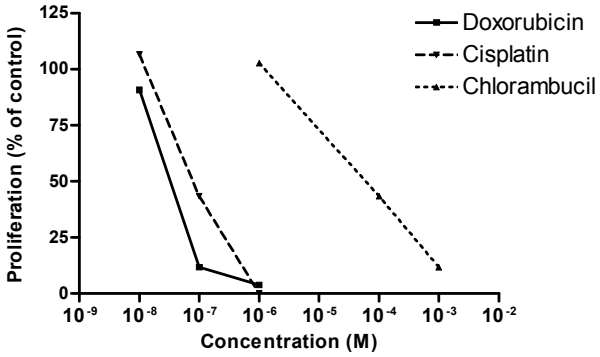

Fig. 1. Typical result of an experiment testing the effect of chlorambucil, cisplatin and doxorubicin on BrdU-incorporation in cultures of primary isolated, culture-activated rat HSC. Data are expressed as a percentage of control.

RESULTS

Effect of drugs on HSC proliferation in vitro

Culture-activated rat HSC were incubated with chlorambucil, cisplatin and doxorubicin in various concentrations. We found that all antiproliferative drugs inhibited BrdU-incorporation in a dose-dependent manner (Fig. 1). Of the tested compounds, doxorubicin was the most potent inhibitor of HSC proliferation. In the concentrations used, cell morphology was not affected as assessed by phase

contrast microscopy (data not shown), which indicates that inhibition of proliferation precedes the cytotoxic effects of these drugs.

Antifibrotic potential of doxorubicin in BDL rats

Based on the results from the *in vitro* study we subsequently investigated the effect of DOX on the fibrotic process *in vivo* (Fig. 2). We found that in BDL animals, treatment with 0.35 mg/kg/day DOX significantly reduced the α-sma-stained area from 8.5 ± 0.8% (PBS-treated BDL rats) to 5.1 ± 0.9% ($P<0.01$). In normal livers only 1.2 ± 0.2% of the total evaluated area of the liver was stained, mainly reflecting α-sma-positive vascular smooth muscle cells in the vessel walls (Fig. 2A-C and J). Treatment with DOX also reduced the amount of collagen, as reflected by a reduction in the collagen type III-stained area within liver sections to 8.9 ± 1.5%, compared to 13.1 ± 1.3% in PBS-treated BDL animals ($P<0.05$). In livers of healthy control rats only 4.9 ± 0.5% of the area was stained for collagen type III (Fig 2. D-F and K). Sirius red staining confirmed the results of DOX on collagen deposition (Fig 2. G-I).

Besides the antifibrotic effect of DOX, treatment with this drug also resulted in significant body weight loss. Furthermore, DOX treatment elicited increased serum γ-GT levels, but not AST and ALT levels, indicating that early hepatocyte or bile duct epithelial cell injury has occurred (Table 1). Yet, the absolute number of bile duct epithelial cells, as assessed by cytokeratin 7 staining (CK7), did not differ between the PBS- and DOX-treated groups (Table 1). Moreover, evaluation of DAB stainings revealed that the number of reactive-oxygen species-producing cells, was also increased in the livers of DOX-treated rats (Table 1). These DAB-positive cells consisted mainly of neutrophils, judged by the presence of polymorphic nuclei in these cells after evaluation of HE-stained liver sections, and based on previous studies (19).

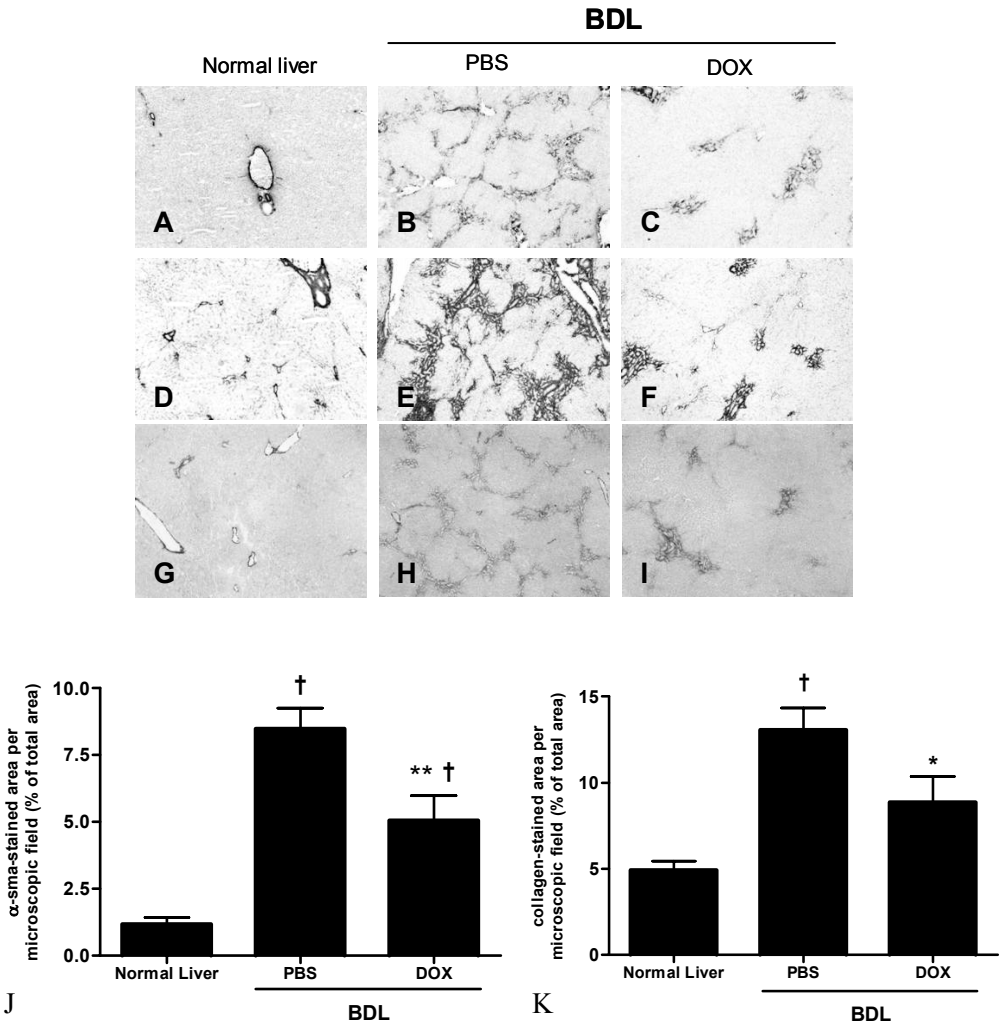

Fig. 2. Effect of treatment with DOX on the number of activated HSC, as assessed by α-sma stainings (A, B, C) and on the amount of collagen present in liver cryostat sections, as assessed by staining with an antibody directed against collagen III (D, E, F) or with picrosirius red (G, H, I). Representative microphotographs were taken at an original magnification of 40x from the livers of healthy animals, PBS-treated BDL-rats and DOX-treated BDL-rats. J: Quantification of α-sma staining by morphometric analysis. K: Quantification of collagen-III-stained area by morphometric analysis. Data are expressed as mean ± SEM. † indicates $P < 0.01$ compared to normal rats, * indicates $P<0.05$ compared to PBS-treated BDL-rats, ** indicates $P<0.01$ compared to PBS-treated BDL rats.

Table. 1. The effect of DOX on toxicity parameters and bile duct epithelial cell proliferation. * indicates P<0.05 compared to PBS-treated BDL rats. N.D: not determined.

	Normal	BDL	
		PBS	DOX
Δ BW (relative to BW at day 3)	N.D.	+ 4.3 ± 1.0%	- 10.1 ± 1.4%*
γ-GT (U/l)	3 ± 0	29.83 ± 4.98	75.70 ± 13.84*
AST (U/l)	50 ± 5	310 ± 53	391 ± 37
ALT (U/l)	30 ± 2	104 ± 32	89 ± 13
AP (U/l)	177 ± 14	436 ± 33	398 ± 42
inflammatory cells (number per microscopic field)	25 ± 1	33 ± 7	97 ± 14*
Bile duct epithelial cells (% CK7-positive area per section)	0.2 ± 0.03	3.9 ± 0.5	3.3 ± 0.4

Synthesis and characterization of M6PHSA-DOX

In order to increase the HSC-specificity of DOX, a conjugate of this drug and M6PHSA was synthesized (Fig. 3A). Spectrophotometric analysis of the construct revealed that per mg of construct 66.7 μg of doxorubicin was present. Of the total amount of doxorubicin in the preparation only 1% was present in uncoupled form, as assessed by HPLC-analysis. SDS-PAGE analysis revealed that no significant amounts of polymeric protein could be detected in the conjugate (Fig 3B). Furthermore, the net negative charge of the conjugate was increased compared to M6PHSA and HSA, which is in agreement with molecules being covalently coupled to the positively-charged amine groups of HSA (Fig 3C). The retention times measured by anion exchange chromatography were 18.9 min, 26.5 min, and 28.0 min for HSA, M6PHSA and M6PHSA-DOX, respectively.

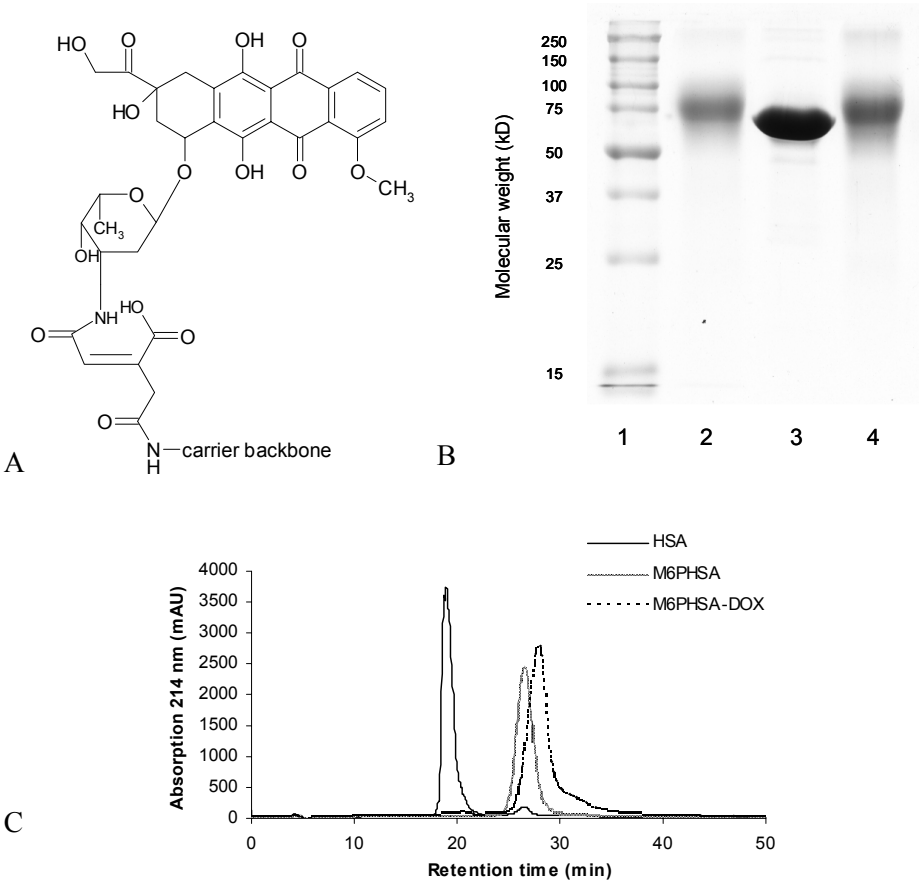

Fig. 3. A: Schematic representation of the chemical bond between DOX and M6PHSA. B: Coommassie Brilliant Blue staining of an SDS-PAGE gel containing the drug carrier and the conjugate. Lane 1: marker, lane 2: M6PHSA-DOX, lane 3: HSA, lane 4: M6PHSA. No significant amount of polymeric protein could be detected. C: Elution profile of HSA, M6PHSA and M6PHSA-DOX on a mono Q anion exchange column. Longer retention times represent an increased net negative charge.

In vivo distribution of DOX and M6PHSA-DOX

In vivo organ distribution of ^{125}I-labeled M6PHSA-DOX

The organ distribution of M6PHSA-DOX in rats with liver fibrosis was assessed 20 minutes after i.v. injection of a radio-labeled tracer dose of the

conjugate. In Fig. 4 it can be seen that already 50 ± 6% of the injected dose distributed to the liver at that time. In heart and kidney, target organs for serious side effects of doxorubicin, only 0.2 ± 0.1% and 1.2 ± 0.5% of the dose accumulated, respectively. In the different parts of the intestine less than 2% of the dose was found and also in the bone marrow no significant radioactivity could be demonstrated (data not shown).

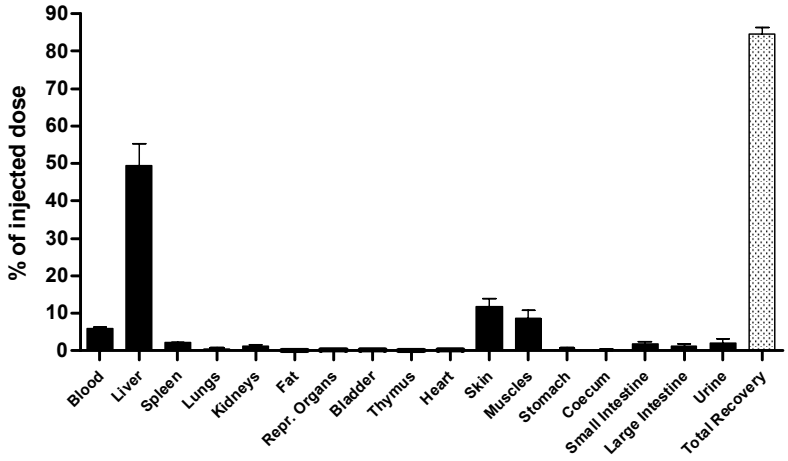

Fig. 4. Organ distribution of radio-labeled M6PHSA-DOX. One week after ligation of the common bile duct, animals were injected with a tracer dose of the ^{125}I-labeled conjugate. Animals were sacrificed 20 minutes after injection. Data represent the average ± SEM of 5 animals.

Localization of the untargeted and targeted drug

To confirm the data of organ distribution studies that were performed with radio-labeled M6PHSA-DOX, immunohistochemical staining for HSA was performed on liver sections and sections of heart and kidney, important organs with respect to DOX toxicity. Strong staining was found in livers in a pattern consistent with accumulation in the non-parenchymal cells of the liver. In hearts and kidneys, complete absence or only minimal staining was found, respectively (Fig. 5 A-C). We also investigated the actual localization of doxorubicin itself by fluorescence microscopy at an excitation wavelength of 450-490 nm and an emission filter > 515 nm, at which DOX fluoresces (Fig. 5 D-I). Administration of free DOX to

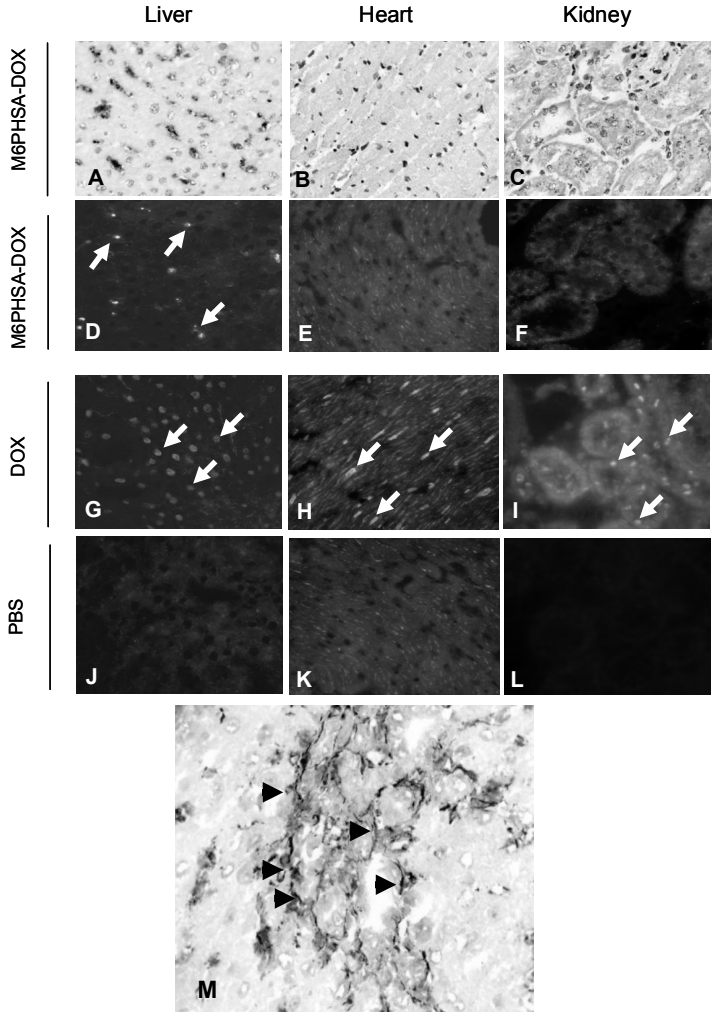

Fig. 5. Images of liver (A, D, G), heart (B, E, H), kidney (C, F, I) from animals receiving M6PHSA-DOX 30 mg/kg (upper two rows) or unconjugated DOX 2 mg/kg (lower row). Immunohistochemical staining for HSA (A-C) was performed to demonstrate the distribution of the drug carrier part of the conjugate (M6PHSA) and fluorescence microscopy was used to detect the drug itself (D-I). Arrows indicate the localization of DOX. Note the change in distribution of DOX after coupling to M6PHSA compared to the uncoupled drug. In the images J, K and L the autofluorescence in livers, hearts and kidneys of BDL rats is shown (original magnification 200x). M: Co-localization of M6PHSA-DOX with HSC-markers in the liver. The conjugate was demonstrated by immunohistochemical staining for HSA (red staining) and HSC were identified with anti-desmin/GFAP antibodies (blue staining). Arrows indicate double-positive cells (original magnification 400x). A full color version of this figure can be found in the appendix.

fibrotic rats resulted in association of the drug with the nuclei of cardiomyocytes and with the nuclei of glomerular and tubular epithelial cells of the kidney, 20 minutes after administration. In the livers, untargeted DOX associated with the nuclei of both hepatocytes and non-parenchymal cells (NPC). However, after coupling of DOX to M6PHSA, no DOX-specific fluorescence could be found at all in heart and kidney. Within the liver, drug-specific fluorescence was notable; animals that received M6PHSA-DOX displayed a non-parenchymal distribution pattern for the drug, with no detectable accumulation in hepatocytes.

Cellular localization of M6PHSA-DOX

To examine in which liver cells the conjugate was taken up, immuno-histochemical double-stainings were performed on liver sections for M6PHSA-DOX together with markers for HSC. We found that M6PHSA-DOX co-localized with HSC-markers (Fig. 5J). As can be seen in the same figure, cells that were HSA-positive but negative for HSC-markers were also found. Further investigation of this revealed that M6PHSA-DOX also co-localized with markers for Kupffer cells (ED2) and liver endothelial cells (RECA-1, data not shown).

In vitro studies with M6PHSA-DOX

To test whether M6PHSA-DOX selectively binds to receptors on HSC, we performed binding studies on culture-activated HSC with ^{125}I-labeled M6PHSA-DOX. In Fig. 6 it can be seen that binding to HSC was reduced by 75.2 ± 6.3% ($P<0.05$) after co-incubation with M6PHSA, which is an M6P/IGF-II receptor ligand. In contrast, the control protein HSA had no significant effect.

Moreover, incubation with M6PHSA-DOX reduced HSC proliferation by 82 ± 15% ($P<0.05$), whereas the drug carrier alone (M6PHSA) exerted no significant effect compared to vehicle-treated control cells (Fig. 7). This indicates that active drug is released, after binding and uptake of the conjugate by the target cells.

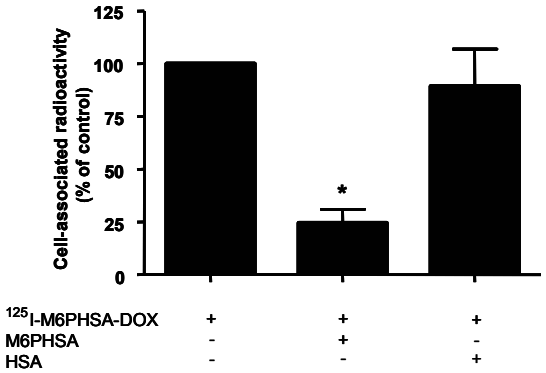

Fig. 6. The influence of competitors on the binding and uptake of ^{125}I-labeled M6PHSA-DOX by culture-activated rat HSC. Note that M6PHSA, a ligand for the M6P/IGF-II receptor, reduces binding of the conjugate by 75.2 ± 6.5%, whereas the control protein HSA exerts no significant effect. Data represent the average ± SEM of 3 independent experiments from 3 different HSC isolations. * indicates P<0.05 compared to control.

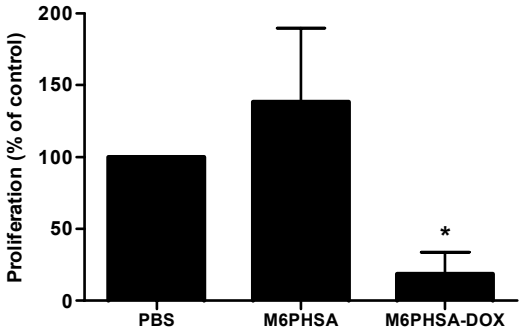

Fig. 7. Effect of M6PHSA and M6PHSA-DOX on HSC proliferation in vitro. * indicates P<0.05 compared to control. Data represent the average ± SEM of 3 independent experiments from 3 different HSC isolations.

DISCUSSION

In the present paper we show that DOX is a potent inhibitor of HSC proliferation *in vitro*, inhibiting cellular proliferation in the nanomolar concentration range. This is in lower concentrations than a number of other typical inhibitors of HSC proliferation *in vitro*, such as mycophenolic acid, statins, the

selective Na+/H+ exchange inhibitor cariporide and the semi-synthetic analogue of fumagillin TNP-470 (4;18;24;25). The higher potency of DOX may be related to the fact that multiple intracellular mechanisms are implicated in its antiproliferative effect, in contrast to these other drugs (26). In this paper we also show that treatment of bile duct ligated rats with doxorubicin reduces the number of activated HSC in the fibrotic rat liver and attenuates the fibrotic process. To our knowledge, this is the first study investigating the use of a cytostatic agent in an experimental model of liver fibrosis and our data indicate that DOX in principle may form a new asset in the treatment of liver fibrosis, for which up till now no pharmacotherapeutics are available. However, the observed side effects will most certainly impede its actual clinical application. In fact, toxicity is a typical problem that forms an obstacle in the application of many other promising antifibrotic drugs as well (27-30).

In this study, the toxicity of DOX was reflected by the loss in body weight, whereas the increased in serum γ-GT levels, but not AST, ALT and AP levels, also suggested hepatocyte or bile duct epithelial cell injury. It is known that during the early stages of hepatocellular injury such an isolated γ-GT increase can precede AP, ALT or AST elevation (31). Very likely, the increased number of DAB-positive cells that we observed is the result of an immune response in reaction to this damage. It is known that drug-induced hepatic inflammation can lead to liver fibrosis, but usually this takes a prolonged period of time. In the present animal model, which is characterized by a very fast proliferation of fibrogenic cells, the antiproliferative effect of DOX on these cells apparently prevails, resulting in the observed antifibrotic effect. It would therefore be interesting to investigate the antifibrotic potential of DOX in animal models in which fibrosis progression is slower, for example in the CCl_4 model. In this BDL model, the antifibrogenic effect of DOX was most prominent in the parenchyma and less clear in the portal areas. Whether this is due to a reduced sensitivity of portal fibroblasts to DOX, or

due to lower drug concentrations in this highly fibrotic area, remains to be established.

Although this DOX-induced hepatic inflammation does not result in a worsening of fibrosis, it should still be considered that an even more potent antifibrotic effect can be obtained, when the influx of inflammatory cells is avoided. The same may be true for the observed weight loss seen in DOX-treated rats, since it has been shown that alcohol in combination with malnutrition causes more severe liver fibrosis in rats (32). In this way HSC-selective delivery of DOX may not only help to avoid general drug-related toxicity, but also contribute to the antifibrogenic potential of DOX via the avoidance of pro-fibrogenic side effects.

Analysis of circulating white blood cell counts revealed no significant differences between DOX-treated BDL rats and PBS-treated BDL rats (data not shown), suggesting that no relevant meyelosuppressive effect was at hand at the present dose of DOX and duration of administration. This renders it unlikely that the antifibrotic effect of DOX we describe here is mediated via the known meyelosuppressive effect of the drug.

Besides the proliferation of HSC, proliferation of ductular epithelial cells occurs in the liver after ligation of the common bile duct. Our data revealed that the ductular response of BDL rats was not significantly affected by treatment with DOX. A possible reason for this is the high expression of mdr1a drug efflux transporters in the apical membrane of the cholangiocytes (33). Since doxorubicin is a substrate for mdr1a, it is conceivable that the resistance of cholangiocytes to DOX is due to a high efflux of the drug from these cells.

To limit the effect of DOX to fibrogenic cells and to avoid the described extra- and intrahepatic toxicity, we set out to investigate the targeted delivery of DOX to the HSC. From physico-chemical analyses we concluded that coupling of DOX to the HSC-selective drug carrier M6PHSA was successful. *In vivo*, the conjugate rapidly and selectively accumulated in the liver, whereas the untargeted drug also accumulated in organs that are prone to DOX toxicity. Within the liver, the uptake

of M6PHSA-DOX was confined to the non-parenchymal cells and the observed co-localization of M6PHSA-DOX with HSC-markers indicated that HSC were reached successfully. Next to the uptake in HSC, also co-localization with Kupffer cell and endothelial cell markers was observed. This very likely reflects scavenger receptor-mediated uptake of M6PHSA-DOX by these cells, since this is a highly negatively charged molecule. To attenuate uptake by these other non-parenchymal cells, the net charge of this construct should be modified. Nevertheless, we could clearly demonstrate that, although not 100% specific, injection with M6PHSA-DOX leads to a significant increase in stellate cell-selectivity compared to the untargeted drug. It remains to be established if the uptake of M6PHSA-DOX in Kupffer cells and liver endothelial cells results in toxicity or whether this contributes to the therapeutic effect of the conjugate. It is known from literature that an attenuation of Kupffer cell functioning may attenuate fibrogenesis (34).

The binding of M6PHSA-DOX to HSC was confirmed by studies performed with a ^{125}I-labeled conjugate in cultures of activated HSC. The association of radio-labeled M6PHSA-DOX with the cells could be inhibited by an excess of M6PHSA but not by HSA, indicating that receptor-mediated uptake of the construct takes place. Moreover, the strong inhibition of cell proliferation by M6PHSA-DOX that we observed also indicates that active drug can be released from the conjugate after uptake by activated HSC.

Although these results show that the targeted delivery of a cytostatic drug to the HSC is possible, it is evident that chronic treatment of fibrotic rats is necessary to test the ultimate antifibrotic potential of this targeted strategy. However, before performing those studies, it will be necessary to better understand the pharmacokinetics of M6PHSA-DOX in fibrotic animals, as well as its intracellular kinetics within HSC. Explicitly, information on the mechanisms through which this new chemical entity is processed by activated HSC, and the rate at which intracellular drug release and elimination occur, will largely dictate the dosage regime of M6PHSA-DOX in chronically treated rats. Based on the expected

differences in cellular handling between the targeted and untargeted drug, this may be very dissimilar for the two compounds. Yet, irrespective of the eventual dosing regimen required, it is likely that by virtue of the improved organ and cell specificity, and the resulting smaller volume of distribution, the total body dose of M6PHSA-DOX can be reduced compared to untargeted DOX, whereas still similar drug concentrations can be obtained within HSC.

In summary, we have shown that treatment of BDL rats with free DOX inhibits the progression of experimental liver fibrosis and strongly inhibits HSC proliferation *in vitro*. Subsequently, we succeeded in delivering this potent antiproliferative drug to HSC *in vitro* as well as *in vivo*. By doing so, accumulation of DOX in extrahepatic tissues as well as hepatocytes was avoided. We conclude that DOX exerts potent antifibrotic effects in bile duct-ligated rats. In conjunction with the here-described drug delivery strategy this may offer perspectives for the use of potent but relatively toxic antiproliferative drugs in the pharmacological treatment of liver fibrosis.

ACKNOWLEDGEMENTS

A. van Loenen, M. de Ruijter, P. Tepper, J.H. Pol and J. Visser are all gratefully acknowledged for their excellent technical assistance. Dr. R.J. Kok is thanked for valuable scientific discussion.

REFERENCE LIST

1. Eng FJ, Friedman SL. Fibrogenesis I. New insights into hepatic stellate cell activation: the simple becomes complex. Am J Physiol Gastrointest Liver Physiol 2000; 279: G7-G11.
2. Friedman SL. Molecular regulation of hepatic fibrosis, an integrated cellular response to tissue injury. J Biol Chem 2000; 275: 2247-50.

3. Kurikawa N, Suga M, Kuroda S, Yamada K, Ishikawa H. An angiotensin II type 1 receptor antagonist, olmesartan medoxomil, improves experimental liver fibrosis by suppression of proliferation and collagen synthesis in activated hepatic stellate cells. Br J Pharmacol 2003; 139: 1085-94.
4. Rombouts K, Kisanga E, Hellemans K, Wielant A, Schuppan D, Geerts A. Effect of HMG-CoA reductase inhibitors on proliferation and protein synthesis by rat hepatic stellate cells. J Hepatol 2003; 38: 564-72.
5. Niki T, Rombouts K, De Bleser P, De Smet K, Rogiers V, Schuppan D, Yoshida M, Gabbiani G, Geerts A. A histone deacetylase inhibitor, trichostatin A, suppresses myofibroblastic differentiation of rat hepatic stellate cells in primary culture. Hepatology 1999; 29: 858-67.
6. Caligiuri A, De Franco RM, Romanelli RG, Gentilini A, Meucci M, Failli P, Mazzetti L, Rombouts K, Geerts A, Vanasia M, Gentilini P, Marra F, Pinzani M. Antifibrogenic effects of canrenone, an antialdosteronic drug, on human hepatic stellate cells. Gastroenterology 2003; 124: 504-20.
7. Di Sario A, Bendia E, Svegliati BG, Ridolfi F, Casini A, Ceni E, Saccomanno S, Marzioni M, Trozzi L, Sterpetti P, Taffetani S, Benedetti A. Effect of pirfenidone on rat hepatic stellate cell proliferation and collagen production. J Hepatol 2002; 37: 584-91.
8. Bland KI, Palin WE, von Fraunhofer JA, Morris RR, Adcock RA, Tobin GR. Experimental and clinical observations of the effects of cytotoxic chemotherapeutic drugs on wound healing. Ann Surg 1984; 199: 782-90.
9. Fausto N. Liver regeneration and repair: hepatocytes, progenitor cells, and stem cells. Hepatology 2004; 39: 1477-87.
10. Beljaars L, Molema G, Weert B, Bonnema H, Olinga P, Groothuis GM, Meijer DK, Poelstra K. Albumin modified with mannose 6-phosphate: A potential carrier for selective delivery of antifibrotic drugs to rat and human hepatic stellate cells. Hepatology 1999; 29: 1486-93.
11. Beljaars L, Molema G, Schuppan D, Geerts A, de Bleser PJ, Weert B, Meijer DK, Poelstra K. Successful targeting to rat hepatic stellate cells using albumin modified with cyclic peptides that recognize the collagen type VI receptor. J Biol Chem 2000; 275: 12743-51.
12. Beljaars L, Weert B, Geerts A, Meijer DK, Poelstra K. The preferential homing of a platelet derived growth factor receptor-recognizing macromolecule to fibroblast-like cells in fibrotic tissue. Biochem Pharmacol 2003; 66: 1307-17.

13. de Bleser PJ, Jannes P, van Buul-Offers SC, Hoogerbrugge CM, van Schravendijk CF, Niki T, Rogiers V, van den Brande JL, Wisse E, Geerts A. Insulinlike growth factor-II/mannose 6-phosphate receptor is expressed on CCl4-exposed rat fat-storing cells and facilitates activation of latent transforming growth factor-beta in cocultures with sinusoidal endothelial cells. Hepatology 1995; 21: 1429-37.
14. de Bleser PJ, Scott CD, Niki T, Xu G, Wisse E, Geerts A. Insulin-like growth factor II/mannose 6-phosphate-receptor expression in liver and serum during acute CCl4 intoxication in the rat. Hepatology 1996; 23: 1530-7.
15. Braulke T, Mieskes G. Role of protein phosphatases in insulin-like growth factor II (IGF II)-stimulated mannose 6-phosphate/IGF II receptor redistribution. J Biol Chem 1992; 267: 17347-53.
16. Dahms NM, Hancock MK. P-type lectins. Biochim Biophys Acta 2002; 1572: 317-40.
17. Geerts A, Niki T, Hellemans K, De Craemer D, Van Den Berg K, Lazou JM, Stange G, Van De Winkel M, De Bleser P. Purification of rat hepatic stellate cells by side scatter-activated cell sorting. Hepatology 1998; 27: 590-8.
18. Greupink R, Bakker HI, Reker-Smit C, Loenen-Weemaes AM, Kok RJ, Meijer DK, Beljaars L, Poelstra K. Studies on the targeted delivery of the antifibrogenic compound mycophenolic acid to the hepatic stellate cell. J Hepatol 2005; 43: 884-92.
19. Poelstra K, Hardonk MJ, Koudstaal J, Bakker WW. Intraglomerular platelet aggregation and experimental glomerulonephritis. Kidney Int 1990; 37: 1500-8.
20. Shen WC, Ryser HJ. cis-Aconityl spacer between daunomycin and macromolecular carriers: a model of pH-sensitive linkage releasing drug from a lysosomotropic conjugate. Biochem Biophys Res Commun 1981; 102: 1048-54.
21. Griffiths GL, Mattes MJ, Stein R, Govindan SV, Horak ID, Hansen HJ, Goldenberg DM. Cure of SCID mice bearing human B-lymphoma xenografts by an anti-CD74 antibody-anthracycline drug conjugate. Clin Cancer Res 2003; 9: 6567-71.
22. Wirth M, Fuchs A, Wolf M, Ertl B, Gabor F. Lectin-mediated drug targeting: preparation, binding characteristics, and antiproliferative activity of wheat germ agglutinin conjugated doxorubicin on Caco-2 cells. Pharm Res 1998; 15: 1031-7.
23. Geerts A. History, heterogeneity, developmental biology, and functions of quiescent hepatic stellate cells. Semin Liver Dis 2001; 21: 311-35.
24. Di Sario A, Bendia E, Taffetani S, Marzioni M, Candelaresi C, Pigini P, Schindler U, Kleemann HW, Trozzi L, Macarri G, Benedetti A. Selective Na+/H+ exchange inhibition by cariporide reduces liver fibrosis in the rat. Hepatology 2003; 37: 256-66.

25. Wang YQ, Ikeda K, Ikebe T, Hirakawa K, Sowa M, Nakatani K, Kawada N, Kaneda K. Inhibition of hepatic stellate cell proliferation and activation by the semisynthetic analogue of fumagillin TNP-470 in rats. Hepatology 2000; 32: 989.
26. Gewirtz DA. A critical evaluation of the mechanisms of action proposed for the antitumor effects of the anthracycline antibiotics adriamycin and daunorubicin. Biochem Pharmacol 1999; 57: 727-41.
27. Pinzani M, Rombouts K, Colagrande S. Fibrosis in chronic liver diseases: diagnosis and management. J Hepatology 2005; 42 Suppl: S22-S36.
28. Bataller R, Brenner DA. Liver fibrosis. J Clin Invest 2005; 115: 209-18.
29. Canbay A, Feldstein A, Baskin-Bey E, Bronk SF, Gores GJ. The caspase inhibitor IDN-6556 attenuates hepatic injury and fibrosis in the bile duct ligated mouse. J Pharmacol Exp Ther 2004; 308: 1191-6.
30. Hagens WI, Olinga P, Meijer DKF, Grootnuis GMM, Beljaars L, Poelstra K. Gliotoxin non-selectively induces apoptosis in fibrotic and normal livers, Liver Int., 2006, in press.
31. Moss DW, Henderson AR. Clinical enzymology. p 686-689. In: Burtis CA, Ashwood ER (ed.). Tietz textbook of clinical chemistry. 3rd ed Saunders, Philadelphia, 1999.
32. Bosma A, Seifert WF, van Thiel-de Ruiter GC, van Leeuwen RE, Blauw B, Roholl P, Knook DL, Brouwer A. Alcohol in combination with malnutrition causes increased liver fibrosis in rats. J Hepatol 1994; 21: 394-402.
33. Gigliozzi A, Fraioli F, Sundaram P, Lee J, Mennone A, Alvaro D, Boyer JL. Molecular identification and functional characterization of Mdr1a in rat cholangiocytes. Gastroenterology 2000; 119: 1113-22.
34. Rivera CA, Bradford BU, Hunt KJ, Adachi Y, Schrum LW, Koop DR, Burchardt ER, Rippe RA, Thurman RG. Attenuation of CCl(4)-induced hepatic fibrosis by GdCl(3) treatment or dietary glycine. Am J Physiol Gastrointest Liver Physiol 2001; 281: G200-G207

6

PHARMACOKINETICS OF A HEPATIC STELLATE CELL-TARGETED DOXORUBICIN CONSTRUCT IN RATS WITH LIVER FIBROSIS

Rick Greupink
Catharina Reker-Smit
Anne-miek van Loenen Weemaes
Marjolijn de Hooge
Johannes H. Proost
Klaas Poelstra
Leonie Beljaars

Submitted

ABSTRACT

Inhibition of hepatic stellate cell (HSC) proliferation is a relevant strategy to inhibit liver fibrosis. Coupling of antiproliferative drugs to the HSC-selective drug carrier mannose-6-phosphate-modified human serum albumin (M6PHSA) may lead to selective inhibition of HSC proliferation, while avoiding systemic side effects. We coupled the antiproliferative drug doxorubicin (DOX) to this drug carrier and in the present study we investigated plasma disappearance, hepatic uptake and intrahepatic distribution of this construct in a rat model of liver fibrosis. In addition, drug release from the construct was studied *in vitro*. M6PHSA-DOX was cleared from the plasma in a biphasic manner. Upon i.v. injection of 4 μg/kg (tracer), 2 and 20 mg/kg, the clearance in the distribution phase of drug disposition (CL_d) significantly decreased in a dose dependent manner from 9.7±0.7 to 4.7±2.3 and 1.0±0.1 $ml.kg^{-1}.min^{-1}$. This indicates that saturation of clearance mechanisms occurs in this phase of drug disposition, likely reflecting saturable receptor-mediated uptake in the target cells. Gamma-camera studies revealed that the conjugate was rapidly and almost completely taken up by the liver, and immunohistochemical double-staining of liver sections demonstrated co-localization of the construct with HSC-markers. Simulation of the release of DOX from the carrier, after cellular uptake by HSC and routing to the lysosomes, showed that a gradual release of the drug takes place over a 9 hour period. Moreover, fluorescence microscopy studies in cultured HSC illustrated that after 24h incubation with the conjugate, DOX was associated with the cell nucleus, indicating that drug release also takes place within HSC. In conclusion, the rapid distribution of M6PHSA-DOX from the blood to HSC in the fibrotic liver, in combination with the expected gradual release of DOX within lysosomes of HSC, make this construct a promising tool for achieving a sustained and selective inhibition of HSC proliferation during liver fibrosis.

INTRODUCTION

Liver fibrosis is characterized by the excessive accumulation of collagen and other extracellular matrix proteins (ECM) as a result of chronic liver injury. The activated hepatic stellate cell (HSC) has been identified as the principal producer of these proteins in the fibrotic liver and therefore this cell type is considered a primary target for the development of new pharmacological treatments for this disease. Because HSC proliferation is a key event during fibrogenesis, the application of antiproliferative drugs for the treatment of this disease is a relevant option (1-3).

In previous work, we have identified doxorubicin (DOX) as a very potent inhibitor of HSC proliferation *in vitro* (4). Furthermore, we have shown that treatment of rats with experimental liver fibrosis with this antiproliferative drug reduced the number of activated HSC in the livers and also reduced collagen deposition (4). However, serious adverse effects preclude its clinical use for the treatment of this chronic liver disease. Coupling of DOX to the HSC-selective drug carrier mannose-6-phosphate-modified human serum albumin (M6PHSA) may reduce the toxicity in non-target tissues.

M6PHSA has been designed to interact with Mannose-6-Phosphate/Insulin-like Growth Factor-II receptors (M6P/IGF-II receptors) (5;6), which are upregulated on activated HSC (7-9). After receptor binding, ligands are internalized and routed to the lysosomal compartment, in which the degradation of the receptor-bound proteins takes place (10). By coupling drugs to M6PHSA, this route can be used for the selective delivery of drugs to M6P/IGF-II receptor bearing cells. Immunohistochemical studies that investigated the M6P/IGF-II receptor expression in experimental liver fibrosis secondary to bile duct ligation, revealed that the receptor is expressed on fibrogenic cells of the liver already during the early stages of experimental liver fibrosis (Greupink et al, manuscript submitted). Indeed, *in vivo* studies in rats with bile duct ligation (BDL)-induced liver fibrosis showed

extensive co-localization of an M6PHSA-DOX conjugate with HSC markers, but detailed information on the pharmacokinetics of this conjugate is still lacking. Such data are very important when employing HSC-targeted cytostatic drugs during liver disease.

The experiments described in this paper therefore serve to gain a further understanding of the pharmacokinetics of M6PHSA-DOX in rats with experimental liver fibrosis. Secondly, the paper investigates the release of DOX from its carrier by *in vitro* techniques. It may form the basis of HSC-selective antiproliferative therapies aimed at reducing liver fibrosis.

MATERIALS AND METHODS

Experimental animals and experimental model of fibrosis

Male Wistar rats (Harlan, Horst, The Netherlands) of 220-240g were housed under a 12-hour dark/light cycle, at constant humidity and temperature. Animals had free access to tap water and standard lab chow (Harlan). All experiments were approved by the local committee for care and use of laboratory animals and were performed according to strict governmental and international guidelines for the use of experimental animals. Liver fibrosis was induced by ligation of the common bile duct (BDL) under O_2/N_2O/Isoflurane anaesthesia as described previously (11).

Synthesis of M6PHSA-DOX

M6PHSA was synthesized and characterized as described by Beljaars et al. (6). DOX (Pfizer, Capelle a/d IJssel, The Netherlands) was coupled to M6PHSA according to the method of Shen and Ryser as described previously (12). Subsequently, M6PHSA-DOX was purified by extensive dialysis against PBS and size exclusion chromatography on a HiLoad Superdex column (GE healthcare, Den Bosch, The Netherlands) with PBS. After dialysis against water, the product was

lyophilized and stored at –20 °C until use. The total amount of DOX and the amount of free DOX present in the preparation were quantitated by spectrophotometric analysis and HPLC analysis, respectively (4).

Radioactive labeling of HSA and M6PHSA-DOX

HSA and M6PHSA-DOX were labeled with ^{123}I for gamma-camera studies or with ^{125}I for plasma disappearance experiments, via a chloramine T method. Protein precipitation with trichloroacetic acid was performed to assess the percentage of free ^{123}I or ^{125}I in the preparations. To investigate whether the labeling procedure resulted in the formation of protein aggregates, we performed size exclusion chromatography on the constructs before administration to the animals. To this end, preparations were injected onto an HPLC system, fitted with a HR 16/300 Superdex 200 column (GE Healthcare), employing isocratic elution with PBS as a mobile phase at a flow of 1 ml/min. Samples were detected online spectrophotometrically at 280 nm and via a gamma-counter.

Plasma disappearance

Ten days after BDL, when plasma bilirubin levels are high and hepatic fibrosis is evident (13), animals were anaesthetized as described above and the carotid artery was cannulated to allow rapid blood sampling. A single dose of 4 µg/kg (tracer, n=2), 2 mg/kg (n=3) or 20 mg/kg (n=3) of M6PHSA-DOX was administered i.v. via the penis vein. To estimate the rate of plasma disappearance, unlabeled dosages of M6PHSA-DOX were supplemented with a tracer dose of 106 cpm of ^{125}I-labeled conjugate.

Blood samples of 0.5 ml were collected in heparinized tubes at 2, 5, 7, 10, 15, 30 and 60, 90 and 120 minutes after administration. During the experiments, the body temperature of the animals was maintained at 37 °C by placing them on thermostatic pads. Blood samples were centrifuged at 7000g for 5 minutes to obtain plasma and subsequently, 100 µl of plasma was treated with an equal

volume of 20% trichloroacetic acid to precipitate proteins. After centrifugation, the radioactivity in the pellet was counted with a γ-counter (Riastar, Packard instruments, Palo Alto, USA). Based on the amount of radioactivity in the pellet and the administered dosages of both radioactive as well as unlabeled material we calculated the total concentration of protein present in the plasma at the various time points after injection. Pharmacokinetic parameters were then derived from the data of individual animals, using the non-linear curvefitting program Multifit (Dr. J.H. Proost, Department of Pharmacokinetics and Drug Delivery, University of Groningen, The Netherlands).

Whole-body distribution and kinetics of hepatic uptake

Ten days after BDL, rats were anaesthetized with 0.4 ml/kg Hypnorm in combination with 2 mg/kg diazepam intramuscularly. The rats were placed on the low-energy all-purpose collimator of a gamma-camera and were i.v. injected with a tracer dose of ^{123}I-M6PHSA-DOX (n=3). Additionally, three animals were injected with ^{123}I-HSA in order to be able to correct for blood-derived radioactivity. For analysis of the scans, the body area that encompasses the liver was highlighted in all rats, and the distribution of radioactivity to this area of interest was dynamically monitored from t=0 to t=20 minutes after injection with a frame-rate of one total body scan per 30 seconds. At the end of the 20 minute scan-period, a final whole-body scan of 5 minutes was performed to assess the distribution at this time-point.

Intrahepatic distribution of M6PHSA-DOX

To investigate the intrahepatic distribution of the conjugate, fibrotic rats received a single i.v. injection of 2 or 20 mg/kg M6PHSA-DOX. Rats were sacrificed 20 minutes after injection and the livers were excised. On 4 μm cryostat sections of the livers immunohistochemical double-stainings were performed for the conjugate and markers for HSC. As a marker for HSC, two monoclonal antibodies were combined: a mouse monoclonal IgG directed against desmin

(Sigma) and mouse monoclonal IgG anti-GFAP (Neomarkers, Fremont, CA, USA), according to standard methods for HSC detection (14). The conjugate itself was visualized with an antibody directed against HSA (Cappel, Zoetermeer, The Netherlands).

Drug release in buffer pH=4.5

To investigate whether DOX could be released from the conjugate in an acidic environment such as present in the lysosomal compartment of cells, M6PHSA-DOX was incubated for 0.75, 2, 3, 9, and 20 hours in a 0.1 M Na_2HPO_4/citric acid buffer, pH=4.5. Release of DOX was monitored by injecting the samples onto an HPLC system fitted with a Waters pump (model 510), a µBondapack C18 guard column, a Thermoquest 250 x 4.6 mm 5µm Hypersil BDS C8 column and a Waters UV detector (model 441) at 254 nm. A solution of 6.7 g trisodiumcitrate in 760 ml water and 240 ml acetonitril (pH adjusted to 4 with formic acid) was used for elution at a flow of 1 ml/min. The amount of released DOX was then calculated from a calibration curve and related to the total amount of coupled DOX.

In vitro studies with HSC

HSC were isolated from male Wistar rats and cultured as described by Geerts et al. (15). Seven days after isolation of HSC, 10,000 cells/well were plated onto glass labteck incubation chambers (Nalge Nunc International, Rochester, NY, USA). Subsequently, after 2 days when HSC have a fully activated phenotype, HSC were incubated with 10 µg/ml of DOX or 50 µg/ml of M6PHSA-DOX for 24 hours, at 37 °C. After washing, the doxorubicin-specific fluorescence in the cells was evaluated with a fluorescence microscope (Leitz, Wetzlar, Germany) equipped with a 450-490 nm excitation / > 515 nm emission filter (16), without embedding the samples in mounting medium.

Statistical analysis

Results were expressed as the mean +/- SD. Data were subjected to a one-way analysis of variance followed by the LSD post-hoc test and differences were considered statistically significant at $P<0.05$. Statistical analyses were performed with the SPSS software package (SPSS Inc, Chicago, IL, USA).

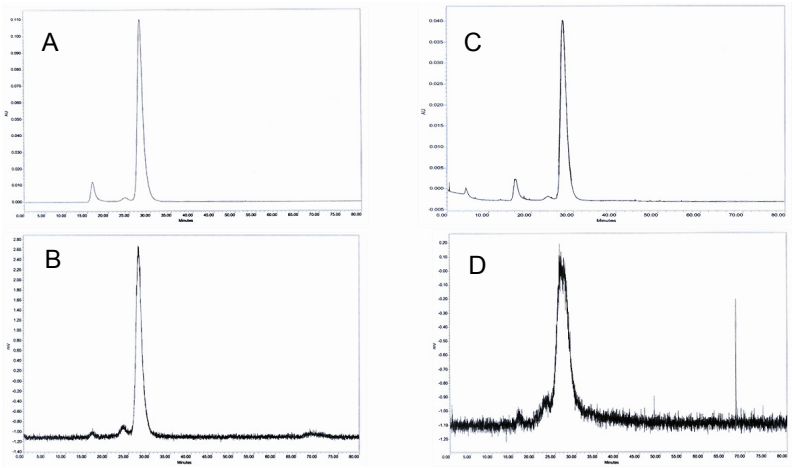

Fig. 1. Size exclusion chromatograms of ^{123}I-labeled HSA (A,B) and ^{123}I-labeled M6PHSA-DOX (C,D). Fig A and C: on-line spectrophotometric detection of the proteins at $UV_{280\ nm}$. Fig B and D: detection of the ^{123}I label in the same HPLC run. The monomeric protein peak elutes at 30 minutes.

RESULTS

Synthesis of M6PHSA-DOX and radioactive labeling

The M6PHSA-DOX conjugate that was used for the present experiments contained 66.7 µg DOX per mg of the construct. HSA, which was used to estimate blood-derived radioactivity in the gamma-camera study, and the DOX-containing conjugate were both successfully labeled without the formation of significant protein aggregates in the preparations (Fig. 1). TCA precipitation of the labeled constructs revealed that the samples did not contain relevant amounts of unbound

iodine (<10%). Size-exclusion chromatography was performed to investigate whether the labeling procedure resulted in the formation of large amounts of protein aggregates. In Fig. 1 it can be seen that the injected proteins contained only minor amounts of polymeric protein (monomeric peak at 30 minutes).

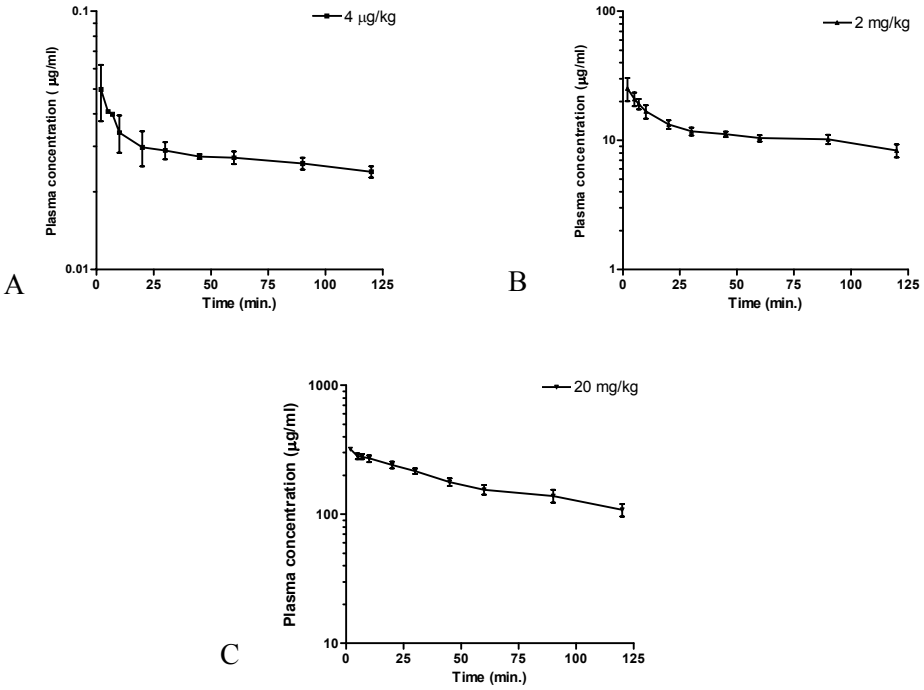

Fig. 2. Plasma disappearance curves after injection of a 4 μg/kg tracer dose (A, n=2), 2 mg/kg (B, n=3) or 20 mg/kg (C, n=3) M6PHSA-DOX in rats with liver fibrosis. Data are expressed as the mean ± SD.

Plasma disappearance and pharmacokinetic parameters

In Fig. 2A-C, the plasma disappearance curves after i.v. injection of M6PHSA-DOX are displayed. To investigate how plasma-disappearance data could be best described, as a first estimation we fitted the parameters of one-, two- and three-compartment models to the plasma concentration data. The best fit, as assessed by calculation of Akaike's Information Criterion, was for all dosages obtained with a two-compartment model. The calculated pharmacokinetic parameters for a two-

compartment model, assuming that elimination takes place from the peripheral compartment, are listed in table 1. We found that the clearance in the distribution phase of disposition (CL_d) significantly decreased when the dose was increased. Clearance (CL), initial volume of distribution (V_1), volume of distribution at steady state (V_{ss}) and terminal half-life ($t_{1/2}$ (2)) did not significantly differ with the dose.

Table 1. Pharmacokinetic parameters of M6PHSA-DOX administered i.v. to fibrotic rats. Plasma concentration data of each animal were analysed separately using a two-compartment model with elimination from the peripheral compartment. Data are expressed as the mean ± SD. † indicates P<0.05 compared to tracer-injected rats, * indicates P< 0.05 compared to rats injected with 2 mg/kg M6PHSA-DOX. $t_{1/2}$ (1): initial half-life, $t_{1/2}$ (2): terminal half-life, AUC0-120: area under the curve up to 120 min, CL_d: distribution clearance, CL: clearance, V_1: initial volume of distribution, V_{ss}: volume of distribution at steady state.

Parameter	4 µg/kg	2 mg/kg	20 mg/kg	Unit
$t_{½}$ (1)	2.29 ± 0.03	6.82 ± 3.86	26.0 ± 2.8*†	Min
$t_{½}$ (2)	362 ± 180	246 ± 107	230 ± 50	Min
$AUC_{0\text{-}120}$	3.4 ± 0.4	1385 ± 194†	20790 ± 2515*†	$min.\mu g.ml^{-1}$
CL_d	9.7 ± 0.7	4.7 ± 2.3	1.0 ± 0.1*†	$ml.kg^{-1}.min^{-1}$
CL	0.28 ± 0.12	0.49 ± 0.18	0.38 ± 0.02	$ml.kg^{-1}.min^{-1}$
V_1	67 ± 21	75 ± 33	64 ± 4	$ml.kg^{-1}$
V_{ss}	131 ± 11	160 ± 18	140 ± 32	$ml.kg^{-1}$

Whole-body distribution, kinetics of hepatic uptake and intrahepatic uptake

Gamma-camera studies were performed to assess the whole-body distribution of M6PHSA-DOX in time after i.v. injection (Fig. 3). Studies were performed 10 days after BDL when fibrosis is rapidly progressing and HSC activation and proliferation is eminent (13). First, ^{123}I-HSA was injected in order to estimate blood-derived radio-activity. After rapid distribution throughout the circulation within 30 seconds after injection, a constant blood-related background signal was found to be associated with well perfused organs such as heart, lungs, kidneys and

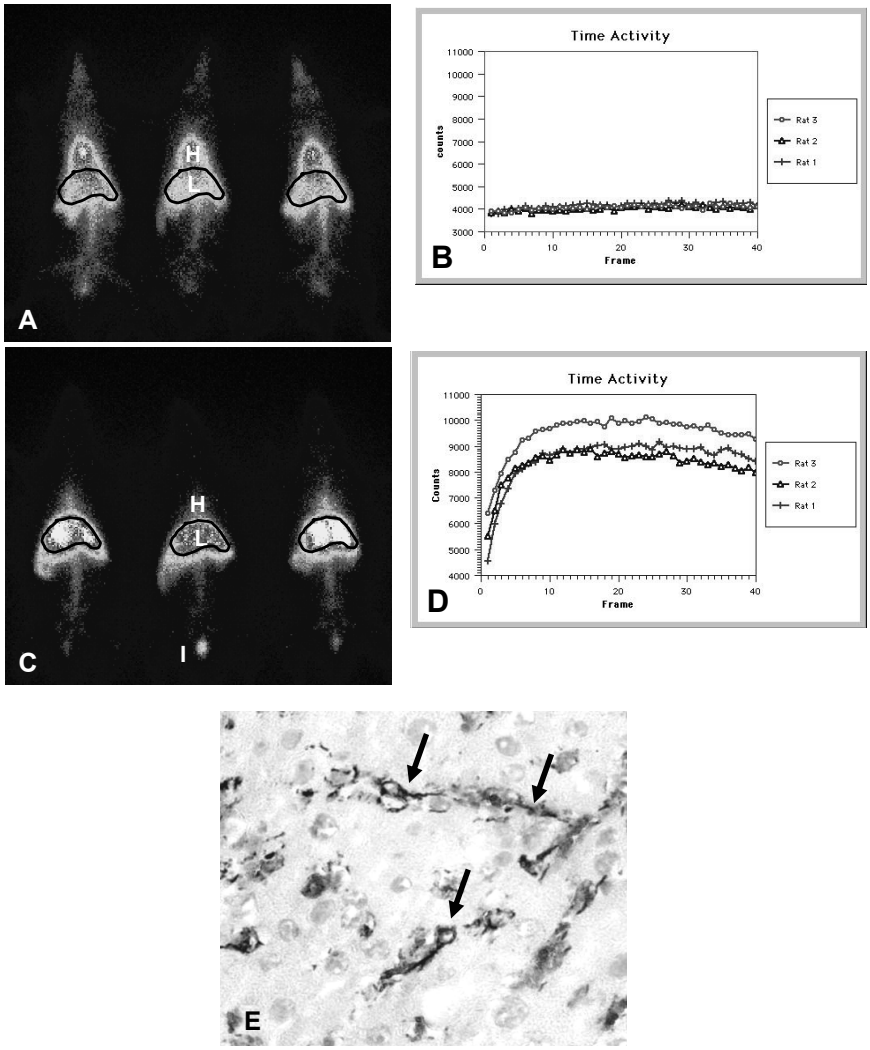

Fig. 3 A. Whole body scan taken with a gamma-camera at the end of the 20 minute test period of 3 animals that received ^{123}I-labeled HSA. B: Accumulation of ^{123}I-labeled HSA within the designated area of interest (the liver), as assessed by image analysis of consecutive γ-camera scans during the first 20 minutes after i.v. injection. C: Whole body scan taken at the end of the 20 minute test period of 3 animals that received ^{123}I-labeled M6PHSA-DOX. D: Association of radio-activity with the liver region during the first 20 minutes after i.v. injection of ^{123}I-labeled M6PHSA-DOX. E: Double-staining for M6PHSA-DOX (red staining) with HSC markers (blue staining) in liver sections (original magnification 200x). Arrows indicate co-localization of the construct with HSC markers. In the whole body scans, H indicates heart, L indicates liver, and I indicates the injection site. A full color version of this figure can be found in the appendix.

the liver (Fig. 3A and B). In contrast, after injection of M6PHSA-DOX, a rapid and high distribution to the livers was found, reaching maximum levels already within 5 minutes after injection. Signals in other organs were reduced as compared to HSA (Fig. 3C and D).

Analysis of the intrahepatic distribution of the conjugate, 20 minutes after injection of 2 or 20 mg/kg indicated that the conjugate clearly co-localized with hepatic stellate cell markers (Fig. 3E), although also uptake could be observed in non-parenchymal cells that were not positive for HSC markers. In addition to this, we observed that after injection of a 2 mg/kg dose, this co-localization with HSC markers was confined to HSC in zone 2 and 3 of the liver, whereas after administration of the 20 mg/kg dose also distribution to the severely fibrotic portal areas could be observed.

Drug release from the carrier

To investigate the rate of drug release from the carrier in an acidic environment, M6PHSA-DOX was incubated in buffer pH=4.5. We found that drug release takes place over a period of approximately 9 hours, amounting to a maximum release of approximately 30% of the total amount of coupled DOX, under the present test conditions (Fig. 4A). *In vitro* studies with rat HSC on the cellular handling M6PHSA-DOX revealed that after exposure to the conjugate, DOX-specific fluorescence could be observed in the nucleus as well as in the cytoplasm (Fig. 4B). The cytoplasmic localization very likely reflects the presence of the conjugate in the lysosomal compartment of the cell after receptor-mediated uptake, whereas the observed association of DOX with the nucleus indicates that DOX is also being released from its carrier and is able to translocate to the cell nucleus. In contrast, cells incubated with unconjugated DOX mainly showed association of DOX with the nuclei (Fig. 4B).

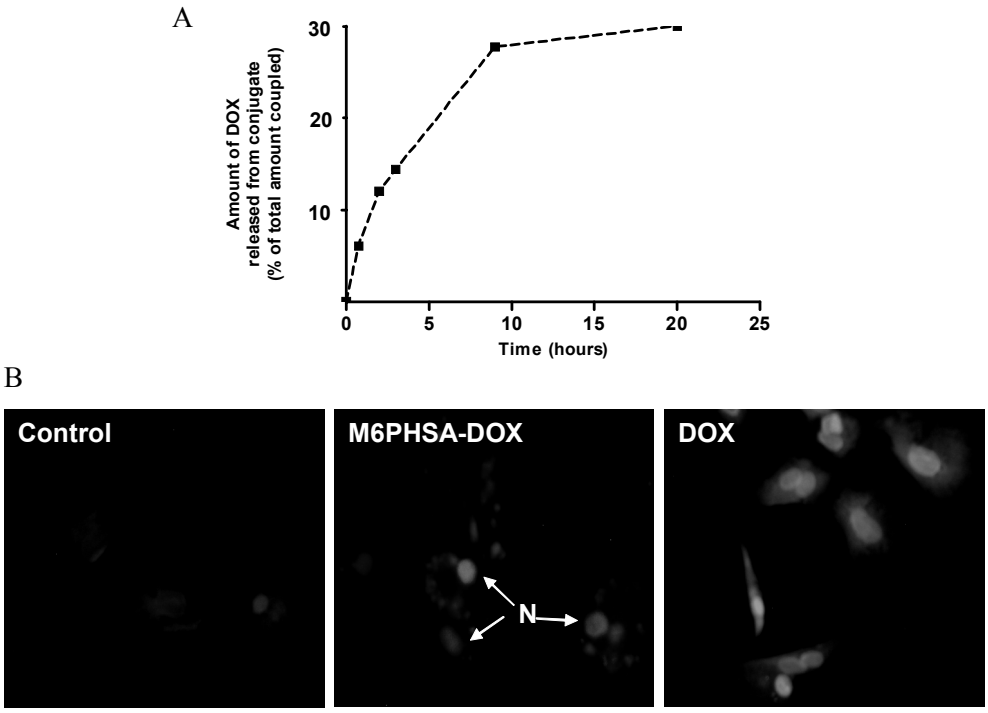

Fig. 4. A: Typical example of an experiment investigating the release of DOX from the conjugate in buffer pH=4.5. B: Fluorescence microscopy study of the binding and uptake of M6PHSA-DOX in activated rat HSC. The red fluorescent pattern (excitation wavelength 450-490 nm emission wavelength > 515 nm) reflects DOX itself. Uncoupled DOX accumulates only in the nuclei of HSC, whereas in the M6PHSA-DOX-treated cells, DOX-specific fluorescence is located in the cytoplasm as well as in the nuclei. Arrows in figure B indicate the nuclei in M6PHSA-DOX-treated cells. The micrographs are representative for data obtained with HSC from three different isolations (original magnification 200x). A full color version of this figure can be found in the appendix.

DISCUSSION

Inhibition of HSC proliferation poses a relevant strategy to inhibit liver fibrosis. However, selective delivery of antiproliferative drugs will be essential to avoid systemic side effects and allow these drugs to be used in a clinical setting (1;3). Although tumour-specific delivery of cytostatics is a well established

strategy, the targeted delivery of antiproliferative drugs to the principal fibrogenic cell type in the liver is a new field of research. This study describes the pharmacokinetic profile of an HSC-targeted construct containing doxorubicin. We found that M6PHSA-DOX is cleared in a biphasic pattern from the circulation, distributes rapidly to the liver and accumulates in HSC. Moreover, the present *in vitro* studies revealed that after this rapid initial distribution to the target cells, a relatively slow release of drug can be expected within HSC.

From *in vitro* studies it is known that M6P-modified proteins are taken up by HSC via receptor-mediated endocytosis (5;6;17). Since the disappearance rate in the initial phase of the curves decreased dose-dependently in the studied dosage range, a saturable transport step that likely reflects receptor-mediated hepatic uptake should be assumed. Based on our current findings, the dose-dependent plasma disappearance pattern should be analyzed according to a model including a Michaelis-Menten type of kinetics in the initial phase of the curve, describing the receptor-mediated transfer from the plasma compartment to the second compartment (liver). Using a population-based approach, as described earlier (18), which includes such a Michaelis-Menten transport process from the central to the peripheral compartment in the two-compartment pharmacokinetic model with elimination from the peripheral compartment, a V_{max} of 400 μg.min^{-1}.kg^{-1} and K_m of 50 μg/ml could be roughly estimated. Since V_1 is approximately 70 ml/kg in the studied population, this implies that at dosages exceeding 3.5 mg/kg, initial plasma decay and hepatic uptake will be significantly slower than at linear conditions ($C_{pl} << K_m$). However, studies that investigate the pharmacokinetics of M6PHSA-DOX in BDL rats across a wider dosage range will be needed to determine these parameters more accurately. Nevertheless, our observations imply that in multiple dosing schemes, at relatively high dosages, the dosing frequency of M6PHSA-DOX may be reduced, which can be considered favourable for the administration of drugs via the intravenous route.

Data from the γ-camera studies indicated that the vast majority of injected construct accumulated in the liver. This is in line with results from an earlier study in which the organ distribution of M6PHSA-DOX was studied in rats with liver fibrosis only at one fixed time-point, 20 minutes after injection. The main novelty of this study therefore is that it also describes the time-course of this hepatic uptake, which revealed that major hepatic uptake already takes place within the first minutes after injection and plateau levels are reached within 5 minutes. It should be realized however that many modified proteins are taken-up by the liver, by virtue of clearance by the mononuclear phagocyte system (19;20). Indeed, as also the case for tumour-targeted proteins, intrahepatic uptake of M6PHSA-DOX by macrophages was observed. However, a clear co-localization of the HSC-targeted DOX construct with HSC-markers was found in our studies, indicative of substantial uptake by these target cells.

Although techniques to study the disposition of HSC-targeted constructs at the body and organ level are readily available, investigation of drug disposition after release from the carrier within HSC *in vivo* is still technically cumbersome. We therefore studied the release of DOX from the conjugate *in vitro* and found that drug release from the carrier occurs relatively slow. Studies in isolated HSC showed that after 24 hour incubation with M6PHSA-DOX, the cytostatic drug was associated with the nuclei of the cells. Because direct translocation of intact albumin-based constructs is very unlikely, this indicates that drug release from the carrier takes place in these cells. Previous studies from our lab (4) showed that M6PHSA-DOX successfully inhibited HSC proliferation *in vitro*, which also indicates that pharmacologically active DOX is released from the carrier in these cells. Yet, drug release in acidic buffer was not complete. This may be explained by the fact that upon conjugation of DOX to the drug carrier an acid-stable stereo-isomer between DOX and the cis-aconityl linker is formed besides the formation of the desired acid-sensitive stereo-isomer (12). In future studies, the percentage of DOX that is released from the conjugate should therefore be optimized by the

insertion of different linkers between the drug and the protein. Of note, it is also possible that *in vivo*, proteases degrade the carrier and additionally contribute to the release of DOX.

The slow rate of drug release may prove an advantage since this may result in a sustained antiproliferative effect within cells even after a single i.v. injection. However, intracellular levels will also depend on the rate of elimination of DOX from HSC. One major elimination pathway for this type of drugs from cells in general, is via active transport by membrane proteins belonging to the ATP binding cassette (ABC) transporter family. In the rat, DOX efflux from cells is mainly mediated by the drug transporters mdr1a and mdr1b, the rodent homologues of human P-glycoprotein (Pgp) (21). Interestingly, Hannivoort et al. demonstrated the presence of mRNA transcripts encoding mdr1a and mdr1b in cultures of activated HSC (22). Yet, to our knowledge there are no studies that have investigated whether the presence of these mRNAs also translates into the presence of a functional drug efflux system in HSC. However, the possible presence of relevant drug efflux pumps with respect to DOX, emphasizes the need for more detailed studies concerning the mechanisms of drug elimination by this particular cell type.

In conclusion, the rapid distribution of M6PHSA-DOX from the blood to the liver in combination with the sustained release of DOX that is expected to take place in the target cells, make this construct a promising tool for achieving a selective inhibition of HSC proliferation during liver fibrosis. Since proliferation of HSC is a key event during fibrogenesis, attenuation of this process may be highly relevant. Studies on the efficacy of this drug delivery construct in experimental liver fibrosis in rats are in progress.

ACKNOWLEDGEMENTS

The help of Mr. J.H. Pol and Mr. H. ter Veen during these studies is greatly appreciated. Mrs. H.I. Bakker, and pharmacy students W. Bouma and M. de Ruijter are thanked for their assistance during *in vitro* experiments. Prof. D.K.F. Meijer is gratefully acknowledged for critical review of the manuscript.

REFERENCE LIST

1. Pinzani M, Rombouts K, Colagrande S. Fibrosis in chronic liver diseases: diagnosis and management. J Hepatol 2005; 42 Suppl: S22-S36.
2. Bataller R, Brenner DA. Hepatic stellate cells as a target for the treatment of liver fibrosis. Semin Liver Dis 2001; 21: 437-51.
3. Bataller R, Brenner DA. Liver fibrosis. J Clin Invest 2005; 115: 209-18.
4. Greupink R, Bakker HI, Bouma W, Reker-Smit C, Meijer DK, Beljaars L, Poelstra K. The antiproliferative drug doxorubicin inhibits liver fibrosis in bile duct-ligated rats and can be selectively delivered to hepatic stellate cells in vivo. J Pharmacol Exp Ther 2006, in press.
5. Beljaars L, Molema G, Weert B, Bonnema H, Olinga P, Groothuis GM, Meijer DK, Poelstra K. Albumin modified with mannose 6-phosphate: A potential carrier for selective delivery of antifibrotic drugs to rat and human hepatic stellate cells. Hepatology 1999; 29: 1486-93.
6. Beljaars L, Olinga P, Molema G, de Bleser P, Geerts A, Groothuis GM, Meijer DK, Poelstra K. Characteristics of the hepatic stellate cell-selective carrier mannose 6-phosphate modified albumin (M6P(28)-HSA). Liver 2001; 21: 320-8.
7. de Bleser PJ, Jannes P, van Buul-Offers SC, Hoogerbrugge CM, van Schravendijk CF, Niki T, Rogiers V, van den Brande JL, Wisse E, Geerts A. Insulinlike growth factor-II/mannose 6-phosphate receptor is expressed on CCl4-exposed rat fat-storing cells and facilitates activation of latent transforming growth factor-beta in cocultures with sinusoidal endothelial cells. Hepatology 1995; 21: 1429-37.
8. Weiner JA, Chen A, Davis BH. E-box-binding repressor is down-regulated in hepatic stellate cells during up-regulation of mannose 6-phosphate/insulin-like growth factor-II receptor expression in early hepatic fibrogenesis. J Biol Chem 1998; 273: 15913-9.
9. de Bleser PJ, Scott CD, Niki T, Xu G, Wisse E, Geerts A. Insulin-like growth factor II/mannose 6-phosphate-receptor expression in liver and serum during acute CCl4 intoxication in the rat. Hepatology 1996; 23: 1530-7.

10. Dahms NM, Hancock MK. P-type lectins. Biochim Biophys Acta 2002; 1572: 317-40.
11. Beljaars L, Poelstra K, Molema G, Meijer DK. Targeting of sugar- and charge-modified albumins to fibrotic rat livers: the accessibility of hepatic cells after chronic bile duct ligation. J Hepatol 1998; 29: 579-88.
12. Shen WC, Ryser HJ. cis-Aconityl spacer between daunomycin and macromolecular carriers: a model of pH-sensitive linkage releasing drug from a lysosomotropic conjugate. Biochem Biophys Res Commun 1981; 102: 1048-54.
13. Hines JE, Johnson SJ, Burt AD. In vivo responses of macrophages and perisinusoidal cells to cholestatic liver injury. Am J Pathol 1993; 142: 511-8.
14. Geerts A. History, heterogeneity, developmental biology, and functions of quiescent hepatic stellate cells. Semin Liver Dis 2001; 21: 311-35.
15. Geerts A, Niki T, Hellemans K, De Craemer D, Van Den Berg K, Lazou JM, Stange G, Van De WM, De BP. Purification of rat hepatic stellate cells by side scatter-activated cell sorting. Hepatology 1998; 27: 590-8.
16. Ismail AA, Amin AM. Cytofluorescence evidence of adriamycin in liver. Neoplasma 1982; 29: 735-40.
17. Greupink R, Bakker HI, Reker-Smit C, Loenen-Weemaes AM, Kok RJ, Meijer DK, Beljaars L, Poelstra K. Studies on the targeted delivery of the antifibrogenic compound mycophenolic acid to the hepatic stellate cell. J Hepatol 2005; 43: 884-92.
18. Proost JH, Beljaars L, Olinga P, Swart PJ, Kuipers ME, Reker-Smit C, Groothuis GM, Meijer DK. Prediction of the pharmacokinetics of succinylated human serum albumin in man from in vivo disposition data in animals and in vitro liver slice incubations. Eur J Pharm Sci 2006; 27: 123-32.
19. Terpstra V, van Amersfoort ES, van Velzen AG, Kuiper J, van Berkel TJ. Hepatic and extrahepatic scavenger receptors: function in relation to disease. Arterioscler Thromb Vasc Biol 2000; 20: 1860-72.
20. Jansen RW, Molema G, Harms G, Kruijt JK, van Berkel TJ, Hardonk MJ, Meijer DK. Formaldehyde treated albumin contains monomeric and polymeric forms that are differently cleared by endothelial and Kupffer cells of the liver: evidence for scavenger receptor heterogeneity. Biochem Biophys Res Commun 1991; 180: 23-32.
21. Leslie EM, Deeley RG, Cole SP. Multidrug resistance proteins: role of P-glycoprotein, MRP1, MRP2, and BCRP (ABCG2) in tissue defense. Toxicol Appl Pharmacol 2005; 204: 216-37.
22. Hannivoort RA, Buist-Homan M, Faber KN, Moshage H. MRP-type transporters protect activated hepatic stellate cells against cell death. Hepatology 2004; 40: 615A.

7

TOWARDS A TARGETED INHIBITION OF HEPATIC STELLATE CELL PROLIFERATION: A SINGLE AND MULTIPLE DOSE STUDY ON THE ANTIFIBROGENIC EFFECTS OF A HEPATIC STELLATE CELL-TARGETED DOXORUBICIN CONSTRUCT IN BILE DUCT-LIGATED RATS

Rick Greupink
Hester I. Bakker
Mariska Geuken
Klaas Nico Faber
Leonie Beljaars
Klaas Poelstra

ABSTRACT

Hepatic stellate cell (HSC) proliferation is a prominent feature of liver fibrosis. The selective delivery of antiproliferative drugs to this cell type therefore constitutes a promising antifibrotic strategy. In the present study we investigated the pharmacological effects of an HSC-targeted doxorubicin construct (M6PHSA-DOX) on experimental liver fibrosis in the rat after single and chronic administration. Seven days after bile duct ligation (BDL), rats were injected i.v. with PBS, M6PHSA (20 mg/kg) or M6PHSA-DOX (20 mg/kg). Twenty-four hours after injection this resulted in a decreased non-parenchymal cell proliferation as well as a diminished local perisinusoidal collagen staining, indicating that pharmacologically active drug is delivered *in vivo*. Chronic treatment of BDL rats for 7 days with i.v. injections of 2 mg/kg/day or 20 mg/kg/day of M6PHSA-DOX, however, did not result in a significant attenuation of overall fibrosis parameters, as assessed by morphometric analysis of collagen-stained and α-sma-stained liver sections. We investigated whether prolonged administration of M6PHSA-DOX upregulated compensatory mechanisms, which may explain the discrepancy between the single and multiple dose study. We found that upon chronic administration of 20 mg/kg M6PHSA-DOX, hepatic mRNA levels of mdr1a, an important drug efflux transporter for DOX, was upregulated. Because DOX is released slowly from its carrier after lysosomal uptake in HSC, this may result in a very effective clearance of the drug from the target cells. In conclusion, despite promising initial effects, chronic administration of M6PHSA-DOX did not result in a profound antifibrotic effect. Further studies should investigate whether the development of more optimal delivery forms of DOX, that exhibit a more rapid intracellular release of DOX, may be instrumental in overcoming this problem.

INTRODUCTION

The activated hepatic stellate cell (HSC) is the principal producer of collagen during fibrogenesis and therefore this cell type is considered a primary target for the development of new pharmacotherapeutics for this chronic disease. Because HSC proliferation is a key event during fibrogenesis, the application of antiproliferative drugs for antifibrotic purposes may be a relevant option (1-3). However, such treatments face serious problems as proliferation of hepatocytes and non-hepatic cells should not be affected.

Previously, we showed that chronic treatment of bile duct-ligated (BDL) rats with the antiproliferative drug doxorubicin (DOX) attenuates the fibrotic process (4). However, toxicity associated with the use of such a potent cytostatic will hamper its actual application as an antifibrotic drug in chronic liver diseases. For this reason we developed an HSC-selective form of DOX by coupling it to the HSC-selective drug carrier mannose-6-phosphate-modified human serum albumin (M6PHSA). In BDL rats we have shown that M6PHSA-DOX is cleared rapidly from the blood and accumulates quickly and selectively in HSC, whereas the uptake of DOX in non-target tissues could be successfully avoided (4). The HSC-selectivity of the conjugate is obtained by virtue of the presence of M6P groups in the protein backbone of the drug targeting construct, which makes it a ligand for Mannose-6-Phosphate/Insulin-like Growth Factor-II receptors (M6P/IGF-II receptors) (5-7). These receptors are specifically upregulated on hepatic stellate cells during the transformation of these cells from a quiescent phenotype into cells with fibrogenic properties (8;9). This transdifferentiation of HSC, referred to as activation, is induced by various mediators that are released upon chronic liver injury (10). M6P/IGF-II receptors on the cell surface are internalized at a high rate and route their bound ligands to the lysosomal compartment. In the acidic lysosomal compartment the degradation of internalized ligands can take place. By coupling DOX to the carrier via an acid-sensitive linker, intracellular release of the

coupled drug can be achieved after internalization of the M6P-containing drug targeting construct (6).

In vitro studies in our laboratory have shown that M6PHSA-DOX indeed binds to culture-activated HSC in a specific manner and results in a successful inhibition of HSC proliferation *in vitro* (4). However, *in vivo* studies that investigate the effect of this HSC-targeted antiproliferative drug have not yet been performed. The work presented in this study therefore explores the intrahepatic effects of single administration of M6PHSA-DOX, as well as the effects of prolonged administration of the conjugate during developing liver fibrosis in bile duct-ligated rats.

MATERIALS AND METHODS

Experimental animals

Male Wistar rats (Out bred strain, Harlan, Horst, The Netherlands) of 220-240g were housed under a 12-hour dark/light cycle, at constant humidity and temperature. Animals had free access to tap water and standard lab chow (Harlan). All experiments were approved by the local committee for care and use of laboratory animals and were performed according to strict governmental and international guidelines. Liver fibrosis was induced by ligation of the common bile duct under O_2/N_2O/Isoflurane anaesthesia as described previously (5).

Synthesis and characterization of M6PHSA-DOX

M6PHSA was synthesized as described by Beljaars et al. (5). DOX was coupled to M6PHSA via cisaconitic acid according to the method of Shen and Ryser, covalently linking the drug and the carrier via an acid-sensitive spacer. This allows drug release within the acidic lysosomal compartment of cells, whereas this bond remains stable in the circulation (11). M6PHSA-DOX was subsequently

purified by dialysis against PBS followed by size-exclusion chromatography on a HiLoad 16/60 Superdex 200 column (Amersham Biosciences, Uppsala, Sweden). After dialysis against water, the product was lyophilized and stored at –20 °C until use. The total amount of coupled DOX was assessed by spectrophotometric analysis and the amount of free drug in the preparation was analyzed by HPLC, as described earlier (4). Monomeric protein content was assessed by SDS-PAGE and size-exclusion chromatography, as described in references (12) and (4).

As a part of the characterization procedure, the synthesized construct was evaluated for its *in vitro* cytotoxicity in cultures of 3T3-fibroblasts, an M6P/IGF-II receptor-expressing cell line. M6P/IGF-II receptor expression in 3T3 fibroblasts was demonstrated via staining of cytospots of 3T3 fibroblasts, using standard indirect immunohistochemical techniques. The primary antibody, a goat polyclonal immunoglobulin directed against the M6P/IGF-II receptor, was obtained from Santa Cruz Biotechnology (Santa Cruz, CA, USA). The effect on cell viability was assessed via Alamar Blue conversion assays, according to the instructions of the manufacturer (Serotec, Kidlington, UK). In brief, cells were seeded at a density of 10,000 cells/well in 96-wells plates, and were allowed to attach to the plates overnight. Subsequently, the cells were incubated with M6PHSA-DOX or vehicle for 24 hours. Alamar Blue was added to the wells 4 hours prior to termination of the experiment. Viable cells convert Alamar Blue into a fluorescent product, which was measured at an excitation wavelength of 560 nm and an emission wavelength of 590 nm.

Single dose study

One week after BDL, rats were given a single i.v. injection of PBS (n=3), M6PHSA (20 mg/kg, n=3) or M6PHSA-DOX (20 mg/kg, n=3). Animals were sacrificed after 24 hours in order to study the acute effects of M6PHSA-DOX in the liver. Liver specimens were fixed in formalin 4% and embedded in paraffin according to standard procedures. The effect of compounds on the proliferation of

HSC and other non-parenchymal cells (NPC) was assessed by staining for Proliferating Cell Nuclear Antigen (PCNA) on 5 µm sections of formalin-fixed liver specimens (PCNA detection kit, Zymed). The number of PCNA-positive NPC was counted in four randomly taken microphotographs per section at a magnification of 200x. To investigate the effect on collagen deposition in the liver, 5 µm thick tissue sections were stained with picrosirius red. Subsequently, the extent of perisinusoidal collagen staining was assessed semi quantitatively by two blinded observers (RG and HIB), using the following scale: + limited staining, ++ clear staining, +++ abundant staining.

Multiple dose study

Eighteen animals were subjected to bile duct ligation at day 0 of the protocol. On day 3, the animals were divided into four groups. The groups were treated with either PBS (n=5), M6PHSA at a dose of 2 mg/kg/day (n=5), M6PHSA-DOX at a dose of 2 mg/kg/day (n=5) or M6PHSA-DOX at a dose of 20 mg/kg/day (n=3). Compounds were administered i.v. via the penis vein, once daily. A total of 7 injections was given, starting on day 3 of the protocol and the animals were sacrificed 24 hours after the last injection on day 10 of the protocol. The livers were excised and were processed according to standard procedures. For optimal results, the number of activated HSC in the livers was assessed immunohistochemically on 4 µm cryostat sections by staining for α-smooth muscle actin (α-sma, Sigma, Gillingham, UK). To study the extent of fibrosis, cryostat sections were immunohistochemically stained with an antibody directed against collagen III (Southern Biotechnology, Birmingham, AL, USA). For both stainings the positive-stained area was subsequently quantified by morphometric analysis of microphotographs obtained at a magnification of 40x. For the analyses the Image J software package (NIH, Bethesda, ML, USA) was used, and the positive-stained area was expressed as a percentage of total area.

Analysis of mdr1a and mdr1b mRNA expression

Total mRNA was isolated from the livers of the animals that were enrolled in the chronic effect study via a solid phase extraction procedure (RNeasy mini kit, Qiagen, Venlo, The Netherlands). Quantification of the amount of isolated RNA was subsequently performed by UV spectrophotometry, using an ND-1000 spectrophotometer (NanoDrop technologies, Wilmington, DE, USA). cDNA was synthesized using the Promega Reverse Transcription System (Promega, Southampton, UK) according to the instructions of the manufacturer. Subsequently, real-time PCR was performed, using appropriate TAQman probes for the analysis of mdr1a and mdr1b mRNA levels. As a reference, mdr1a and mdr1b mRNA levels were analyzed in whole liver samples taken from rats that were chronically treated with untargeted DOX, equivalent to 2 mg/kg of targeted DOX. Chronic treatment with untargeted DOX, which was equivalent to 20 mg/kg of targeted DOX was lethal to fibrotic rats, and could therefore not be included as a reference.

Statistical analysis

Results were expressed as the mean +/- SEM. Data were subjected to the Mann-Whitney U test and differences were considered statistically significant at $P<0.05$.

RESULTS

Synthesis and characterization of M6PHSA-DOX

Spectrophotometric analysis of the construct revealed that per mg of construct 66.7 µg of doxorubicin was present. Of the total amount of doxorubicin in the preparation only 1% was present in uncoupled form, as assessed by HPLC-analysis. SDS-PAGE and size-exclusion chromatography revealed that no significant amounts of polymeric protein could be detected in the conjugate. As a

part of the characterization we evaluated the synthesized construct for its *in vitro* efficacy, and we found that M6PHSA-DOX successfully reduced the viability of M6P/IGF-II receptor-expressing fibroblasts (Fig. 1). This effect could not be explained by the presence of the negligible amount of uncoupled DOX in the preparation, indicating that active drug is released from the carrier in this cellular system.

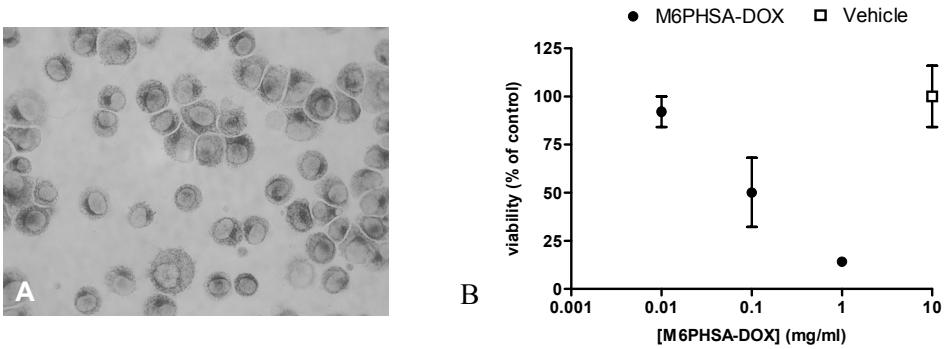

Fig. 1. A: Cytospots of 3T3-fibroblasts stained positive for the M6P/IGF-II receptor. B: Demonstration of the pharmacological activity of M6PHSA-DOX in cultures of 3T3-fibroblasts. Twenty-four hours of incubation with the conjugate resulted in reduced cell viability, as assessed by alamar blue conversion assays. Data are the average ± SD of one experiment, performed in triplicate.

Single dose study

Although profound antifibrogenic effects were not anticipated 24 hours after a single injection, previous studies from our laboratory on the pharmacokinetics and release of DOX from the drug carrier, indicated that effects directly related to the drug may be expected at this time point. Therefore, NPC proliferation in the liver was assessed by immunohistochemical staining for PCNA, which revealed that NPC proliferation was decreased in the M6PHSA-DOX-treated animals compared to animals that were treated with the control protein ($P<0.05$, Table 1). In addition to cell proliferation, we also assessed the effect on intrahepatic collagen deposition. Picrosirius red staining revealed that in the livers of M6PHSA-DOX-treated animals, the staining for perisinusoidal collagen was reduced, compared to animals

that were treated with a single injection of PBS or the control protein M6PHSA (Table 1). In previous studies on the localization of M6PHSA-DOX in fibrotic livers, we found that the conjugate mainly co-localized with perisinusoidal HSC in zone 2 and 3 of the liver and to a lesser extent with fibrogenic cells in the portal areas (Greupink et al., manuscript submitted, thesis chapter 6). The effect we now observe, therefore, is consistent with the intrahepatic localization of M6PHSA-DOX and is an indication that pharmacologically active DOX is also delivered *in vivo*.

Table 1. Effects of M6PHSA-DOX and control substances on non-parenchymal cell proliferation and perisinusoidal collagen deposition 24 hours after one single i.v. injection. * indicates P<0.05 compared to the control protein. +: limited collagen staining, ++: clear collagen staining, +++ abundant collagen staining.

	PCNA-positive NPC per microscopic field (% of control)	**Perisinusoidal collagen score**
PBS	100 ± 8	+++
M6PHSA	101 ± 2	+++
M6PHSA-DOX	90 ± 5*	+

Multiple dose study

Subsequently, we investigated whether chronic treatment with M6PHSA-DOX could effectively attenuate the numbers of activated HSC in the liver and fibrosis. Despite the successful delivery of DOX, chronic treatment of BDL rats with M6PHSA-DOX did not result in a reduction in the numbers of activated HSC. Although after daily injections of 20 mg/kg of M6PHSA-DOX the α-sma-stained area appeared to be reduced, this did not reach statistical significance (Fig. 2A). Moreover, the extent of liver fibrosis did not differ between the groups at all (Fig. 2B). In addition, on the mRNA level we could also not observe any statistically significant effects of M6PHSA-DOX on markers for (activated) HSC and fibrosis.

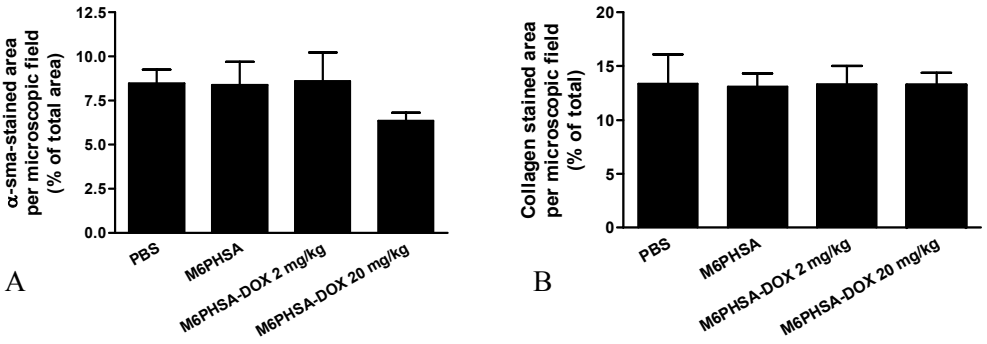

Fig. 2. A: Results of the morphometric analysis of α-sma-stained liver sections obtained from rats after chronic treatment with M6PHSA-DOX or control substances, reflecting the number of activated HSC in the livers. B: Evaluation of the effect of chronic treatment with M6PHSA-DOX on intrahepatic collagen deposition, as assessed by morphometric analysis of collagen III-stained liver sections. PBS (n=5), M6PHSA (n=5), M6PHSA-DOX 2 mg/kg/day (n=5), M6PHSA-DOX 20 mg/kg/day (n=3).

mRNA expression levels of mdr1a and mdr1b

The combined observations from the acute and chronic study prompted us to investigate whether compensatory mechanisms might be activated in the fibrotic liver upon chronic exposure to M6PHSA-DOX. We tested whether clearance mechanisms for DOX are upregulated in the M6PHSA-DOX-treated rats. Such a drug resistance mechanism has been well documented for tumour cells that are exposed to DOX (13). We evaluated mRNA expression levels of mdr1a and mdr1b, which are the rodent equivalents of P-glycoprotein, known to eliminate DOX from cells (14). We found that hepatic mdr1a mRNA expression was significantly increased 1.6 ± 0.1 fold in the animals treated with 20 mg/kg M6PHSA-DOX compared to the PBS-treated BDL rats (Fig. 3A). In contrast to mdr1a expression, mdr1b mRNA levels were not upregulated after chronic exposure to the conjugate (Fig. 3B).

In Fig. 4A and 4B the expression levels of mdr1a, mdr1b in the livers of rats that were chronically treated with untargeted DOX are shown as a reference. Upon

chronic exposure to untargeted DOX, mdr1a and mdr1b mRNA expression were increased 2.3 ± 0.3 fold and 2.8 ± 0.2 fold over PBS-treated BDL rats, respectively.

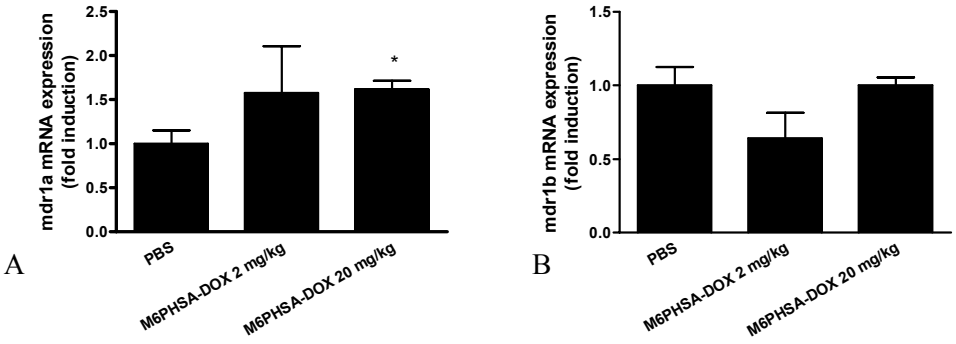

Fig. 3. The influence of chronic treatment with M6PHSA-DOX and control substances on hepatic mdr1a (A) and mdr1b (B) mRNA expression. * indicates $P<0.05$ compared to PBS-treated controls.

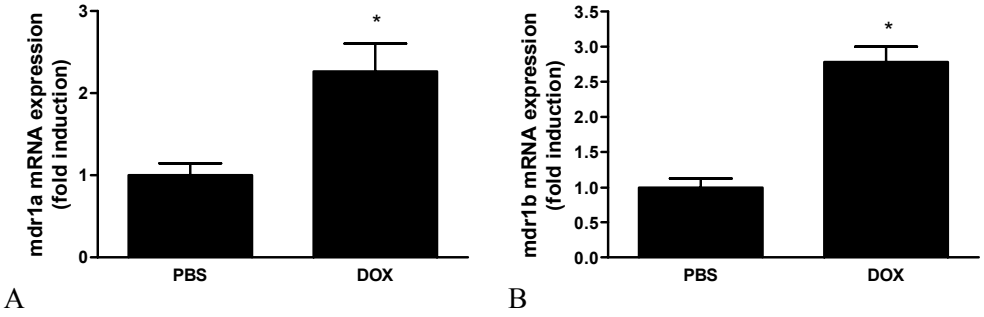

Fig. 4. Effect of chronic treatment with unconjugated DOX on hepatic mdr1a (A) and mdr1b (B) mRNA expression. * indicates $P<0.05$ compared to controls.

DISCUSSION

In the present study the intrahepatic effects of a single dose of M6PHSA-DOX, as well as the effects of prolonged administration of the conjugate on liver fibrosis in bile duct-ligated rats were investigated. We could show that non-parenchymal cell proliferation was significantly reduced after a single injection of M6PHSA-

DOX, which is indicative for the successful delivery of pharmacologically active DOX *in vivo*. The cell type that is affected here could not be addressed, but previous studies have shown that this construct accumulates in HSC, liver endothelial cells and Kupffer cells (4). In addition to the antiproliferative action of M6PHSA-DOX, a reduction in perisinusoidal collagen staining could be observed within the livers of M6PHSA-DOX-treated animals. This may be due to a reduced number of HSC, although this could not be detected by immunohistochemical staining for HSC markers. It is also known that DOX inhibits collagen synthesis via the inhibition of enzymes that are crucial to collagen biosynthesis, examples of which are prolyl-4-hydroxylase and prolidase (15-18). In line with these reports, preliminary data from our own lab showed that collagen protein deposition in the HSC-T6 cell-line was inhibited by the drug. However, further studies will be needed to investigate this phenomenon in more detail. Given the rapid reduction in perisinusoidal collagen staining within 24h post injection, these studies should also explore the possibility that the decreased perisinusoidal collagen staining may be the consequence of an increased activity of collagenases within the Space of Disse.

Despite the observed effects in the single dose study, no favourable antifibrotic effects could be observed anymore in the long-term study, in which the construct was dosed daily for 7 consecutive days. Nor collagen deposition, nor α-sma staining, nor markers for HSC and fibrosis on the mRNA level had changed after treatment. We therefore considered the possibility that after multiple dosing, the intracellular concentration of the active drug in HSC was decreased, either due to increased hepatic clearance, increased hepatic redistribution or insufficient release of the drug from the carrier.

In relation to increased hepatic clearance and/or redistribution from HSC we found that an upregulation of mdr1a mRNA takes place in the livers of animals treated with M6PHSA-DOX. Based on whole liver mRNA expression data it can not be differentiated whether HSC participate in this upregulation, or if this is limited to the hepatocyte population. This may be examined in more detail in future

studies. However, previous studies by Hannivoort et al. demonstrated that high mRNA levels of mdr1a and mdr1b are present in culture-activated HSC *in vitro* (19). It would therefore be relevant to investigate whether DOX is capable of inducing mdr mRNA levels in the culture-activated cells *in vitro* as well as *in vivo*, and also if this results in an overexpression of the mdr transporter on the protein level.

In figure 4 it is shown that in animals that were treated with untargeted DOX, the mdr mRNA levels were induced as well. Yet, in a previous study (4), an antifibrogenic effect of DOX was evident in these animals and thus it seems that an upregulation of mdr1 expression itself cannot fully explain why HSC-targeted DOX fails to exert an antifibrotic effect. However, differences in cellular handling between DOX and M6PHSA-DOX should also be taken into account. Peak levels of pharmacologically active drug may be higher in the liver after administration of the untargeted drug than after administration of the targeted compound. Although the distribution of the M6PHSA-DOX prodrug is superior to that of the native drug with respect to liver uptake (4), lysosomal degradation of the drug-carrier complex may be a rate-limiting step in the release of pharmacologically active drug from the conjugate. In contrast, the untargeted drug directly enters the cell in an active form. In a previous study we have shown that after rapid distribution of M6PHSA-DOX to HSC, drug release following cellular internalization will be slow (Greupink et al., manuscript submitted, thesis chapter 6). It is conceivable that upon the slow release of pharmacologically active DOX from the lysosomes into the cytosol, DOX will be very effectively cleared if drug efflux pumps are upregulated either in the cell membrane of HSC or in the hepatocytes. Despite the high HSC-selectivity of M6PHSA-DOX, in this case the cytosolic concentrations of pharmacologically active DOX may therefore remain too low to exert pharmacological effects in the nucleus. Co-administration of a Pgp-blocker such as verapamil may elucidate the role of mdr1a here (20;21).

In summary, this is the first study aiming at an attenuation of HSC proliferation during liver fibrosis, using an HSC-targeted, doxorubicin-containing construct. A single dose of M6PHSA-DOX resulted in a reduction in hepatic non-parenchymal cell proliferation and perisinusoidal collagen staining in bile duct-ligated rats. However, this did not translate into a profound antifibrotic effect after chronic administration. Possibly this is the consequence of an upregulation of intrahepatic drug efflux mechanisms, which could also be demonstrated. A significant increase in mRNA levels for one of the major efflux pumps for DOX (i.e. mdr1a) was at hand. In combination with a slow release of DOX from the conjugate this may lead to sub-therapeutic concentrations within the nucleus. Further studies on HSC-targeted DOX constructs that display rapid release of the drug, or dose regimen optimization should address these items.

In conclusion, the concept of an antifibrotic therapy based on an HSC-selective delivery of antiproliferative drugs is feasible, but higher peak levels of DOX within the target cells are required. This can be achieved either by increasing the efficacy and rate at which DOX is released from the carrier, or by blocking mdr1-mediated efflux. Alternatively, drugs may be used that are not subject to P-glycoprotein-mediated extrusion from the target cells.

REFERENCE LIST

1. Pinzani M, Rombouts K, Colagrande S. Fibrosis in chronic liver diseases: diagnosis and management. J Hepatol 2005; 42 Suppl: S22-S36.
2. Bataller R, Brenner DA. Hepatic stellate cells as a target for the treatment of liver fibrosis. Semin Liver Dis 2001; 21: 437-51.
3. Friedman SL. Molecular regulation of hepatic fibrosis, an integrated cellular response to tissue injury. J Biol Chem 2000; 275: 2247-50.
4. Greupink R, Bakker HI, Bouma W, Reker-Smit C, Meijer DKF, Beljaars L, Poelstra K. The antiproliferative drug doxorubicin inhibits liver fibrosis in bile duct-ligated rats and can be selectively delivered to hepatic stellate cells in vivo. J.Pharmacol.Exp.Ther. 2006, in press.

5. Beljaars L, Molema G, Weert B, Bonnema H, Olinga P, Groothuis GM, Meijer DK, Poelstra K. Albumin modified with mannose 6-phosphate: A potential carrier for selective delivery of antifibrotic drugs to rat and human hepatic stellate cells. Hepatology 1999; 29: 1486-93.
6. Dahms NM, Hancock MK. P-type lectins. Biochim Biophys Acta 2002; 1572: 317-40.
7. Ghosh P, Dahms NM, Kornfeld S. Mannose 6-phosphate receptors: new twists in the tale. Nat Rev Mol Cell Biol 2003; 4: 202-12.
8. de Bleser PJ, Jannes P, van Buul-Offers SC, Hoogerbrugge CM, van Schravendijk CF, Niki T, Rogiers V, van den Brande JL, Wisse E, Geerts A. Insulinlike growth factor-II/mannose 6-phosphate receptor is expressed on CCl4-exposed rat fat-storing cells and facilitates activation of latent transforming growth factor-beta in cocultures with sinusoidal endothelial cells. Hepatology 1995; 21: 1429-37.
9. de Bleser PJ, Scott CD, Niki T, Xu G, Wisse E, Geerts A. Insulin-like growth factor II/mannose 6-phosphate-receptor expression in liver and serum during acute CCl4 intoxication in the rat. Hepatology 1996; 23: 1530-7.
10. Eng FJ, Friedman SL. Fibrogenesis I. New insights into hepatic stellate cell activation: the simple becomes complex. Am J Physiol Gastrointest Liver Physiol 2000; 279: G7-G11.
11. Shen WC, Ryser HJ. cis-Aconityl spacer between daunomycin and macromolecular carriers: a model of pH-sensitive linkage releasing drug from a lysosomotropic conjugate. Biochem Biophys Res Commun 1981; 102: 1048-54.
12. Greupink R, Bakker HI, Reker-Smit C, Loenen-Weemaes AM, Kok RJ, Meijer DK, Beljaars L, Poelstra K. Studies on the targeted delivery of the antifibrogenic compound mycophenolic acid to the hepatic stellate cell. J Hepatol 2005; 43: 884-92.
13. Hardman J, Limbird L, Goodman Gilman A. Antineoplastic agents. In: Goodman and Gilman's the Pharmacological basis of therapeutics, p 1425-1432, 10th ed, McGraw-Hill publishers, 2001.
14. Leslie EM, Deeley RG, Cole SP. Multidrug resistance proteins: role of P-glycoprotein, MRP1, MRP2, and BCRP (ABCG2) in tissue defense. Toxicol Appl Pharmacol 2005; 204: 216-37.
15. Muszynska A, Wolczynski S, Palka J. The mechanism for anthracycline-induced inhibition of collagen biosynthesis. Eur J Pharmacol 2001; 411: 17-25.
16. Sasaki T, Holeyfield KC, Uitto J. Doxorubicin-induced inhibition of prolyl hydroxylation during collagen biosynthesis in human skin fibroblast cultures. Relevance to imparied wound healing. J Clin Invest 1987; 80: 1735-41.
17. Gunzler V, Hanauske-Abel HM, Myllyla R, Kaska DD, Hanauske A, Kivirikko KI. Syncatalytic inactivation of prolyl 4-hydroxylase by anthracyclines. Biochem J 1988; 251: 365-72.

18. Saika S, Ooshima A, Yamanaka O, Kimura M, Okada Y, Tonoe O, Tanaka S, Ohnishi Y. In vitro effects of doxorubicin and mitomycin C on human Tenon's capsule fibroblasts. Ophthalmic Res 1997; 29: 91-102.
19. Hannivoort RA, Buist-Homan M, Faber KN, Moshage H. MRP-type transporters protect activated hepatic stellate cells against cell death. Hepatology 2004; 40: 615A.
20. Gigliozzi A, Fraioli F, Sundaram P, Lee J, Mennone A, Alvaro D, Boyer JL. Molecular identification and functional characterization of Mdr1a in rat cholangiocytes. Gastroenterology 2000; 119: 1113-22.
21. Wang JC, Liu XY, Lu WL, Chang A, Zhang Q, Goh BC, Lee HS. Pharmacokinetics of intravenously administered stealth liposomal doxorubicin modulated with verapamil in rats. Eur J Pharm Biopharm 2006; 62: 44-51.

8

SUMMARY, GENERAL DISCUSSION AND CONCLUSIONS

SUMMARY

Liver fibrosis is the response to a variety of chronic injurious events to the liver, induced by chronic viral hepatitis, iron or copper overload disease, certain autoimmune diseases, toxicity by certain drugs or chronic alcohol abuse and metabolic disorders, such as the metabolic syndrome. The disease is characterized by the deposition of excessive amounts of scar tissue in the liver, which disturbs liver structure and functioning. In an advanced stage, the fibrotic process acquires a self-perpetuating character, and fibrosis will gradually progress into its end-stage called cirrhosis even when the injurious stimulus is removed. Finally, healthy liver cells are largely replaced by connective tissue. This remodelling of the liver parenchyma also results in impaired blood flow through the liver, which subsequently leads to portal hypertension and many secondary problems. In contrast to the early stages of the disease, when loss of functional liver parenchyma can still be compensated for by virtue of a functional over-capacity of the liver, liver function becomes de-compensated in the cirrhotic end-stage of the disease, ultimately leading to death. To date, no effective antifibrotic drug is available for treatment and the only curative intervention is a liver transplantation (1).

Within the fibrotic liver, activated hepatic stellate cells (HSC) are the main source of the excessive amounts of extracellular matrix proteins, which are the building blocks of the connective tissue. Under the influence of fibrogenic stimuli derived from damaged hepatocytes, activated Kupffer cells and liver endothelial cells, HSC transdifferentiate from a quiescent cell type into a cell with a myofibroblast-like phenotype. During fibrosis, the number of active fibrogenic cells in the liver also dramatically increases, mainly as a result of an increased local proliferation of HSC. Because the latter process plays an important role in the progression of the disease, inhibiting HSC proliferation could be a relevant strategy to inhibit liver fibrosis in a pharmacological manner (2;3).

The development of clinically applicable antifibrotic drugs based on the understanding of the pathogenesis of liver fibrosis and HSC biology has thus far met with limited success. One important reason for this is that candidate compounds exert too many adverse effects to be of any practical use. This is particularly true for antiproliferative drugs that are usually applied as anticancer agents, i.e. the adverse effects of such antitumour drugs are well known. Therefore, these drugs have not yet been tested for their antifibrotic potential during liver fibrosis. As summarized in **chapters 1 and 2**, toxicity in non-target cells may be avoided by the selective delivery of drugs to the HSC. HSC-selective drug carriers have recently been developed and the work described in this thesis explores the concept of HSC-selective delivery of antiproliferative drugs as a potential strategy to treat liver fibrosis. This is the first time this item is addressed.

In the studies described in this thesis, mannose-6-phosphate-modified human serum albumin (M6PHSA) was used as a drug carrier to which drugs were covalently coupled in order to improve their HSC-selectivity. M6PHSA has been designed to interact with mannose-6-phosphate/insulin-like growth factor receptors (M6P/IGF-IIR). In isolated HSC with an activated phenotype this receptor is upregulated. Previous data from our laboratory have shown that M6PHSA, as a consequence of this, selectively accumulates in the HSC of rats with advanced liver fibrosis induced by bile duct ligation (BDL) (4-6). However, at the start of this project there were no systematic data available regarding the M6P/IGF-II receptor expression in the livers of BDL rats. Particularly, these data were needed to predict whether HSC-selectivity of the constructs may also be expected in an early stage of the disease, when HSC proliferation is most prominent (7).

In **chapter 3** we therefore explored the upregulation of M6P/IGF-II receptor expression during experimental liver fibrosis, at various time points after BDL. We found that M6P/IGF-IIR mRNA expression was increased during the early stages after ligation and immunohistochemical staining for M6P/IGF-IIR revealed a clear presence of this receptor on α-sma-positive cells with spindle-shaped nuclei. To

investigate the possibility of an upregulation of this receptor on other fibrogenic cells during fibro-proliferative disease in other organs as well, we also studied M6P/IGF-II receptor expression in the renal vasculature of homozygous TGR(mRen2) rats. In these renin transgenic animals, hypertension-induced fibrotic vascular lesions develop, which are characterized by a thickening of renal capillaries associated with vascular smooth muscle cell proliferation (8). In the kidneys of TGR(mRen2) rats the number of M6P/IGF-IIR-positive blood vessels per microscopic field was indeed increased, indicating that this receptor is also expressed in early fibrotic vascular lesions in renal tissue.

Our findings thereby opened perspectives for the selective delivery of drugs to HSC in the fibrotic rat liver already in an early stage of the disease. Moreover, targeting antiproliferative drugs to vascular smooth muscle cells in vascular lesions via this receptor may be a possibility as well. This is one example of disease-induced targeting (9).

In **chapter 3** we also studied whether delivery of the immunosuppressive drug mycophenolic acid (MPA) to M6P/IGF-II receptor-expressing fibroblasts is possible via receptor-mediated uptake *in vitro*, and subsequently whether this resulted in pharmacological effects within these cells. Besides the well known immunosuppressive action of the drug, it has been shown by others that MPA inhibits the proliferation of fibroblast-like cells directly (10-12). Selective delivery of MPA to fibrogenic cells may therefore enhance this antiproliferative effect on fibrogenic cells, while simultaneously the potential systemic immunosuppressive effects could be reduced. In fibrotic patients, the latter can be considered a serious side effect. In the studies described in this chapter we demonstrated that MPA was successfully conjugated to M6PHSA and that the resulting construct was capable of inhibiting 3T3-fibroblast proliferation. Additionally, we showed that the effect of M6PHSA-MPA was significantly reversed by co-incubation with an excess of M6PHSA, an M6P/IGF-IIR ligand, but not by an excess of human serum albumin (HSA). This indicated that the construct was indeed taken up by receptor-mediated

endocytosis before exerting its antiproliferative effect within the cells.

To this point, the effects of MPA on HSC had not yet been investigated. In **chapter 4** we demonstrated that the proliferation of culture-activated rat HSC can be completely inhibited by this drug in the micromolar concentration range. Co-incubation of the MPA-treated cells with exogenous guanosine completely restored the proliferative potential of the cells. This is in line with an inhibitory action of this drug on inosine monophosphate dehydrogenase, an enzyme that is crucial for *de novo* guanosine synthesis in cells. We also investigated in this chapter whether the results obtained with the M6PHSA-MPA conjugate in 3T3-fibroblasts could be established in cultured HSC. On the basis of these studies we concluded that in HSC this conjugate also binds to specific receptors, and that this results in a successful inhibition of HSC proliferation. Importantly, *in vivo* studies demonstrated that our conjugate accumulated selectively in HSC, whereas extensive uptake in extrahepatic organs was avoided.

Upon chronic treatment of fibrotic rats with the drug carrier alone (M6PHSA), we discovered that this neoglycoprotein elicits an influx of inflammatory cells within the liver. However, this did not negatively influence fibrogenesis. Interestingly, the carrier-induced hepatic inflammation was completely suppressed in the animals treated with M6PHSA-MPA, whereas this was not the case in the animals that were co-injected with M6PHSA and an equivalent amount of the untargeted drug. M6PHSA-MPA also reduced mRNA expression of α-β-Crystallin, a specific marker for HSC activation. Although these data indicated that pharmacologically active drug can be successfully delivered to HSC, hepatic collagen content and HSC numbers were not significantly affected. This raised the possibility that the delivered amount of MPA to the HSC was too low, which is conceivable since the MPA to protein ratio of the conjugate used in this study was only 0.5:1. Attempts to synthesize a pharmacologically active construct with an increased drug to protein ratio via alternative synthesis strategies were unsuccessful. Our data may also indicate that *in vivo*, HSC have an alternative

metabolic pathway in place in order to maintain intracellular guanosine levels.

In **chapter 5** we therefore investigated the antifibrotic potential and HSC-selective delivery of the more potent antiproliferative drug, doxorubicin (DOX). DOX can also be coupled in higher amounts to the drug carrier, and as an additional advantage over MPA, this drug is detectable by fluorescence microscopy techniques. The latter characteristic of the drug enabled a more optimal investigation of the cellular localization of the targeted and untargeted drug within the liver. We found that DOX inhibits the proliferation of cultured HSC in the nanomolar range and, in this respect, was the most potent cytostatic drug available. Moreover, we could show that chronic treatment of bile duct ligated rats with DOX reduced the number of activated HSC and attenuated collagen deposition. This showed that treatment with this cytostatic drug can in principle exert favorable effects during experimental liver fibrosis. Yet, as expected, we observed clear adverse effects. These were reflected by a significant body weight loss, increased serum γ-GT levels, and an influx of inflammatory cells in the liver. To increase the HSC-specificity of DOX in order to overcome this toxicity, the drug was coupled to M6PHSA via an acid-sensitive linker. The resulting construct (M6PHSA-DOX) accumulated preferentially in the liver and was found to be substantially co-localized with HSC-markers, as assessed by immunohistochemical double-staining for HSA and desmin/GFAP. Taking advantage of the fluorescence of DOX itself, the distribution of the coupled drug could be tracked individually and its selective uptake in non-parenchymal liver cells, about 8% of the liver volume, was clearly demonstrated. In contrast, the livers of rats that were injected with the free drug displayed an extensive uptake of DOX in hepatocytes. It may therefore be expected that during treatment with M6PHSA-DOX hepatocytes retain their functionality and proliferative capacity, unlike treatment with the untargeted drug. From *in vitro* studies, described at the end of this chapter, it could be concluded that the drug targeting construct bound in a selective manner to cultured HSC and strongly inhibited HSC proliferation.

The experiments described in **chapter 6** served to gain a better understanding of the pharmacokinetics of M6PHSA-DOX in rats with liver fibrosis. We observed that the initial plasma disappearance of the construct was inversely correlated to the injected dose, which is in line with clearance by a saturable receptor-mediated clearance mechanism. We also performed γ-camera studies, in which we monitored the hepatic uptake of a ^{123}I-labeled tracer dose in time. This confirmed that the liver was the principal organ of accumulation, and now also revealed that hepatic uptake at relatively low doses occurs rapidly. Within the first 5 minutes after injection, most of the administered dose was already present in the target organ. *In vitro* we evaluated the potential release of DOX from the carrier in an acidic environment, which served to simulate drug release from the construct in the lysosomal compartment of cells to which the endocytosed material is routed. These studies showed that a relatively slow release of DOX from its carrier can be expected to take place within the target cells (9-hour period for maximal release). Such a slow release of DOX from the carrier could ensure a prolonged antiproliferative effect within HSC after rapid initial delivery of the construct to the cells. In cultures of primary isolated rat HSC, fluorescence microscopy studies indicated that untargeted DOX accumulated quickly and mainly in the cell nucleus, whereas M6PHSA-DOX incubation resulted in a granular accumulation pattern in the cytoplasm and, later on, also within the nucleus. The latter is consistent with an accumulation of the construct in the lysosomal compartment. The nucleus-associated DOX in the M6PHSA-DOX-treated cells confirms that release of DOX from the carrier can take place. These observations are in line with the results presented in chapter 5, in which an antiproliferative effect of the construct in cultures of HSC was evident.

Chapter 7 subsequently describes the pharmacological effects of both a single-dose and chronic administration of M6PHSA-DOX on experimental liver fibrosis in rats. In the single-dose study we found that non-parenchymal cell proliferation was reduced in the M6PHSA-DOX-treated animals compared to animals treated

with the control protein. Moreover, a reduction in perisinusoidal collagen deposition was observed. However, despite the apparent successful delivery of pharmacologically active DOX *in vivo* after single dosing, fibrosis parameters were not significantly affected after chronic administration of the conjugate. Recent studies by the group of Faber and Moshage (Dept. of Liver, Digestive and Metabolic diseases, University Medical Centre Groningen) demonstrated the presence of mdr1a and mdr1b mRNA in cultured HSC (13). We therefore hypothesized that chronic exposure to M6PHSA-DOX may induce the cellular expression of these ATP-dependent efflux pumps, also called multi drug resistance transporters. These pumps remove DOX from the target cells and combined with the relatively slow release of pharmacologically active DOX from the intralysosomal depot of intact conjugate (chapter 6), this increase in cellular extrusion mechanisms for DOX may lead to sub-therapeutic drug concentrations in the cytoplasm and nucleus. In line with this hypothesis, we found that chronic treatment of BDL rats with M6PHSA-DOX significantly induced mdr1a mRNA liver levels. Interestingly, mdr1b expression remained unaffected. To test this hypothesis in more detail in the future, immunohistochemical staining of liver sections should elucidate whether, apart from hepatocytes, activated HSC are indeed involved in the observed upregulation of multi drug resistance genes in whole liver samples, and if this leads to mdr-related efflux phenomena in this cell type. Simultaneously, DOX-induced upregulation of mdr1a and mdr1b may be studied in cultures of HSC.

In conclusion, it remains to be established at which dose therapeutic levels of doxorubicin can be attained in HSC following chronic administration of its M6PHSA conjugate. So far, pharmacologically active DOX can be delivered to HSC, but therapeutic levels are not obtained yet, possibly due to the observed mdr1a upregulation in these livers.

GENERAL DISCUSSION AND PERSPECTIVES

Optimization of HSC-selective constructs

Although the HSC-selectivity of antiproliferative drugs was successfully enhanced, undesired uptake of the developed constructs by liver macrophages was still evident (chapters 4, 5 and 6). This clearance by the mononuclear phagocyte system is not unique for HSC-targeted constructs but poses a problem in drug targeting in general. Although it will be difficult to completely avoid macrophage uptake, a successfully applied tactic for the avoidance of protein clearance by these cells is by modification of the proteins with polyethylene glycol (PEG). Pegylation may be applied to improve HSC-targeted preparations as well, but a serious draw-back of this strategy might be that the interaction with M6P/IGF-II receptors also becomes impaired. Since the observed uptake of the present conjugates in Kupffer cells is very likely mediated via scavenger receptors, an alternative strategy to avoid clearance by macrophages would be to reduce the net-negative charge of the constructs (14). As illustrated in chapter 5, this high net negative charge is determined in part by the negatively charged phosphate groups coupled to the protein backbone. In the PDGF-receptor and collagen VI-receptor recognizing HSC-selective drug carriers, circular receptor-recognizing peptides serve as homing devices. As a result, the net negative charge of drug targeting constructs will be lower, which will help to avoid clearance by macrophages. In addition, the absence of possible immunogenic sugar residues in these carriers may also avoid a pro-inflammatory effect, as was observed after administration of M6PHSA (see chapter 4).

Obviously, drugs other than MPA and DOX may be coupled to the drug carriers as well. As outlined in chapter 2, many candidates are available. According to the theory presented in chapter 7, it may be important to make a pre-selection of these drugs by screening the compounds with respect to their Pgp-substrate specificity. Still, whether a drug is a suitable candidate for HSC-selective drug

delivery depends not only on the pharmacological properties of the drug, but is also determined by the presence of proper chemical groups for its conjugation to the drug carrier (carboxylic acid-, amine-, hydroxyl- or sulphide-groups). By investing in technology that allows the conjugation of drugs that can not be coupled to the drug carriers by current conjugation techniques, perspectives can be offered for the targeting of a wider range of promising antifibrotic drugs to HSC. Recently, substantial progress has been made with respect to this. In our lab, the potential antifibrotic drug pentoxifylline was successfully coupled to M6PHSA. This drug, which lacks traditional functional groups for coupling strategies, was conjugated to M6PHSA via the aromatic nitrogens of the drug, using a novel platinum-based linker technology. Since aromatic nitrogens are commonly found in pharmacologically active molecules, this technique may be successfully applied to a wide range of therapeutics (20).

Portal Fibroblasts

The results described in this thesis strengthen the notion that liver fibrosis is a resilient disease. Particularly, studies in bile duct-ligated rats have shown that, besides activated HSC, also portal fibroblasts contribute to fibrogenesis. A simultaneous inhibition of the proliferation of these cells may thus result in a more effective attenuation of fibrosis. Portal fibroblasts are situated in close proximity to the proliferating bile ductules, in zone 1 of the liver. In chapter 6 we have described that fibrogenic cells that are located in the centre of the severely fibrotic portal zones are only reached when high dosages of conjugate are administered. This may be the result of reduced perfusion and accessibility of the fibrogenic cells within these areas. In contrast, accumulation of constructs in activated HSC at the interface of fibrotic and healthy tissue is attained much easier, at lower dosages. As an alternative to the hypothesis posed in chapter 7, it could thus be possible that for a more successful inhibition of fibrogenesis in BDL rats a better penetration of targeting constructs in zone 1 is required. To gain a better understanding of the

antifibrogenic potential of antiproliferative drugs targeted to fibrogenic cells in zone 2 and 3 of the liver, it would therefore be relevant to explore the antifibrotic potential of the developed constructs in fibrosis models that are characterized by fibrosis in these zones. A suitable model for these purposes is the CCl_4 model (See fig. 1, chapter 2), in which fibrogenesis is characterized by a gradual formation of bridges of connective tissue between central veins. With respect to cirrhosis in man, this model is also more relevant since the very rapid and extensive portal expansion that is so characteristic for the BDL model is absent in most forms of the human disease (see chapter 2). We therefore set out to implement this model in our laboratory and currently both a mouse and a rat model of CCl_4-induced liver fibrosis have been introduced.

Although HSC are the principal extracellular matrix-producing cells in the fibrotic liver, progression of fibrosis is also the result of a complex interplay between these fibrogenic cells and other liver cell types (see chapter 2).It should therefore be considered that a more successful inhibition of liver fibrosis may require a pharmacological intervention not only on the level of HSC, but also on the level of other liver cell types.

Role of M6P/IGF-II receptors in disease

Besides the described experiments that can be performed to further investigate the HSC-selective targeting of drugs, another interesting line of research would be to explore the role of the M6P/IGF-II receptor in fibrotic diseases in more detail. Our current data show that these receptors are upregulated on vascular smooth muscle cells in fibrotic vascular lesions and myofibroblasts in fibrotic livers. It is known from literature that activation of latent TGF-β into its active fibrogenic form is mediated by this receptor, as well as the regulation of extracellular levels of insulin-like growth factor (15;16). Interestingly, pro-renin can serve as a ligand for the M6P/IGF-IIR as well, which may lead to its activation or degradation via internalization and subsequent degradation in the lysosomes (17;18). The binding

of pro-renin is of special interest since the development of hypertension-induced vascular lesions in renin transgenic rats is mainly due to an increased activity of the renin angiotensin aldosterone system. Moreover, recent reports have also demonstrated the profibrogenic role of angiotensin II during liver fibrosis (19). M6P/IGF-II receptors on the cell surface of fibrogenic cells may therefore be involved in fibrogenesis by regulating local angiotensin II concentrations via the modulation of renin levels in the direct vicinity of these cells.

Our finding of enhanced expression of the M6P/IGF-II receptor in the renal capillary walls of the TGR(mRen2) rats is new and quite interesting. The receptor appears to be expressed relatively early in the pathogenesis of vascular injury. Receptor expression could be clearly observed, whereas thickening of the capillary vascular walls was still relatively mild. Besides serving as a possible target for fibrogenic cell-selective drug delivery, it is therefore possible that this receptor can be used as an early marker for the development of fibrotic vascular lesions. To explore this in more detail, further efforts are needed to examine the time-course of receptor expression in relation to other disease markers. To this end, animal models for hypertension-induced vascular lesions and atherosclerosis, as well as human pathological tissues should be studied.

CONCLUSIONS

The work presented in this thesis demonstrates that treatment with an antiproliferative drug in principle constitutes a viable antifibrotic strategy for the treatment of liver fibrosis. In addition, we could unequivocally demonstrate that such drugs can be selectively delivered to the key fibrogenic cells in the livers of animals with liver fibrosis. The developed constructs represent the first generation of HSC-targeted drugs and were shown to bind selectively to activated HSC *in vitro* and exert pharmacological effects *in vitro* as well as *in vivo*. Further optimization of targeting constructs in combination with the testing of these second

generation constructs in other models of liver fibrosis should elucidate whether HSC-selective targeting of antiproliferative drugs can ultimately be employed to treat this chronic disease.

REFERENCE LIST

1. Pinzani M, Rombouts K, Colagrande S. Fibrosis in chronic liver diseases: diagnosis and management. J Hepatol 2005; 42 Suppl: S22-S36.
2. Bataller R, Brenner DA. Liver fibrosis. J Clin Invest 2005; 115: 209-18.
3. Eng FJ, Friedman SL. Fibrogenesis I. New insights into hepatic stellate cell activation: the simple becomes complex. Am J Physiol Gastrointest Liver Physiol 2000; 279: G7-G11.
4. Beljaars L, Molema G, Schuppan D, Geerts A, de Bleser PJ, Weert B, Meijer DK, Poelstra K. Successful targeting to rat hepatic stellate cells using albumin modified with cyclic peptides that recognize the collagen type VI receptor. J Biol Chem 2000; 275: 12743-51.
5. de Bleser PJ, Jannes P, van Buul-Offers SC, Hoogerbrugge CM, van Schravendijk CF, Niki T, Rogiers V, van den Brande JL, Wisse E, Geerts A. Insulinlike growth factor-II/mannose 6-phosphate receptor is expressed on CCl4-exposed rat fat-storing cells and facilitates activation of latent transforming growth factor-beta in cocultures with sinusoidal endothelial cells. Hepatology 1995; 21: 1429-37.
6. de Bleser PJ, Scott CD, Niki T, Xu G, Wisse E, Geerts A. Insulin-like growth factor II/mannose 6-phosphate-receptor expression in liver and serum during acute CCl4 intoxication in the rat. Hepatology 1996; 23: 1530-7.
7. Hines JE, Johnson SJ, Burt AD. In vivo responses of macrophages and perisinusoidal cells to cholestatic liver injury. Am J Pathol 1993; 142: 511-8.
8. de Borst MH, Navis G, de Boer RA, Huitema S, Vis LM, van Gilst WH, van Goor H. Specific MAP-kinase blockade protects against renal damage in homozygous TGR(mRen2)27 rats. Lab Invest 2003; 83: 1761-70.
9. Meijer DK, Beljaars L, Molema G, Poelstra K. Disease-induced drug targeting using novel peptide-ligand albumins. J Control Release 2001; 72: 157-64.
10. Raisanen-Sokolowski A, Vuoristo P, Myllarniemi M, Yilmaz S, Kallio E, Hayry P. Mycophenolate mofetil (MMF, RS-61443) inhibits inflammation and smooth muscle cell proliferation in rat aortic allografts. Transpl Immunol 1995; 3: 342-51.
11. Heinz C, Hudde T, Heise K, Steuhl KP. Antiproliferative effect of mycophenolate mofetil on cultured human Tenon fibroblasts. Graefes Arch Clin Exp Ophthalmol 2002; 240: 408-14.

12. Hauser IA, Renders L, Radeke HH, Sterzel RB, Goppelt-Struebe M. Mycophenolate mofetil inhibits rat and human mesangial cell proliferation by guanosine depletion. Nephrol Dial Transplant 1999; 14: 58-63.
13. Hannivoort RA, Buist-Homan M, Faber KN, Moshage H. MRP-type transporters protect activated hepatic stellate cells against cell death. Hepatology 2004; 40: 615A.
14. Terpstra V, van Amersfoort ES, van Velzen AG, Kuiper J, van Berkel TJ. Hepatic and extrahepatic scavenger receptors: function in relation to disease. Arterioscler Thromb Vasc Biol 2000; 20: 1860-72.
15. Dennis PA, Rifkin DB. Cellular activation of latent transforming growth factor beta requires binding to the cation-independent mannose 6-phosphate/insulin-like growth factor type II receptor. Proc Natl Acad Sci U S A 1991; 88: 580-4.
16. Dahms NM, Hancock MK. P-type lectins. Biochim Biophys Acta 2002; 1572: 317-40.
17. van den Eijnden MM, Saris JJ, de Bruin RJ, de Wit E, Sluiter W, Reudelhuber TL, Schalekamp MA, Derkx FH, Danser AH. Prorenin accumulation and activation in human endothelial cells: importance of mannose 6-phosphate receptors. Arterioscler Thromb Vasc Biol 2001; 21: 911-6.
18. Admiraal PJ, van Kesteren CA, Danser AH, Derkx FH, Sluiter W, Schalekamp MA. Uptake and proteolytic activation of prorenin by cultured human endothelial cells. J Hypertens 1999; 17: 621-9.
19. Bataller R, Gabele E, Parsons CJ, Morris T, Yang L, Schoonhoven R, Brenner DA, Rippe RA. Systemic infusion of angiotensin II exacerbates liver fibrosis in bile duct-ligated rats. Hepatology 2005; 41: 1046-55.
20. Gonzalo Lazaro T, Talman EG, Van de Ven A, Temming K, Greupink R, Beljaars L, Meijer DKF, Molema G, Poelstra K, Kok RJ. Selective targeting of pentoxifylline to hepatic stellate cells using a novel platinum-based linker technology. Journal of Controlled Release 2006; 111(1-2):193-203.

SAMENVATTING

Leverfibrose en de rol van de hepatische stellaat cel

Leverfibrose is een chronische ziekte die het gevolg is van langdurig optredende leverschade. Deze schade kan verschillende oorzaken hebben, bijvoorbeeld een chronische virale leverinfectie (hepatitis B of C), auto-immuunziektes, metabole aandoeningen waaronder obesitas, het chronisch gebruik van alcohol en het gebruik van sommige geneesmiddelen. Leverfibrose wordt gekarakteriseerd door de vorming van grote hoeveelheden littekenweefsel (collageen) in dit orgaan.

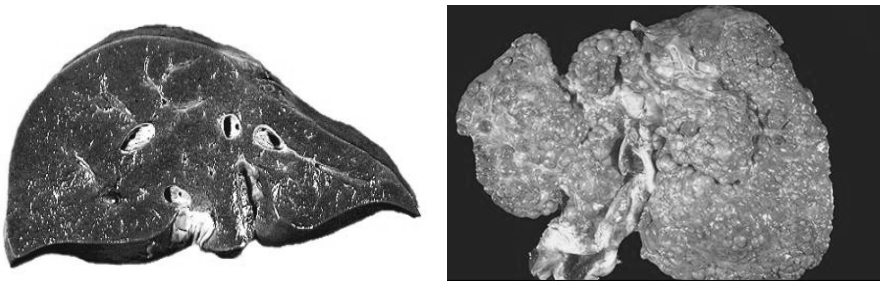

Fig. 1. Doorsnedes van een gezonde menselijke lever (links) en een door leverfibrose aangetaste lever (rechts). Het onregelmatige uiterlijk van de fibrotische lever wordt veroorzaakt door de aanwezigheid van overmatige hoeveelheden littekenweefsel.

De verstoring van de weefselarchitectuur heeft onder andere tot gevolg dat de doorbloeding van de lever verslechtert, wat vervolgens leidt tot een achteruitgang in leverfunctie. In combinatie met allerlei secundaire complicaties die ontstaan als gevolg van de verhoogde collageen afzetting in de lever kan dit uiteindelijk leiden tot de dood. Een ander kenmerk van lever fibrose is dat het ziekteproces in een gevorderd stadium onomkeerbaar is, zelfs wanneer de prikkel die de schade veroorzaakt wordt weggenomen. Tot op heden is er geen enkele farmaco-therapeutische behandeling die het fibrose proces kan remmen of omkeren en de enige curatieve behandeling is het uitvoeren van een lever transplantatie.

Omdat aan een transplantatie grote risico's kleven en er bovendien een gebrek is aan donororganen, is de ontwikkeling van een farmacologische behandeling dringend gewenst. Die zoektocht naar een antifibrotisch geneesmiddel kreeg een belangrijke impuls toen de hepatische stellaat cel (HSC) werd geïdentificeerd als spil in het ziekteproces. Er werd aangetoond dat de HSC onder invloed van mediatoren van verschillende andere celtypen in de lever (hepatocyten, bloedvat endotheel cellen en immuuncellen) na het optreden van chronische leverschade transformeert van een rustende cel in een geactiveerde cel die verantwoordelijk is voor de overmatige productie van collageen. Bovendien neemt het aantal geactiveerde HSC in de fibrotische lever sterk toe als gevolg van een sterk toegenomen celdeling van deze fibrogene cellen. Omdat de proliferatie van HSC zo'n belangrijke rol speelt bij de ontwikkeling van leverfibrose zou het remmen van de groei van deze cellen een relevante strategie kunnen zijn voor de farmacologische behandeling van deze ziekte.

Drug Targeting

Wanneer patiënten met leverfibrose behandeld zouden worden met antiproliferatieve middelen (bijvoorbeeld cytostatica), dan zou dit echter zeer waarschijnlijk leiden tot ernstige bijwerkingen omdat het groei-remmende effect niet alleen zal optreden in HSC, maar ook in andere organen en andere levercellen. De cytostatica zullen na toediening namelijk niet alleen ophopen in de HSC, maar ook opgenomen worden in andere cellen en weefsels in het lichaam. Met name door deze grote kans op ernstige bijwerkingen is het gebruik van antiproliferatieve farmaca voor de behandeling van leverfibrose nooit goed onderzocht.

Zoals uiteengezet in **hoofdstuk 1 en 2**, kan de toxiciteit van antiproliferatieve geneesmiddelen worden beperkt door deze stoffen alleen af te leveren in het lichaam waar hun effect gewenst is, in dit geval de HSC, terwijl de ophoping in de andere lichaamscellen wordt voorkomen. Dit principe wordt drug targeting genoemd. Om dit te bewerkstelligen zullen de farmacokinetische eigenschappen

van bestaande antiproliferatieve middelen moeten worden veranderd. Een mogelijkheid hiervoor is het koppelen van een cytostaticum aan een dragermolecuul dat wel selectief ophoopt in de gewenste doelcel. Drager moleculen voor HSC waren tot voor kort nog niet bekend, maar in de afgelopen jaren zijn zulke HSC-selectieve dragermoleculen in ons laboratorium ontwikkeld. In de studies beschreven in dit proefschrift wordt hiervan gebruik gemaakt om te onderzoeken of het mogelijk is antiproliferatieve stoffen selectief af te leveren in de HSC en te bepalen of dit een kansrijke strategie vertegenwoordigt in de ontwikkeling van een farmacologische behandeling voor leverfibrose.

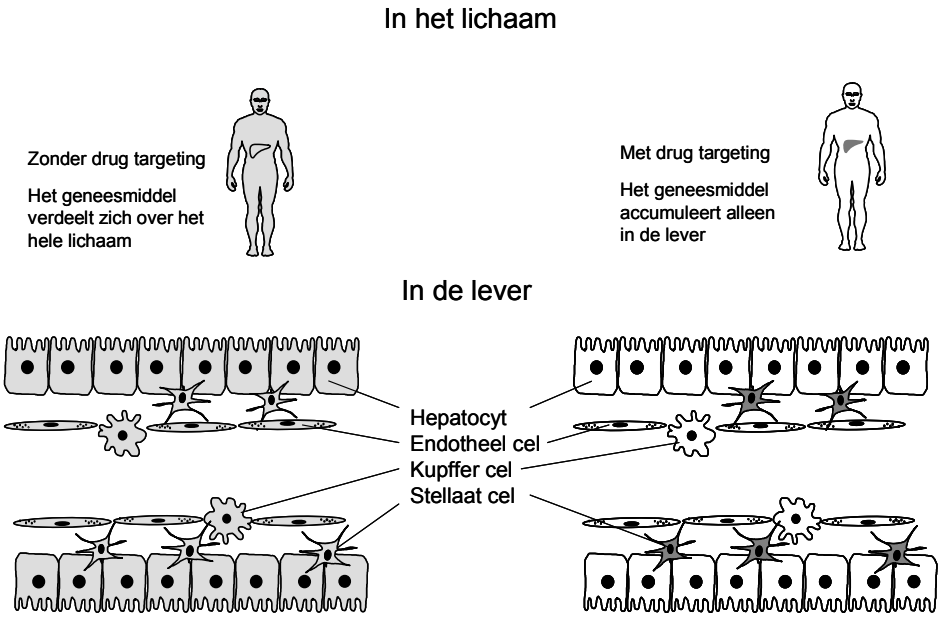

Fig. 2. Schematische weergave van het drug targeting principe. De intensiteit van de grijze kleur geeft de concentratie van het geneesmiddel weer in organen en cellen. In het linker gedeelte van de figuur wordt de situatie afgebeeld na toediening van een geneesmiddel dat niet aan een stellaat cel specifiek dragermolecuul is gekoppeld, in het rechter gedeelte de situatie na toediening van een geneesmiddel dat selectief naar de stellaat cellen wordt gestuurd. Idealiter wordt het geneesmiddel dan niet alleen afgeleverd in het juiste orgaan, maar binnen dat orgaan bovendien in het juiste celtype.

In de studies beschreven in dit proefschrift staat de HSC-selectieve geneesmiddeldrager "mannose-6-fosfaat gemodificeerd humaan serum albumine" (M6PHSA) centraal. Mannose-6-fosfaat is een suikergroep die herkend wordt door receptoren die verhoogd tot expressie worden gebracht op de geactiveerde HSC, de mannose-6-fosfaat/insuline-achtige groeifactor type II receptoren (M6P/IGF-II receptoren). Door de mannose-6-fosfaat suikergroepen te koppelen aan een eiwit (albumine) ontstaat een neoglycoproteine dat selectief bindt aan de opgereguleerde receptoren op de geactiveerde HSC. Naast de mannose-6-fosfaat groepen kan aan het albumine een geneesmiddel worden gekoppeld, dat op deze wijze net zo selectief ophoopt in de HSC als het dragermolecuul.

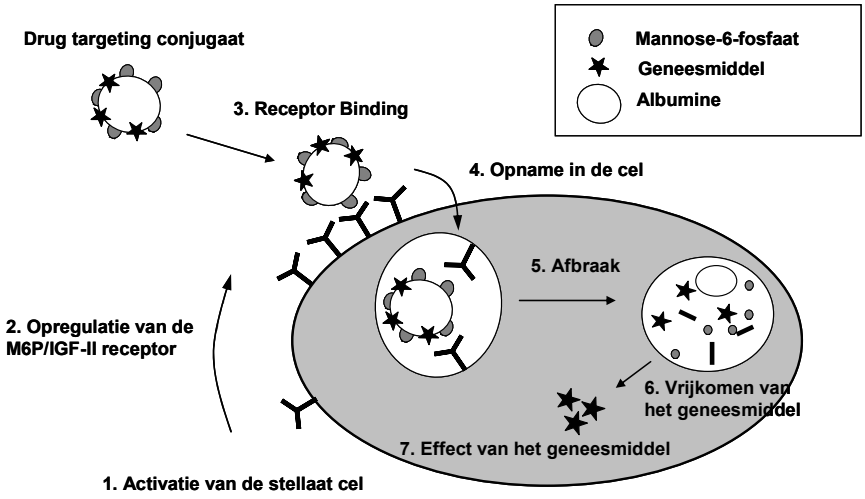

Fig. 3. Schematische weergave van de drug targeting strategie.

Het onderzoek

Om onze drug targeting strategie te testen is in dit proefschrift gebruik gemaakt van een diermodel voor leverfibrose, het "galgang ligatie model" (bile duct ligation model, afgekort BDL). Door de galgang van een rat af te binden ontstaat chronische leverschade doordat galzouten, die normaal worden uitgescheiden via de gal, nu ophopen in de lever met als gevolg een fibrotische respons. De HSC proliferatie treedt in dit model al op binnen de eerste 10 dagen na inductie van de

ziekte. In **hoofdstuk 3** is daarom eerst onderzocht of in deze vroege fase van fibrogenese de doelwit receptor op de geactiveerde HSC tot expressie wordt gebracht. Dit is een absolute voorwaarde wil het selectief afleveren van antiproliferatieve stoffen bij de HSC succesvol zijn. Het bleek dat de M6P/IGF-II receptor expressie in de levers van BDL ratten op zowel mRNA als op eiwit niveau was verhoogd op alle onderzochte tijdstippen, nl. 3, 7 en 10 dagen na inductie van de ziekte. Bovendien konden we aantonen dat de toename in receptor expressie in de fibrotische levers kon worden toegeschreven aan een opregulatie op α-smooth muscle actine positieve lever cellen, een kenmerk van geactiveerde HSC. De opregulatie van M6P/IGF-II receptoren op fibrogene cellen vindt echter niet alleen plaats tijdens fibrose in de lever. In hoofdstuk 3 laten we namelijk ook zien dat tijdens hypertensie-geinduceerde fibrose in bloedvaten in de nier een verhoogde expressie van deze receptor aanwezig is, wederom op de fibrogene cellen. Deze vindingen openen mogelijkheden om geneesmiddelen af te leveren in HSC in een vroege fase van het fibrose proces in de lever, wanneer de HSC proliferatie het meest prominent is. Bovendien biedt dit perspectieven voor het afleveren van geneesmiddelen in fibrogene cellen tijdens fibrose in andere organen, waaronder de nier. Uit de studies beschreven in hoofdstuk 3 bleek bovendien dat het koppelen van het geneesmiddel mycophenolzuur aan het drager molecuul M6PHSA mogelijk is en een product opleverde dat farmacologisch actief was: in *vitro* remde ons construct de groei van fibroblasten. Dit onderstreept de haalbaarheid van het drug targeting concept verder.

Mycophenolzuur is bekend als immuunsuppressivum (CellCept), dat wordt toegepast om afstoting van donororganen te voorkomen na een orgaantransplantie. Minder bekend zijn de directe antiproliferatieve effecten op sommige fibroblasten. Bij de behandeling van patiënten met leverfibrose is met name het antiproliferatieve effect van dit geneesmiddel gewenst (in de HSC) terwijl de immuunsuppressie bij deze patiëntengroep als ongewenste bijwerking kan worden beschouwd. Het gericht afleveren van mycophenolzuur in HSC lijkt daarom zinvol.

Alhoewel het antiproliferatieve effect van mycophenolzuur aangetoond is in fibroblast-achtige cellen in nier, oog en vaatwand, was het effect van dit farmacon op HSC nog nooit onderzocht. In **hoofdstuk 4** tonen we aan dat mycophenolzuur in micromolaire concentraties de proliferatie van uit rattenlevers geïsoleerde HSC volledig kan remmen. Analoog aan de resultaten die behaald zijn in de fibroblast-cellijn, vonden we dat wanneer dit geneesmiddel werd gekoppeld aan M6PHSA, het resulterende drug targeting construct ook selectief bond aan receptoren op HSC en het de deling van deze cellen effectief remde. Uit *in vivo* studies bleek dat het HSC-gerichte mycophenolzuur na intraveneuze injectie in ratten met lever fibrose bijna exclusief werd opgenomen door de lever terwijl opname in andere organen kon worden voorkomen. In de lever werd het HSC-gestuurde mycophenolzuur inderdaad voor een belangrijk deel opgenomen door HSC. Effect studies, waarin het conjugaat meerdere malen intraveneus werd gegeven, lieten zien dat een vroege marker voor HSC activatie afnam in ratten die behandeld werden met het HSC-selectieve mycophenolzuur terwijl dit bij behandeling met het vrije, niet getargete geneesmiddel niet het geval was. Dit geeft aan dat het ook *in vivo* mogelijk is met deze drug targeting techniek farmacologisch actief mycophenolzuur in de HSC af te leveren.

Het fibrose proces en de toename van het aantal HSC in de lever werden echter niet significant geremd. Mogelijk is dit het gevolg geweest van de lage koppelingsratio tussen mycophenolzuur en M6PHSA, waardoor slechts een sub-therapeutische hoeveelheid van dit farmacon in de doelcel werd afgeleverd. Pogingen om meer mycophenolzuur te koppelen aan de geneesmiddel drager waren echter niet succesvol.

In **hoofdstuk 5** hebben wij daarom het antifibrotische effect en de HSC-selectieve aflevering van het sterker werkzame antiproliferatieve geneesmiddel doxorubicine (DOX) onderzocht. DOX kon in grotere hoeveelheden aan de geneesmiddeldrager worden gekoppeld met als bijkomend voordeel dat doxorubicine in weefsels gemakkelijk kan worden gelokaliseerd met behulp van

een fluorescentie microscoop. Zo kon het verschil in de intrahepatische verdeling tussen het HSC-getargete en het vrije, niet HSC-getargete geneesmiddel goed met elkaar worden vergeleken. We vonden dat DOX in nanomolaire concentraties, dus in lagere concentraties dan mycophenolzuur, de proliferatie van HSC remde. Bovendien remde doxorubicine de progressie van fibrose *in vivo*, in het rattenmodel voor deze ziekte. Zoals verwacht traden er bij behandeling met het vrije, niet getargete geneesmiddel wel bijwerkingen op. Er waren aanwijzingen voor schade aan hepatocyten en een toegenomen infiltratie van ontstekingscellen in het leverweefsel. Dit illustreert wederom het belang van de HSC-selectieve drug targeting strategie. In dit hoofdstuk laten we ook zien dat doxorubicine na koppeling aan M6PHSA, selectief naar de fibrogene levercellen kan worden gestuurd. Wanneer met de fluorescentie microscoop de distributie van het HSC-gerichte doxorubicine (M6PHSA-DOX) werd vergeleken met dat van het vrije doxorubicine, bleek dat het vrije farmacon detecteerbaar was in alle organen waar bijwerkingen van dit cytostaticum plaats kunnen vinden. Het HSC-gerichte doxorubicine hoopte daarentegen vrijwel alleen op in de lever. In de lever konden we bovendien waarnemen dat het HSC-gerichte geneesmiddel voor een belangrijk deel terug te vinden was in HSC, terwijl hepatocyten gespaard bleven voor opname van doxorubicine. Dit in tegenstelling tot het vrije geneesmiddel, dat niet-selectief in alle levercellen accumuleerde. *In vitro* studies, beschreven aan het einde van dit hoofdstuk, bevestigden de selectieve binding van M6PHSA-DOX aan HSC. Bovendien resulteerde de incubatie van de *in vitro* gekweekte HSC met M6PHSA-DOX in een afname van de celdeling, daarmee aantonende dat farmacologisch actief doxorubicine vrij kan komen van de geneesmiddel drager.

De experimenten beschreven in **hoofdstuk 6** hadden tot doel meer te weten te komen over de farmacokinetiek van M6PHSA-DOX in ratten met leverfibrose. Het bleek dat na injectie van dit drug targeting construct de plasmaspiegel bi-fasisch afnam en dat, naarmate meer M6PHSA-DOX werd toegediend, de snelheid van plasmaverdwijning in de eerste verdelingsfase verminderde. Dit is te rijmen met de

manier waarop M6PHSA-DOX uit het plasma verwijderd wordt, namelijk via receptor-medieerde opname. Een verzadiging van dit opname proces zou het gevonden farmacokinetisch profiel prima kunnen verklaren. Naast de kinetiek van de plasmaverdwijning is met behulp van gamma-camera studies de snelheid geëvalueerd waarmee radio-actief gelabeld M6PHSA-DOX zich na injectie over het lichaam verdeelt. Deze studies bevestigden dat de lever het belangrijkste doelwit orgaan is voor het construct, maar illustreerden bovendien dat deze opname zeer snel verloopt. Al binnen 5 minuten werd in de lever een plateau-waarde bereikt. Op basis van *in vitro* studies beschreven in dit hoofdstuk is het te voorspellen dat na de snelle opname van M6PHSA-DOX in de lever, het doxorubicine relatief langzaam van de geneesmiddeldrager zal vrijkomen, gedurende een periode van uren. Hoewel bij gewone geneesmiddelen een snelle verdwijning uit het plasma vaak geassocieerd is met een kortdurend effect, hoeft dit bij HSC-gerichte geneesmiddelen dus niet zo te zijn.

In **hoofdstuk 7** zijn vervolgens de farmacologische effecten van M6PHSA-DOX op het fibrose proces onderzocht, na enkelvoudige injectie, alsmede na chronische toediening. In de studie waarin eenmalig werd gedoseerd was de celdeling van de zogenaamde non-parenchymale levercellen, de populatie levercellen waarvan de HSC onderdeel uit maken, afgenomen. Bovendien kon in de gebieden van de lever waar het drug targeting construct werd afgeleverd een afname in de collageen afzettingen worden waargenomen. Echter, ondanks het feit dat farmacologisch actief doxorubicine *in vivo* succesvol werd afgeleverd, bleek dat na meerdere doseringen het fibrose proces niet significant werd beïnvloed. Een verklaring hiervoor was moeilijk te vinden tot dat zeer recentelijk werd beschreven dat HSC de eiwitten mdr1a en mdr1b in hun celmembraan tot expressie kunnen brengen. Deze transport eiwitten, varianten van het humane P-glycoproteine, kunnen doxorubicine de cel uit pompen. Daarom hebben wij bestudeerd of chronische blootstelling van fibrotische ratten aan M6PHSA-DOX de expressie van deze geneesmiddel pompen in de lever induceert. Inderdaad konden we

aantonen dat chronische toediening van het drug targeting construct leidde tot een verhoogde mdr1a mRNA expressie, maar dat de mdr1b mRNA expressie niet werd beïnvloed. Een verhoogde expressie van mdr1a, in combinatie met de relatief langzame afgifte van doxorubicine van de geneesmiddeldrager (hoofdstuk 6) zou kunnen leiden tot sub-therapeutische concentraties in de cel. Toekomstig onderzoek zal nog wel moeten uitwijzen of deze op-regulatie inderdaad plaats vindt in HSC en of dit ook plaats vindt op eiwit niveau. Daarnaast zullen studies waarin deze drug efflux pompen geblokkeerd worden (via het tegelijkertijd toedienen van bijvoorbeeld verapamil) moeten uitwijzen of de antifibrotische effecten na chronische toediening van M6PHSA-DOX dan wel zijn waar te nemen.

Samenvattend kan worden gesteld (**hoofdstuk 8**) dat het in dit proefschrift gepresenteerde onderzoek aantoont dat een behandeling met antiproliferatieve stoffen een relevante strategie kan zijn in de behandeling van leverfibrose. Daarbij laten we zien dat in een diermodel voor deze ziekte antiproliferatieve geneesmiddelen selectief kunnen worden afgeleverd in hepatische stellaat cellen, in een farmacologisch actieve vorm. De ontwikkelde constructen vertegenwoordigen de eerste generatie van geneesmiddelen die selectief kunnen worden afgeleverd bij de hepatische stellaat cellen. Hiermee is de basis gelegd voor het verder uitwerken van een antifibrotische therapie die selectief aangrijpt op dit celtype.

APPENDIX:

LIST OF ABBREVIATIONS

COLOR FIGURES

DANKWOORD

CURRICULUM VITAE

LIST OF PUBLICATIONS

LIST OF ABBREVIATIONS

α-sma	alpha-smooth muscle actin
γ-GT	γ-glutamyltransferase
AIH	autoimmune hepatitis
ALT	alanine transaminase
AP	alkaline phosphatase
ASH	alcoholic steatohepatitis
AST	aspartate transaminase
BDL	bile duct-ligated/ligation
BrdU	5-bromo-2'-deoxyuridine
CCl_4	carbontetrachloride
DAB	diaminobenzidine
DDR-2	discoidin domain-2 receptors
DOX	doxorubicin
EC	endothelial cells
ECM	extracellular matrix
EGF	epidermal growth factor
HSA	human serum albumin
HBV	hepatitis B virus
HCV	hepatitis C virus
HSC	hepatic stellate cell
IFN	interferon
IGF	insulin-like growth factor
IMPDH	inosine monophosphate dehydrogenase
KC	Kupffer cell
M6P	mannose-6-phosphate
M6P/IGFII	mannose-6-phosphate/insulin-like growth factor-II
M6PHSA	mannose-6-phosphate-modified human serum albumin
MMP	matrix metalloproteinase
MPA	mycophenolic acid
NASH	non-alcoholic steatohepatitis
NPC	non-parenchymal cells
PAF	platelet activating factor
PBC	primary biliary cirrhosis
PBS	phosphate-buffered saline
PCNA	proliferating cell nuclear antigen
PDGF	platelet derived growth factor
PSC	primary sclerosing cholangitis
TGF	transforming growth factor
TGR(mRen2)27	renin transgenic rats
TIMP	tissue inhibitor of metalloproteinase
TNF	tumor necrosis factor

COLOR FIGURES

Chapter 3, figure 2

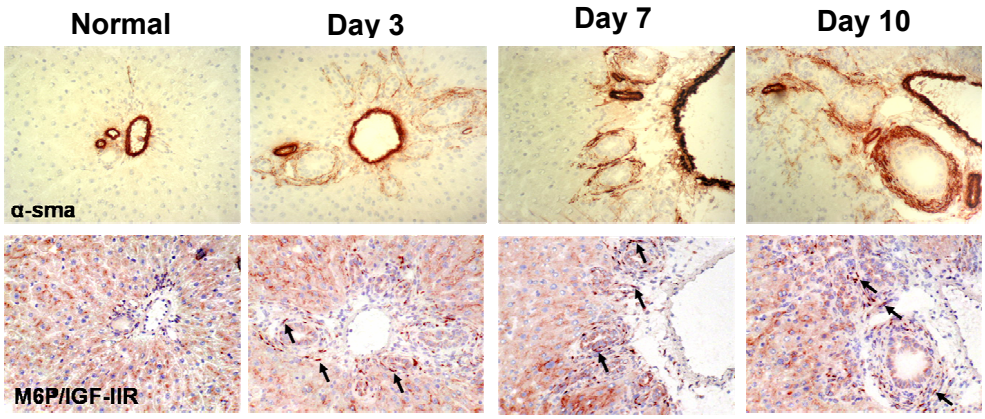

Chapter 3, figure 3A

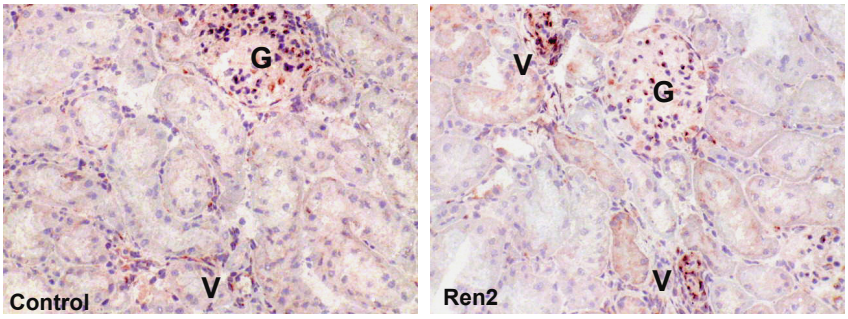

Chapter 5, figure 5

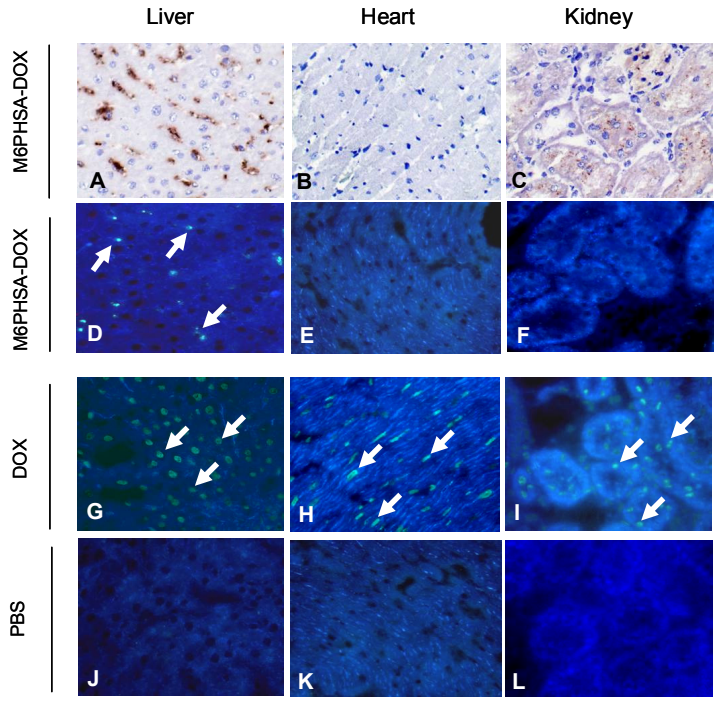

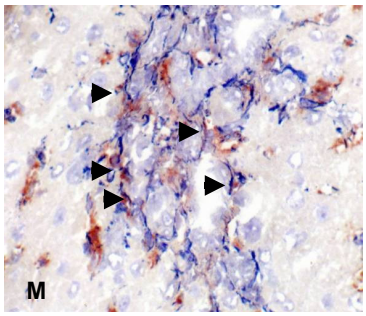

Chapter 6, figure 3

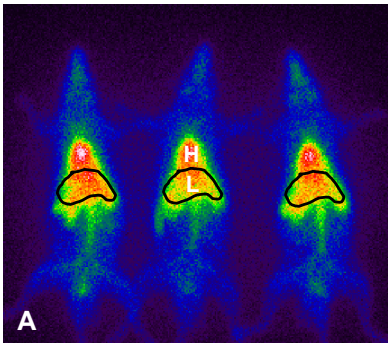

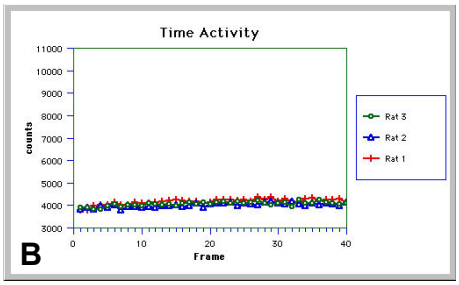

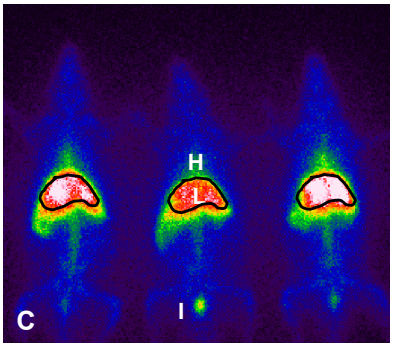

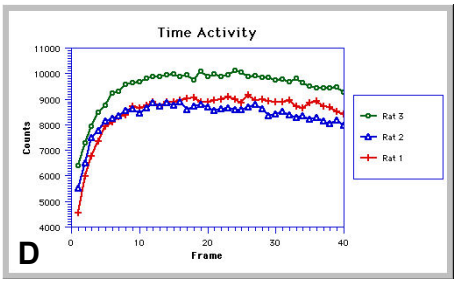

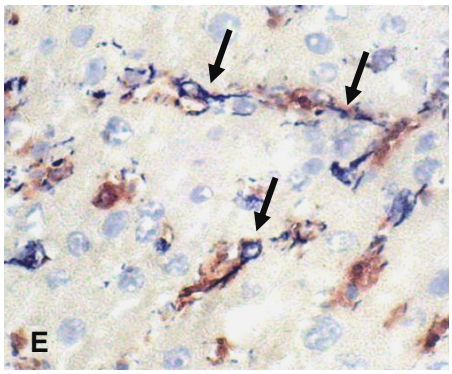

Chapter 6, figure 4B

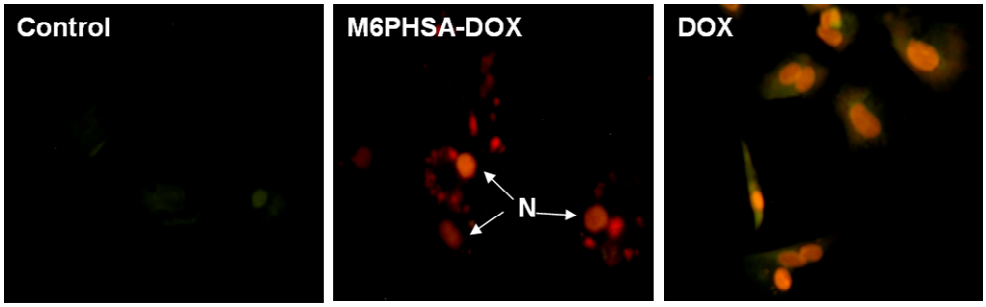

DANKWOORD

Heel veel plezier heb ik de afgelopen jaren beleefd aan het doen van het onderzoek dat beschreven staat in dit proefschrift. Het enthousiasme waarmee allerlei mensen aan dit onderzoek hebben bij gedragen heeft daarbij een belangrijke rol gespeeld en hen wil ik op deze plek daar heel hartelijk voor bedanken.

In de eerste plaats Klaas. Als eerste promotor en bovendien dagelijks begeleider heb jij een belangrijke bijdrage geleverd aan mijn ontwikkeling tot onderzoeker. Ondanks je drukke bestaan als vers benoemde hoogleraar wist je altijd weer tijd vrij te maken om de voortgang van het lopende onderzoek te bediscussiëren. Je enthousiasme voor, kennis van, en kijk op de pathologie van ziekteprocessen zijn inspirerend en mijns inziens een verrijking voor het farmacokinetisch en farmacologisch onderzoek binnen de farmacie. Terugkijkend kan ik dan ook oprecht zeggen dat ik erg blij ben dat ik de afgelopen jaren mijn promotie-onderzoek onder jouw hoede heb mogen doen.

Dick, als tweede promotor stond jij meer op afstand van mijn project, maar was ook jij altijd geïnteresseerd in de vorderingen die ik maakte. Onze regelmatige gesprekken, ook na je emeritaat, heb ik als zeer prettig en leerzaam ervaren. Bovendien was het toezicht op de kwaliteit van de farmacokinetische aspecten van mijn onderzoek bij jou in goede handen. Hiervoor zeer bedankt.

Leonie, zonder jouw bemoeienis was dit proefschrift nog een lang en moeilijk verhaal geworden. Je probleemoplossend vermogen op velerlei vlak is enorm, waarvan ik dan ook zeer dankbaar gebruik heb gemaakt. Het is mooi en niet meer dan terecht dat het stellaat cel onderzoek nu een vervolg krijgt met het goedkeuren van je eigen STW project. Heel veel succes!

De analisten van ons fibrose groepje: Hester, Catharina, Alie en Anne-miek bedankt voor de vele stellaat cel isolaties, syntheses, (dubbel-)kleuringen, deskundige hulp met de dierexperimenten en ga zo maar door. Jullie inzet en praktische expertise maken het ook echt mogelijk om binnen het lab onze eigen antifibrotische geneesmiddelen te maken en uitvoerig te testen. Hester, ik heb nog eens staan kijken naar de enorme rij met mappen gevuld met data die jij hebt vergaard en ik realiseer me dat ik heel veel geluk heb gehad met jou als analist op het project. Fijn dat ik je heb kunnen overreden om als paranimf op te treden!

Zonder iedereen bij naam te noemen natuurlijk ook een woord van dank voor de rest van de (oud-)leden van de vakgroep Kinetiek. Dankzij de ontwikkeling van de digitale fotografie staat mijn harde schijf gelukkig vol met foto's van de jaarlijkse labdagen, een mooie herinnering dacht ik zo. In het bijzonder Robbert-Jan bedankt voor velerlei synthese advies, Hans voor het vol enthousiasme "tackelen" van farmacokinetische vraagstukken, Jan voor het draaiende houden van het lab en in dit kader zeker ook Willem bedankt voor het verhelpen van het tot twee keer toe crashen van de thuiscomputer. Er staat weer een zeer functioneel model, nu bovendien met een goede game-configuratie! Werner, kamergenoot van (bijna) het eerste uur en mede fibrose-AIO, ik ben je zeer erkentelijk voor alle gevraagde en ongevraagde adviezen (een adviserende functie is zeker wat voor jou) en ook

voor de gezelligheid de afgelopen jaren, zowel in als buiten het lab. Succes met de afronding van je eigen proefschrift. All other PhD-students, Teresa, Janja, Adriana, Kai, Jai, Asia, Esther, Marja, Annemarie, Ansar, and (at TGM) Willemijn and Antoine also the best of luck finishing your theses. I very much enjoyed your international company. Als veelvuldig CO gebruiker op ons lab hoort ook Mattijs J in dit rijtje thuis: succes met de laatste loodjes. Verder Peter bedankt voor het wegwijs maken in the US of A tijdens de congressen in Boston 2003 en 2004, en tenslotte dienen hier natuurlijk de dames Linda, Marieke en Wilma genoemd te worden die als bijvakstudent hebben bijgedragen aan de diverse hoofdstukken. Ik hoop dat jullie er wat van hebben op gestoken, ik vond het prettig samenwerken.

Buiten de Farmacokinetiek, bij de afdeling Pathologie en Laboratorium Geneeskunde, ben ik Harry van Goor zeer erkentelijk voor het vol enthousiasme uit de vriezer opduiken van vriescoupes van diverse nierziektemodellen en, bij de Nucleaire Geneeskunde, Marjolijn de Hooge, Hans ter Veen en Hans Pol voor het mogelijk maken van de gamma-camera studies en het radioactief labelen van de verschillende conjugaten. Dank ook Pieter en Ulrike bij de farmacochemie voor het vakkundig reduceren van NO_2 groepen tot NH_2 groepen en, bij de afdeling Maag- Darm- en Leverziekten, Klaas-Nico Faber en Mariska Geuken voor het mij uit de brand helpen door wel op heel erg korte termijn de mdr1 mRNA levels in de laatste leversamples te bepalen.

Dan wil ik natuurlijk de leden van de beoordelingscommissie, Prof. Dr. Moshage, Prof. Dr. Haisma en Prof. Dr. Verkade, op deze plaats ook zeer hartelijk bedanken voor het snelle beoordelen van mijn proefschrift.

Buiten het werk, Matthijs (principieel klimmer/schaatser) en Bart (principieel koffiedrinker in modderig Roskilde) bedankt voor de broodnodige relativerende niet-wetenschappelijke kijk op de zaken. En natuurlijk de Farmaboys: Peer, Peder, Raoul, Jeroen, Antoon, Aldo en Mark, de jaarlijkse uitjes waarmee we tijdens de studie begonnen zijn, waren ook de afgelopen 4,5 jaar weer een welkome afwisseling met het werk. Het lijkt mij dat we hier zeker mee door moeten gaan. Peer, ik ben dan ook blij dat je als vriend uit deze groep als paranimf wilt optreden.

Lieve Mama en Minke, bedankt voor alles. Zonder jullie doorzettingsvermogen in de afgelopen jaren was dit proefschrift er nooit geweest, dat weet ik zeker. Dat geldt ook voor oom Dick en tante Gerrie, door jullie bekommeringen is veel op zijn pootjes terecht gekomen terwijl dat ook heel anders had kunnen zijn geweest. Ik ben blij dat jullie er allemaal zijn. Daarnaast ook bedankt voor het zakwoordenboek der therapie van Prof. Klencke waarvan de tekst nu op de voorkant van dit boekje prijkt!

Tenslotte, lieve Annelies. Als geen ander heb jij van dichtbij gezien hoe dit proefschrift vorm kreeg. Ik ben je heel dankbaar voor alle grote en kleine bijdragen eraan, maar veel meer nog voor alle andere dingen.

Rick

CURRICULUM VITAE

Rick Greupink werd op 20 september 1976 geboren te Rheden en groeide op in Ruurlo. In 1994 voltooide hij het VWO aan het Staring College te Lochem en in dat zelfde jaar begon hij met de studie farmacie aan de Rijksuniversiteit Groningen. Zijn afstudeeronderzoek betrof een studie naar het selectief afleveren van farmaca in de nier met behulp van eiwitten van een laag moleculair gewicht. Rick studeerde in 2000 cum laude af om vervolgens de opleiding tot apotheker te volgen. Het apothekersdiploma behaalde hij in 2001, waarna hij in dienst trad als Onderzoeker in Opleiding bij de vakgroep Farmacokinetiek en Drug Delivery van de afdeling Farmacie van de RuG. Deze vakgroep maakt deel uit van het Groningen University Institute for Drug Exploration (GUIDE), waarin zowel farmaceutische als medische onderzoeksgroepen participeren. Het project werd door de Stichting Technische Wetenschappen gefinancierd en is uitgevoerd onder begeleiding van dr. L. Beljaars, prof. dr. D.K.F. Meijer en prof. dr. K. Poelstra. De resultaten hiervan zijn vastgelegd in dit proefschrift.

LIST OF PUBLICATIONS (FULL PAPERS)

Greupink R, Bakker HI, Reker-Smit C, van Loenen-Weemaes A, Kok RJ, Meijer DKF, Beljaars L, Poelstra K. Studies on the targeted delivery of the antifibrogenic compound mycophenolic acid to the hepatic stellate cell. *Journal of Hepatology 2005; 43(5): 884-892.*

Gonzalo Lazaro T, Talman EG, Van de Ven A, Temming K, **Greupink R**, Beljaars L, Meijer DKF, Molema G, Poelstra K, Kok RJ. Selective targeting of pentoxifylline to hepatic stellate cells using a novel platinum-based linker technology. *Journal of Controlled Release 2006; 111(1-2):193-203*

Greupink R, Bakker HI, Bouma W, Reker-Smit C, Meijer DKF, Beljaars L, Poelstra K. The antiproliferative drug doxorubicin inhibits liver fibrosis in bile duct-ligated rats and can be selectively delivered to hepatic stellate cells in vivo. *Journal of Pharmacology and Experimental Therapeutics 2006; 317(2): 514-521.*

Greupink R, Bakker HI, Van Goor H, de Borst MH, Beljaars L, Poelstra K. Mannose-6-phosphate/insulin-like growth factor-II receptors may represent a target for the selective delivery of mycophenolic acid to fibrogenic cells. *Pharmaceutical Research, in press*

Greupink R, Reker-smit C, van Loenen-Weemaes A, de Hooge MN, Proost JH, Poelstra K, Beljaars L. Pharmacokinetics of a hepatic stellate cell-targeted doxorubicin preparation in rats with liver fibrosis. *Submitted.*

Greupink R, Bakker HI, Meijer DKF, Beljaars L, Poelstra K. Towards a targeted inhibition of hepatic stellate cell proliferation: a single and multiple dose study on the antifibrogenic effects of a hepatic stellate cell-targeted doxorubicin construct in bile duct-ligated rats. *In preparation.*

Hagens WI, Pinto A, **Greupink R,** De Jager-Krikken A, Poelstra K, Beljaars L. Targeting 15d-prostaglandin J_2 to Hepatic Stellate Cells: M6P-HSA versus pPB-HSA. *In preparation.*

Beljaars L, Hagens WI, **Greupink R**, Van Luin M, Reker-Smit C, Meijer DKF, Mallat A, Lotersztajn S, Poelstra K. Aggravation of liver fibrosis after selective inhibition of cyclo-oxygenase-2 (COX-2) in hepatic stellate cells. *In preparation*.